

# **IPS Meeting 2016**

## **7 - 8 March**



Institute of Physics Singapore

## **Conference Program**

(post-print version, status: March 4, 2016, 16:41SGT)

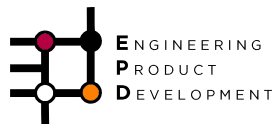
The IPS Meeting 2016 thanks its sponsors  
for their generous support



ACEXON TECHNOLOGIES PTE LTD



Institutional Sponsors:

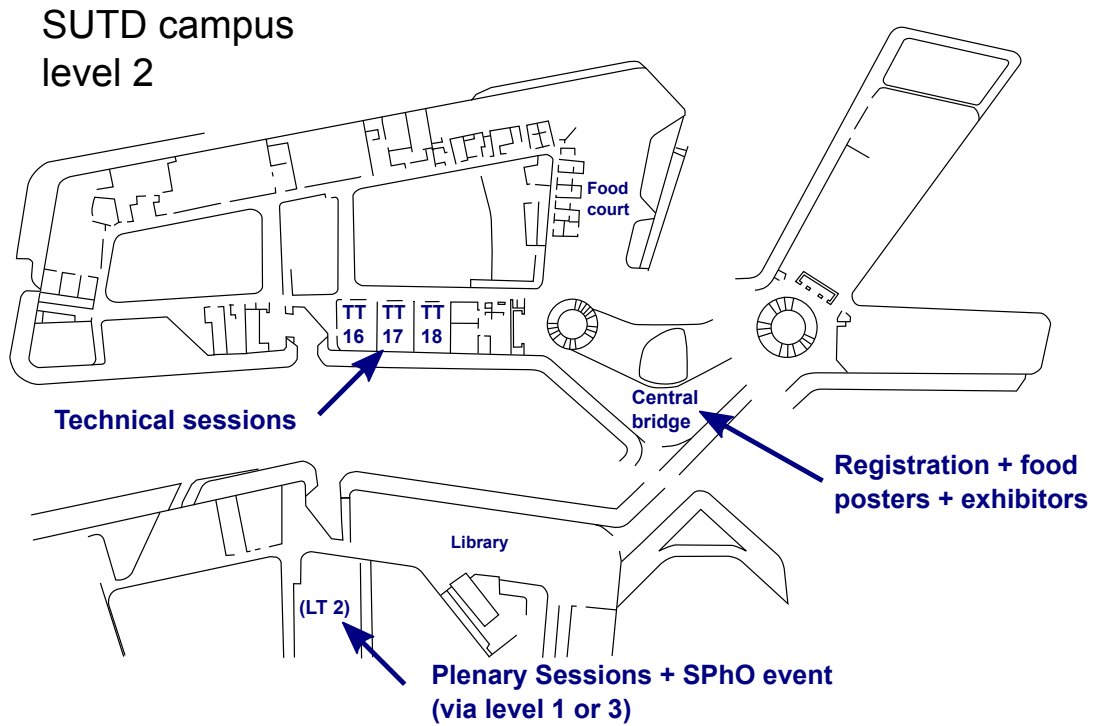


# Contents

<b>1</b>	<b>Location Map</b>	<b>2</b>
<b>2</b>	<b>Schedule</b>	<b>3</b>
<b>3</b>	<b>Plenary sessions</b>	<b>5</b>
	P1: Benoit Taisne, EOS: The Sound of Nature's Fury . . . . .	5
	P2: Shaffique Adam, Yale-NUS College / CA2DM: Effects of disorder ... . . . . .	6
	P3: Alexander Ling, NUS Physics Dept / CQT: Operating quantum devices in space . . . . .	7
	P4: Joel Yang, SUTD: Nanostructure Designs For Plasmonic Color Printing . . . . .	8
<b>4</b>	<b>Poster Sessions</b>	<b>9</b>
	PO1: Rapid fire poster pitch student competition . . . . .	9
	IPS Best Poster Award . . . . .	9
	PO2: General poster presentation . . . . .	9
<b>5</b>	<b>Technical Sessions</b>	<b>50</b>
	T1: Solid State Physics 1 . . . . .	50
	T2: Solid State Physics 2 . . . . .	52
	T3: Soft Condensed Matter . . . . .	54
	T4: Optics and Photonics 1 . . . . .	57
	T5: Energy Conversion and Storage . . . . .	60
	T6: Quantum Information . . . . .	63
	T7: Topological Systems . . . . .	66
	T8: Optics and Photonics 2 . . . . .	69
	T9: Atomic, Molecular and Optical Physics 1 . . . . .	72
	T10: 2D Materials - Future Directions . . . . .	74
	T11: Solid State Physics 3 . . . . .	76
	T12: Solid State Physics 4 . . . . .	78
	T13: Atomic, Molecular and Optical Physics 2 . . . . .	79
	T14: Optics and Photonics 3 . . . . .	81
	T15: Density Functional Theory of 2D Materials . . . . .	84
<b>6</b>	<b>Committees</b>	<b>86</b>
	<b>Author List</b>	<b>87</b>

# 1 Location Map

Most events take place at level 2 around the center of the SUTD campus:



The big lecture theater LT2 for plenary sessions, posterpitch presentations and the SPhO event can be reached either via level 3 or via level 1.

You can find a browsable map with all levels at <http://sutdmap.appspot.com/>.

## 2 Schedule

### Monday, 7 March

8.30 AM	Registration		
9.00 AM	Opening Address (LT2)		
9.15 AM	Plenary talk 1 (LT2)		
10.00 AM	Plenary talk 2 (LT2)		
10.30 AM	Coffee/Tea Break + Exhibition + Poster mounting		
11.15 AM	Technical Sessions		
	T1 (TT16) Solid State Physics 1	T2 (TT17) Solid State Physics 2	T3 (TT18) Soft Condensed Matter
12.30 PM	Lunch + Poster mounting + Exhibition		
1.30 PM	Technical Sessions		
	T4 (TT16) Optics and Photonics 1	T5 (TT17) Energy Conservation and Storage 2	T6 (TT18) Quantum Information
3.00 PM	Coffee/Tea Break + Exhibition		
3.30 PM	Technical Sessions		
	SPHO (LT2) Physics Olympiad Awards + University presentations + Refreshments	T7 (TT16) Topological Systems	T8 (TT17) Optics and Photonics 2
			T9 (TT18) Atomic, Molecular and Optical Physics 1
5.00 PM	Coffee/Tea Break + Exhibition		
5.30 PM	Plenary talk 3 (LT2)		
6.30 PM	End of Monday sessions		

## Tuesday, 8 March

8.30 PM	Registration		
9.00 AM	Plenary talk 4 (LT2)		
10.00 AM	Technical Sessions		
	T10 (TT16) 2D Materials - Future Directions	T11 (TT17) Solid State Physics 3	T12 (TT18) Solid State Physics 4
10.45 AM	Coffee/Tea Break + Exhibition + Poster mounting		
11.15 AM	Technical Sessions		
	T13 (TT16) Atomic, Molecular and Optical Physics 2	T4 (TT17) Optics and Photonics 3	T15 (TT18) Density Functional Theory for 2D Materials
12.30 PM	Lunch + Posters + Exhibition		
1.30 PM	PO1: Rapid Fire poster Pitch session (LT2)		
2.30 PM	PO2: Poster + Exhibition		
4.00 PM	Coffee/Tea Break + Exhibition		
4.30 PM	PO2: Poster, continued + Exhibition		
6.00 PM	Poster awards + Pizza + Drinks		
7.30 PM	End of Tuesday sessions		

### **3 Plenary sessions**

We have four distinguished plenary speakers this year – with a nice overview of recent activities in physical sciences in Singapore. Some of the topics are not really our daily business, but we hope you can sit back and enjoy the wide scope of topics physicists are working on!

#### **P1: The Sound of Nature's Fury**

Asst. Prof. Benoit TAISNE, Asian School of the Environment, Earth Observatory Singapore

Monday, 7 March, 9:15am, Venue: LT2

#### **Abstract**

Infrasound are sounds below the human hearing threshold, the vibrations that you feel in your body in a movie theatre when Godzilla wrecks The City, or the aliens fire the Death Ray. Infrasound can travel in the atmosphere around Earth. For instance, the eruption of mount Kelut, Indonesia, was recorded in Alaska, USA, more than 11000 kilometers away. And a giant meteor that exploded over Russia produced deep sounds recorded in Antarctica, twice. What can we learn from them? How can we get early warning about Natural Hazards from infrasound? And finally, why should we care in Singapore? In this presentation you will be listening to the sounds produced by Natural Hazards all around the world and get a sense on how we can get precious minutes of early warning that could save thousands of lives and billions of dollars in economic losses.

#### **About the Speaker**

Benoit Taisne is a geophysicist by training, and started his academic career at the famous Ecole Normale Supérieure de Paris. In 2008, he received his PhD in geophysics with distinction at the Institut de Physique du Globe de Paris, CNRS, with work on magma dynamics in the terrestrial crust. He worked as a Seismologist and a Postdoctoral researcher at the Montserrat Volcano Observatory, IPGP until 2012, when he joined the Earth Observatory of Singapore, one of the research centres of excellence, as a Principal investigator. His current research focuses on the early anticipation of the style and size of volcanic eruptions. He uses new tomographic methods (muon telescopes) to shed light on two crucial parts of the volcanic system that have so far remained elusive for volcanologists and hazard managers, and which are key inputs for ash dispersal models. He complements results from muon tomography experiments by more traditional data and methods from different disciplines like geophysics (seismologic studies), geodesy (GPS studies), geochemistry (petrology and gas chemistry) and physics-based models of magma migration to get quantitative values for key physical parameters controlling the eruption style, and hence anticipate the style and size of eruptions to come.

## **P2: Effects of disorder and interactions in graphene**

Asst. Prof. Shaffique Adam, YaleNUS College and Centre for Advanced 2D Materials, National University of Singapore

Monday, 4 March, 10:00am, Venue: LT2

### **Abstract**

Almost ten years ago, a new electronic material appeared – notable not only for its ease of preparation and theoretical simplicity, but also by its promise for future electronic devices. Single monatomic sheets of carbon, known as graphene, are described as weakly interacting massless Dirac fermions and in many ways, are a textbook system to test physical models. In this talk, I will begin by briefly reviewing [1] the theory for graphene at the Dirac point where competing effects of disorder, electron-electron interactions, and quantum interference conspire together to give a surprisingly robust state whose properties can be described using a weakly-interacting semi-classical picture. Motivated by some very recent experiments, I will then report on our theoretical progress towards understanding how strong electron-electron interaction effects can be observed in strained graphene and in graphene on hexagonal boron nitride [2-3].

- [1] S. Das Sarma, S. Adam, E. H. Hwang, and E. Rossi, “Electronic transport in two dimensional graphene”, *Rev. Mod. Phys.* **83**, 407 (2011).
- [2] H. Tang, E. Laksono, J.N.B. Rodrigues, P. Sengupta, F.F. Assaad, and S. Adam, “Interaction driven metal-insulator transition in strained graphene”, *Phys. Rev. Lett.* **115**, 186602 (2015).
- [3] D. Y. H. Ho, I. Yudhistira, B. Y-K Hu and S. Adam, (in preparation), (2015).

This work is supported by the National Research Foundation Singapore under its Fellowship program (NRF-NRFF2012-01).

### **About the Speaker**

Dr. Adam was born in Nairobi, Kenya. After completing his A-levels in Kenya, he went to Stanford University where he received his BS, majoring in Physics with a minor in Mathematics. He graduated with departmental honors and a University distinction. After spending four months as an exchange student at Magdalen College in Oxford University, Dr. Adam went on to pursue his doctorate in Theoretical Physics at Cornell University, where he worked on the magnetic properties of nanoscale conductors. He then moved to the Condensed Matter Theory Center at the University of Maryland where he worked on the electronic transport properties of graphene. Before joining Yale-NUS College, Dr. Adam spent three years as a National Research Council Fellow in the Center for Nanoscale Science and Technology at the US National Institute of Standards and Technology.

### **P3: Operating quantum devices in space**

Asst. Prof. Alexander LING, Centre for Quantum Technologies and Department of Physics, National University of Singapore

Monday, 7 March, 5:30pm, Venue: LT2

#### **Abstract**

The Centre for Quantum Technologies is planning a series of fundamental science experiments in LEO using very small spacecraft. These tests will investigate the in-orbit generation of light particles (photons) that are in a special quantum state called entanglement. Space-based entangled photon systems will enable fundamental tests probing the overlap of quantum physics and gravity. Developing good control over the generation of entangled photons also has practical uses as they can be used to perform quantum communication, and currently the most mature technological pathway to a global quantum network is to use satellite-based quantum systems. Prof Ling will discuss the highs and lows of the CQT program, the future missions, and also efforts to make every smaller sources of entangled photons.

#### **About the Speaker**

Alexander Ling first came to Singapore in 1996 to study physics at the National University of Singapore under the Goh Keng Swee Scholarship program. After graduating, he worked on education technology by day while racing bicycles by night. He returned to academia in 2004 as a graduate student, working on various projects that later became incorporated into the Centre for Quantum Technologies. After receiving his PhD in 2008, he worked as a postdoctoral fellow on quantum photonics at the National Institute of Standards and Technology in the USA. He returned to CQT in mid-2010 to lead a team that is developing rugged quantum devices that can operate reliably outside the lab.

## **P4: Nanostructure Designs For Plasmonic Color Printing**

Assistant Prof. Joel K.W. Yang, Engineering Product Development pillar at the Singapore University of Technology and Design Tuesday, 8 March, 09:00am, Venue: LT2

### **Abstract**

A new approach for generating a whole range of colors using only a limited number of components is actively being investigated. Unlike pigments or inks, plasmonic colors arise from precise geometric control of metallic nanostructures. Plasmonic colors printing promises ultra-high resolution with sub-wavelength pixel dimensions, and degradation-resistant colors. They are also suitable for large-area manufacturing processes. In this talk we will discuss the various approaches to fabricate and study plasmonic colors of different designs, and some of their interesting optical properties.

### **About the Speaker**

Dr. Joel Yang received his Master of Science (2005) and PhD (2009) from the Massachusetts Institute of Technology in Electrical Engineering and Computer Science. He holds a joint appointment as Senior Scientist I at the Institute of Materials Research and Engineering (IMRE) of A\*STAR, where he co-heads the Plasmonic and Semiconductor Nanostructures Lab.

Highlights of his work includes the printing of color at the ultimate resolution limit (100,000 dpi) using plasmonic resonators, and for study of the “salty-developer” to improve the resolution of hydrogen silsesquioxane electron-beam resist. His scientific contribution is recognized through several local and international awards, including the MIT Technology Review TR35@Singapore award, and the 2012 Singapore Young Scientist Award.

He teaches several courses at SUTD including Circuits and Electronics, Engineering in the Physical World, and Electromagnetism.

## **4 Poster Sessions**

### **PO1: Rapid fire poster pitch student competition**

As in the last two years, we have a full session (Tuesday after lunch) with no parallel technical sessions where all IPS participants get your audience for a supershort (3 minutes) presentation on a poster if the authors want to participate. In order to encourage authors to participate, we will choose the Best Poster Award this year from those submissions where there was short presentation in this session.

For this, we just project your poster on the screen in the lecture hall (please provide us with a PDF file for that purpose). You can email this to us via [postersipsmeeting.org](mailto:postersipsmeeting.org), or leave it with the reception desk.

### **IPS Best Poster Award**

During the conference the program committee will select the three best poster presentations for the IPS Best Poster Award. The award will be handed over to the winners at the Poster & Pizza session at the end of PO2 on Tuesday evening, probably around 6pm-7pm at (Venue: TBD).

### **PO2: General poster presentation**

#### **Timing**

Posters are presented during the whole conference; perhaps you can make sure that the posters are up as soon as you can. We encourage everyone to browse around during coffee breaks and lunchtime (catered lunch is nearby). We would recommend that the best time for the poster presenters to be around at the poster is the Thursday evening session that comes together with some food and drinks as well. Please take down the posters by latest at the end of the conference, i.e., on Tuesday evening.

#### **Location**

The poster area will be in the foyer. Each poster is assigned a panel which corresponds to the easychair number. We will provide Velcro strips to mount the posters on the wall, please see the reception desk for this.

#### **Format**

The poster walls fit a A1 sized poster (portrait orientation).

## Abstracts

Below, we show a list of abstracts submitted by the authors. You can locate the poster of your interest via the easychair number from the poster submission, they are sorted and labelled by these numbers.

### **PO.9 Pushing single photon counting technology towards better Size, Weight and Power (SWAP) performance.**

Rakhitha Chandrasekara\*, Kadir Durak, Cliff Cheng, Alexander Ling\* (Centre for Quantum Technologies)

Single photon counting is widely used in low-light sensing and communications experiments. However, the development of detector technology often does not keep pace with the development of new optical sources or protocols, restricting the deployment of quantum communication infrastructure. Our team is working on a number of quantum experiments where the Size, Weight and Power (SWAP) requirements are too challenging for commercial-off-the-shelf detector modules and necessitate the development of fast, compact and efficient detector circuits.

In this poster, we present a novel in-situ measurement method that extracts the pulse height from silicon Geiger-mode avalanche photodiodes (GM-APDs) while it is performing photon counting. This technique will enable fine control of the GM-APD when it is actively quenched, and enable a compact and efficient detector circuit that is capable of detecting millions of photon events per second. We also consider the interplay of photon statistics (from a single photon source) and detector circuit response in order to develop a model that predicts the performance of a quantum communication system based on entangled photons from Spontaneous Parametric Downconversion sources.

### **PO.11 Photonic Floquet topological insulators with single Dirac cones and anomalous edge states**

Daniel Leykam\*, Mikael Rechtsman, Yidong Chong (Nanyang Technological University)

We introduce a class of photonic Floquet topological insulators created by staggered helical waveguide arrays. In these lattices, the topological phase can be tuned by changing the inter-waveguide coupling strength, significantly reducing radiative losses compared to previous designs. At topological phase transitions, the Floquet bandstructure hosts a single Dirac cone, revealing novel chiral propagation effects such as a discrete analogue of conical diffraction and suppression of Anderson localization by weak antilocalization. As well as trivial and Chern insulator phases, an "anomalous" Floquet phase with vanishing Chern number and unidirectional edge states is also accessible. We also present an efficient numerical method for computing the Floquet bandstructure and radiative losses of these systems.

### **PO.12 Quantum random numbers from vacuum fluctuations**

Yicheng Shi\*, Brenda Chng, Kurtsiefer Christian (center for quantum technologies)

We implement a quantum random number generator based on a balanced homodyne measurement of vacuum fluctuations of the electromagnetic field. The digitized signal is directly processed with a fast randomness extraction scheme based on a linear feedback shift register. The

random bit stream is continuously read in a computer at a rate of about 480 Mbit/s and passes an extended test suite for random numbers.

**PO.13 Complete achromatic optical switching between two waveguides with a sign flip of the phase mismatch**

Wei Huang\*, Andon Rangelov\*, Elica Kyoseva\* (Singapore University of Technology and Design)

We present a two-waveguide coupler which realizes complete achromatic all-optical switching. The coupling of the waveguides has a hyperbolic-secant shape, while the phase mismatch has a sign flip at the maximum of the coupling. We derive an analytic solution for the electric field propagation using coupled-mode theory and show that the light switching is robust against small to moderate variations in the coupling strength and phase mismatch. Thus, we realize an achromatic light switching between the two waveguides. We further consider the extended case of three coupled waveguides in an array and pay special attention to the case of equal bidirectional achromatic light beam splitting.

**PO.14 Broadband and ultra-broadband modular half-wave plates**

Emiliya Dimova, Wei Huang, George Popkirov, Andon Rangelov\*, Elica Kyoseva\* (Singapore University of Technology and Design)

We experimentally demonstrate broadband and ultra-broadband spectral bandwidth modular half-wave plates. Both modular devices comprise an array of rotated single half-wave plates (HWPs), whereby for broadband and ultra-broadband performance we use standard and commercial achromatic HWPs, respectively. The bandwidth of the modular HWPs depends on the number  $N$  of individual HWPs used and in this paper we experimentally investigate this for  $N=3,5,7,9$ . The elements in the arrays are rotated at specific angles with respect to their fast-polarization axes, independent of the nature of the birefringent material. We find the rotation angles using an analogy to the technique of composite pulses, which is widely used for control in nuclear magnetic resonance.

**PO.15 A SU(3) Topological Insulator in the 2D Honeycomb Lattice**

Ulrike Bornheimer\*, Christian Miniatura, Benoît Grémaud (CQT, MajuLab, NUS)

We investigate a particular realization of a topological insulator with spin-1 bosons propagating in a 2D honeycomb optical lattice and subjected to a SU(3) spin-orbit coupling. This physical situation is equivalently obtained from a gauge transformation of the Harper model and can be realized experimentally. We focus on the analysis of the single-particle spectrum and the edge states obtained when open boundary conditions are imposed in one direction. Indeed, their very existence reflects the topology of the bulk system through the bulk-edge correspondence. We also examine the localization properties of these edge states, stability and dependence on symmetries of the Hamiltonian.

**PO.16 3D Porous Hierarchical Nickel-Molybdenum Nitrides Synthesized by RF Plasma as Highly Active and Stable Hydrogen Evolution Reaction Electrocatalysts**

Yongqi Zhang, Hong Jin Fan\* (Nanyang Technological University)

Development of a robust and efficient noble metal-free catalyst for hydrogen evolution reaction (HER) is highly desirable for the carbon dioxide-free hydrogen production. Transition metal nitrides are widely used as catalysts for electro-water splitting. Here we report a fast and environmental friendly N<sub>2</sub> plasma activation method to fabricate nickel molybdenum bimetallic nitride (NiMoN) on carbon cloth with a 3D porous dendritic nanostructure. The as-prepared catalyst demonstrates outstanding HER performance rendered by the porous surface, enhanced mass and charge transport properties. The nanostructured bimetallic nitrides exhibits an excellent catalytic activity for HER, namely, 10 mA cm<sup>-2</sup> at an overpotential of around 109 mV, and an exchange current density of 0.92 mA cm<sup>-2</sup>, and good stability in an alkaline electrolyte.

### **PO.17 Coherent multiple scattering across the Anderson transition**

Sanjib Ghosh\* (CQT)

The transition from a metallic extended phase to the insulating localized phase of a disordered system is known as the Anderson transition. We show that the coherent back scattering (CBS) peak in the momentum space is capable of giving a full description for the Anderson transition. We develop a finite time scaling theory for the width of the CBS peak and extract the various critical parameters for the transition.

### **PO.20 Quantum assisted Gaussian process regression**

Zhikuan Zhao\*, Jack Fitzsimons, Joseph Fitzsimons (Singapore University Of Technology And Design)

Gaussian processes (GP) are powerful models for regression problems in supervised machine learning, and have been widely applied across a broad spectrum of applications, ranging from robotics, data mining, geophysics and climate modelling all the way to predicting price behaviour of commodities in financial markets. Implementation of GP regression is often limited by the typically required  $O(n^3)$  logic gates. We show that the quantum linear systems algorithm [Harrow et al., Phys. Rev. Lett. 103, 150502 (2009)] can be applied to Gaussian process regression (GPR), leading to an exponential reduction in computation time in some instances. We show that even in some cases not ideally suited to the quantum linear systems algorithm, a polynomial increase in efficiency still occurs.

### **PO.24 Tin based Oxides and Sulfides as Anodes for Lithium-ion Batteries**

Bruce Wen, M. V. Venkatesh Reddy\* (National University of Singapore)

The principal objective of this project is to investigate the electrochemical performance of tin based oxides and sulfides as prospective anode material for Lithium-ion Batteries. Nano-sized tin oxide (SnO<sub>2</sub>), tin sulfide (SnS), and tin disulfide (SnS<sub>2</sub>) have been evaluated at low synthesis temperatures ranging from 150°C to 240°C. The prepared powders are characterized by X-ray diffraction, Brunauer-Emmett-Teller surface area analysis, and scanning electron microscopy. The electrochemical properties are analysed by galvanostatic cycling and cyclic voltammetry studies, under two different voltage ranges, 0.005V-1.0V and 0.005V-3.0V. Hexadecyltrimethylammoniumbromide (CTAB), is added to tin oxide material to investigate its effects on cycling performance. Galvanostatic cycling studies, at a current rate of 100mA g<sup>-1</sup>, showed that nano-sized SnO<sub>2</sub> prepared at low temperature of 180°C using the molten salt method (MSM) displays reversible capacities of 478mAh g<sup>-1</sup>, with a capacity of retention of 71.7% over 50 cycles in

the voltage range 0.005V-1.0V, and 1056mAh g<sup>-1</sup>, with a capacity retention of 44.9% over 50 cycles, in the voltage range 0.005-3.0V. SnS prepared at the optimal temperature of 180°C using the solvothermal method showed a superior reversible capacity of 1131mAh g<sup>-1</sup> in the voltage range of 0.005V-3.0V, with good capacity retention of 85% over 30 cycles, at a current rate of 60mA g<sup>-1</sup>. Cyclic voltammetry studies corroborate typical electrochemical reactions. The current observations suggest that tin based anodes prepared under optimal synthesis methods and cycled in the optimal voltage range can have good electrochemical performance in terms of both capacity and capacity retention.

### **PO.26 Morphology Controlled Synthesis of NiCo2O4 nano structures and their applications for Li-ion batteries**

Tian Yi Lim\*, M. V. Reddy\* (Advanced Batteries Lab, National University of Singapore)

To study the effects of different synthesis methods of NiCo2O4 compounds, molten salt, sol-gel and urea combustion methods were employed. Their morphology and electrochemical properties were studied. Two combinations of salts for the molten salt method were used, Ni-chloride–Co-hydroxide, and Ni-acetate–Co-acetate, prepared at 650°C. The obtained powders were characterized using X-ray diffraction, BET surface area, SEM, cyclic voltammetry, and galvanostatic cycling techniques. Differing morphologies for each of the preparation methods were noted, with the urea combustion method giving the smallest particle sizes with largest porosity. For electrochemical performance, initial capacity ranged from 1800 mAh g<sup>-1</sup> for urea combustion to 800 mAh g<sup>-1</sup> for Ni-acetate – Co-acetate prepared by molten salt methods. The sol-gel and urea combustion methods provide best performance with smallest capacity fading. We report the process of synthesis and their performance for the three synthesis methods.

### **PO.27 First-principles Study of Asymmetric Monolayer of Transition Metal Dichalcogenides and Related Nanostructures**

Yong Sheng Soh\*, Yuan Ping Feng (National University of Singapore)

Two-dimensional (2D) transition metal dichalcogenides (TMDs), MX<sub>2</sub> (M=Mo, W, etc, X=S, Se, Te, etc), have attracted much attention in recent years. A large number of 2D-TMDs have been theoretically predicted and many of them have been synthesized. Typical 2D-TMD structures consist of a symmetric tri-atomic-layer structure, with a hexagonal atomic layer of metal atoms sandwiched between two atomic layers of the same type of chalcogens. However, there is no reason to believe that asymmetric 2D-TMDs, made of a metal atomic layer between two atomic layers of different chalcogens, cannot exist. If stable and can be grown, the asymmetric structure may have unexpected properties and open new applications.

We propose to investigate asymmetric 2D-TMD structures such as S/Mo/Se, Se/Mo/Te, S/Mo/Te from first-principles using density functional theory (DFT). The structures will be optimised and their stability will be analysed first. For stable structures identified from the stability analysis, we will carry out first-principles calculations to study their physical properties and explore their potential applications.

Compared to symmetric 2D structures, the asymmetric 2D structures break the inversion symmetry which we expect to lead to properties different from those of symmetric structures. For example, the two surfaces of S/Mo/Te, terminated by S and Te respectively, are expected to behave differently which may lead to segregated adsorption of atoms and molecules. The asym-

metric structure may also result in asymmetric charge distribution, an internal electric field, and a net dipole moment in the surface normal direction which can be explored for nanoelectronic and photonic applications. Layers of S/Mo/Te stacked up vertically will be bound together by dipole-dipole interaction, instead of the weak van der Waals interaction. Interesting results can be expected if such materials are put together to form 2D superlattices.

In asymmetric TMD structures such as S/Mo/Te, due to the smaller lattice constant of MoS<sub>2</sub> compared to MoTe<sub>2</sub>, there could be a small tensile strain in the Mo-S bonds and a small compressive strain in the Mo-Te bonds. This small internal strain may result in natural curling of the S/Mo/Te monolayer and formation of nanotubes or spherical shell structures. We will study the stability of such structures and their physical properties.

### **PO.29 Strong Influence of Coupling for Polarization Control of Light in Metasurfaces**

Longqing Cong\*, Yogesh Srivastava, Ranjan Singh (Nanyang Technological University)

The inductive coupling between the SRR meta-atoms in a double SRR meta-molecular system has been thoroughly investigated that depends on the geometrical distance. This is intuitive according to Faraday's law from the aspect of magnetic flux. Here, we investigated two non-intuitive aspects of inductive coupling phenomenon (defined as intra coupling): the inter unit cell coupling effect on the intra coupling spectra and the orientation dependent intra coupling switch. In the first part, we investigate the spectral features of co- and cross-polarized by engineering the periodicity of the unit cells that changes the inter unit cell coupling strength. The inter unit cell coupling is demonstrated to play key roles in determining the spectral amplitude and bandwidth. In the second part, we investigate the effect of SRR orientation in the meta-molecular unit cell. In the orthogonally arranged double SRR system, the opposite orientations of one SRR could switch the intra coupling channel between on and off states. The intra coupling induces the cross-polarized light and thus the far field polarization states can be engineered by engineering the inter coupling strength or the SRR orientations. The proposed SRR configuration could be applied as polarizer or quarter wave plate.

### **PO.31 Microlandscaping of Nanoparticles on 2D Transition Metal Dichalcogenides Films for Enhanced Functionality**

Belle Sow Miaoer\*, Jun Peng Lu, Chorng Haur Sow (NUS High School)

Recent research has shown that monolayer transition metal dichalcogenides (TMDs) have interesting photoluminescence properties which differ from their bulk layer counterparts, with the presence of fluorescence concentric patterns. WS<sub>2</sub> is an interesting 2D TMDs with rich phenomena that is sensitively dependent on any structural and chemical heterogeneity in the monolayer. The sample is structurally rich with S atoms covering the monolayer and playing critical role in dictating the physical properties of the monolayer. Gold nanoparticles (Au NPs) have been demonstrated to show strong affinity towards S in nanomaterials. Thus from fundamental science viewpoint, it is interesting to investigate how Au NPs would decorate onto the surface of the WS<sub>2</sub>. In this work, Au NPs was deposited on 2D WS<sub>2</sub> to explore the effects of Au NPs deposition on the photoluminescence intensity of WS<sub>2</sub> TMDs, and the possible chemical or physical changes to the system after successful decoration of gold nanoparticles. Results have shown that the photoluminescence intensity and wavelength vary along different regions on the monoflake,

and Au NPs selectively deposit on various regions within the monoflake, namely at the edge, at steps and fluorescence boundaries. We observed photoluminescence enhancement in selected regions within the  $WS_2$  monolayer. The density of Au NPs also affects the photoluminescence enhancement after the deposition. Hence, Au NPs act as nanoexplorers which probe the chemical and structural heterogeneity of the system, allowing us to understand the properties of the system better.

### **PO.32 Microencryption on Atomic Monolayers Enabled by Direct Laser Writing**

Hou Chua\*, Pinxi Tan\*, Ashwin Venkatakishnan\* (NUS High School of Math and Science)

Tungsten disulfide ( $WS_2$ ), a 2D transition metal dichalcogenide, exhibits different chemical and physical properties in both its monolayer and bulk layer crystal forms. As  $WS_2$  monolayer flakes exhibit direct band gaps, they fluoresce when excited by light. They show strong edge fluorescence, as well as weak non-edge fluorescence that comes in a variety of distinct patterns and intensity. In contrast, such fluorescence is not present in bulk layer flakes. This project investigates the utilization of a focused laser beam to exfoliate  $WS_2$  bulk layer flakes into thinner monolayers that also show strong fluorescence comparable to that of monolayer flakes. In addition, we examine how a laser beam can also modify monolayer flakes to increase its natural non-edge fluorescence intensity. Interestingly, when flakes are modified under deprivation of oxygen, such changes are no longer observable, implying that oxygen is responsible for the modification of fluorescence as well as the exfoliation of bulk layer flakes. A redshift in photoluminescence peak wavelength and changes in the surface height and phase of modified monolayer flakes also support the theory that oxidation is responsible for laser modification. This opens up opportunities for the exfoliation and encryption applications of laser modification on bulk layer and monolayer flakes respectively.

### **PO.37 Theory of Quantum Cavity and Diode**

Alexandre Roulet\*, Jibo Dai, Pierre-Olivier Guimond, Huy Nguyen Le, Valerio Scarani (Centre for Quantum Technologies, National University of Singapore)

Optical emitters strongly coupled to photons propagating in one-dimensional waveguides are a promising platform for optical quantum information processing.

In [1], we investigate the Rabi oscillation of an atom placed inside a quantum cavity where each mirror is formed by a chain of atoms trapped near a one-dimensional waveguide. We show that in the Markovian regime the lifetime of the photon inside the cavity is not enhanced by the presence of the mirrors, and therefore sustained Rabi oscillation analogous to that observed in conventional CQED setups cannot be obtained. Thus, the delay must be taken into account and the dynamics of the problem is inherently non-Markovian. Parameters of interest such as the Rabi frequency and the cavity loss rate due to photon leakage through the mirrors are obtained.

In [2], we present a full quantum mechanical analysis of a proposed diode based on a pair of atoms with different detunings [3]. We show that, in this device, rectification is a purely multi-photon effect. Therefore, it cannot achieve rectification for single-photon states, contrary to the hope stated in the initial proposal. On the other hand, when the incident light is a coherent pulse, the efficiency of the diode can reach up to 70% in an optimal range of input power. We also study the dynamics and explain the results obtained by tracking the atomic excitation, yielding a

clear physical picture for the origin of the rectification. This detailed understanding may inspire improved designs of passive and state-independent optical diodes.

These works belong to a series of studies where devices that are usually considered classical are replaced by quantum objects allegedly performing the same functionality. A better understanding of the physics of these quantum devices opens the door for exciting applications such as delayed-choice experiments or superposition of gates in quantum circuits.

[1] Phys. Rev. A 93, 023808 (2016) [2] Phys. Rev. A 92, 063848 (2015) [3] Phys. Rev. Lett. 113, 243601 (2014)

### **PO.39 Optical Intensity Interferometry through Atmospheric Turbulence**

Peng Kian Tan\*, Aik Hui Chan, Christian Kurtsiefer (Centre for Quantum Technologies)

Conventional ground-based astronomical observations suffer from image distortion due to atmospheric turbulence. This can be minimised by choosing suitable geographic locations or adaptive optical techniques, and avoided altogether by using orbital platforms outside the atmosphere. One of the promises of optical intensity interferometry is its independence from atmospherically induced phase fluctuations. By performing narrowband spectral filtering on sunlight and conducting temporal intensity interferometry using actively quenched avalanche photon detectors (APDs), the Solar  $g^{(2)}(\tau)$  signature was directly measured. We observe an averaged photon bunching signal of  $g^{(2)}(\tau) = 1.693 \pm 0.003$  from the Sun, consistently throughout the day despite fluctuating weather conditions, cloud cover and elevation angle. This demonstrates the robustness of the intensity interferometry technique against atmospheric turbulence and opto-mechanical instabilities, and the feasibility to implement measurement schemes with both large baselines and long integration times.

### **PO.43 Identification of DNA Nucleobases by Excitonic Shift in Monolayer WS<sub>2</sub>: Towards Label-Free Optical Biosensing**

Shun Feng, Yu Chen, Namphung Peimyoo, Jingzhi Shang, Chunxiao Cong, Chenji Zou, Bingchen Cao, Ting Yu\* (Nanyang technological University)

Two-dimensional transition metal dichalcogenides (2D TMDs) have attracted increasing attention due to the underlying fundamental physics like strong excitonic behaviour which leads to the tunable light emission that varies with external condition like electric field, strain and chemical doping. This unique property may give birth to future sensing applications. Monolayer WS<sub>2</sub> has stood out as a promising platform for such applications with its unique electronic properties and relatively higher intrinsic emission quantum yield than the one of MoS<sub>2</sub>, another popular family member of 2D TMDs. Though much progress has been made, the direct applications utilizing their excitonic properties in bio-related fundamental research are still rare. In this work, we successfully synthesis monolayer WS<sub>2</sub> flake with strong and uniform light emission using chemical vapor deposition (CVD) technique. Photoluminescence (PL) characterization is performed as a powerful tool to probe the emission states as well as the electronic and optical physics behind them, as four kinds of nucleobases are applied as P/N type dopants to tune the physical state via charge transfer process. The nucleobase- WS<sub>2</sub> interaction is further illustrated by electrical transport and the concentration based spectroscopic measurements, unambiguously confirming the origin of the excitonic evolution in WS<sub>2</sub> (i. e. charge transfer) and paving a pathway for future applications with tunable optical response. Our results show a

series of dopant-selective behaviour which is useful for distinguishing different nucleobases and indicates a potential sensing strategy to overcome the DNA sequencing difficulty.

#### **PO.44 Device-independent parallel self-testing of two singlets**

Xingyao Wu\*, Jean-Daniel Bancal\*, Matthew McKague\*, Valerio Scarani\* (Centre for Quantum Technologies)

Device-independent self-testing is the possibility of certifying the quantum state and the measurements, up to local isometries, using only the statistics observed by querying uncharacterized local devices. In this paper, we study parallel self-testing of two maximally entangled pairs of qubits: in particular, the local tensor product structure is not assumed but derived. We prove two criteria that achieve the desired result: a double use of the Clauser-Horne-Shimony-Holt inequality and the  $3 \times 3$  Magic Square game. This demonstrates that the magic square game can only be perfectly won by measuring a two-singlets state. The tolerance to noise is well within reach of state-of-the-art experiments.

#### **PO.46 SpooQySats: producing entangled photons in nanosatellites to enable future Quantum physics experiments and long-range Quantum Key Distribution.**

Robert Bedington\*, Cliff Cheng, Yue Chuan Tan, Edward Truong Cao, Xueliang Bai, Alexander Ling\* (Centre for Quantum Technologies, NUS)

SpooQySats are 10x10x30cm nanosatellites that will be assembled and operated from the Centre For Quantum Technologies (CQT) to test and validate our upcoming SPEQS (Small Photon Entangling Quantum System) entangled photon sources, in preparation for future space-to-ground QKD (Quantum Key Distribution) demonstration missions.

QKD, secure communications enabled by Quantum Mechanics, is currently performed on the ground using fibre optics or point-to-point free-space links. These implementations are subject to restrictive coverage and range limitations however arising from factors such as the curvature of the Earth, losses to the atmosphere/optical fibres and the challenges of keeping a ground-based node secure.

QKD links between satellites and ground stations however need only pass through a few 10s of kilometres of atmosphere, can achieve global coverage, and are well suited to be secure nodes due to their relative inaccessibility. By using entanglement-based QKD (such as E91), the quantum nature of the link can be verified by means of a Bell's inequality test.

To this end CQT is developing the SPEQS miniaturised, ruggedised entangled photon sources designed for use on board satellites. By locating the photon source on the satellite (and the detectors on the ground) losses due to atmospheric turbulence can be minimised and potential future space-based experiments with entangled photons enabled.

To further develop such prototypes into space missions would traditionally require collaborations with space agencies and satellite engineering companies and institutes. These would then require lengthy and costly design processes whereby the experiment design is rigorously de-risked through the use of extensively verified space-compatible parts (costly components that have previously been used in space and that can be proved to be resistant to radiation, vacuum and temperature cycling for many years) before a full-scale, large-budget demonstration mission

is launched. As a small country with no space agency Singapore is not well suited to produce such a space mission.

Through a high degree of standardisation and some batch production however, CubeSats have enabled cheaper, off-the-shelf nanosatellite components and turnkey solutions greatly simplifying the process of building a satellite and greatly reducing the cost. Being nanosatellites, CubeSats are very small and lightweight making them very much cheaper to launch. Since costs are so greatly minimised, higher failure risks become acceptable, less extensive testing is required, and cheaper off-the-shelf components are often used. Since CubeSats are so small they are launched as piggy-back payloads alongside traditional large satellites, and are also deployed from the International Space Station (ISS). The launch interface is standardised and adapted to most of world's satellite-launching rockets greatly reducing the planning and negotiation time before launches and thus enabling rapid incremental development cycles of satellites.

Accordingly the CQT SpooQySats are allowing for the streamlined incremental development of our SPEQS miniaturised entangled photon sources into devices that will be capable of enabling space-to-ground QKD.

Early SPEQS devices have already been integrated and demonstrated on third-party CubeSats, but the CQT-developed SpooQySats will allow the whole spacecraft to be more closely designed around the requirements of the upcoming, more advanced, SPEQS payloads. As these are the first satellites to be built at CQT the objectives are modest, no photons will be beamed outside of the satellite and the SPEQS sources will simply produce and analyse entangled photons in-situ to verify that the device can survive the launch and the space environment conditions.

Establishing optical links between spacecraft and ground stations is non-trivial but is possible with CubeSats and is being actively researched by a number of research groups around the World. By collaborating with such groups we are hopeful that space to ground QKD links can be demonstrated with nanosatellites and possibly act as an early stepping stone towards space-based global QKD networks.

### **PO.50 Towards atom interferometry with guided matter wave in optical fiber**

Wui Seng Leong Wui Seng\*, Mingjie Xin, Roy Arpan, Wei Sheng Chan (Nanyang Technological University)

Precision measurement with light-pulse grating atom interferometry in free space have been used in the study of fundamental physics and applications in inertial sensing. However, the sensitivity of measurement is mainly limited by the inhomogeneity of beam wavefront after several optical components. Recent development of photonic bandgap fibers allows light for travelling in a hollow region while preserving its fundamental Gaussian mode. Optically guided matter waves inside a hollow-core photonic bandgap fiber solves the limitation of beam inhomogeneity and provides the potential in research field of atomic sensing and precision measurement to the next level of compactness and accuracy. Here, we will show our experimental progress towards an atom interferometer inside an optical fiber.

### **PO.51 Towards Hybrid Quantum Systems of Atoms and Superconductors**

Christoph Hufnagel\*, Chin Chean Lim\*, Alessandro Landra\*, Chee Howe Ew\*, Deshui Yu\*, Yisheng Lei\*, Rainer Dumke\* (Centre for Quantum Technologies and Nanyang Technological University)

Hybridisation of atomic systems with solid state systems could offer a viable mean to achieve better quantum state manipulation and to study interesting physical phenomena. In our experimental direction, we work towards the coupling between ultracold atoms and superconductors under applied microwave field. This will be done by trapping ultracold Rb atoms in proximity of a superconducting cavity cooled to  $<100\text{mK}$  with a dilution refrigerator, and applying a microwave field to induce coupling with the atoms. We predict coherent coupling between trapped  $^{87}\text{Rb}$  atoms and the resonator, and would attempt to manipulate atomic states through the superconducting resonator.

### **PO.53 An Array of Quantum Wires in a Planar Microcavity**

Kristin Bjorg Arnardottir\*, Ivan Iorsh, Alexander Alodjants, Ivan Shelykh (Nanyang Technological University)

We consider theoretically a system of excitons in a periodic array of wires embedded in a planar microcavity. The excitons can couple strongly to the cavity photon mode and the periodicity of the wires leads to the emergence of quasi-momentum along the axis perpendicular to the wires, which leads to a two dimensional exciton-polariton which have Brillouin zones along one direction. This anisotropy leads to a hyperbolic region in the lower-polariton dispersion branch, where the effective masses along two perpendicular directions have opposite signs. This property leads to interesting effects. We have found that our system supports dark soliton solutions as well as non-trivial propagation of incident pump pulses.

### **PO.56 A random number generator based on avalanche photodiode dark counts**

James Grieve\*, Rakhitha Chandrasekara, Sara Engardt, Jatadhari Mishra, Alexander Ling (Centre for Quantum Technologies)

The generation of physical random number generators is an area of active research, with extant applications in the areas of computing, gaming and cryptography. Recent years have seen an explosion in the demand for high quality unpredictable, well distributed random numbers and the search for and development of well characterized physical systems that can provide them.

We propose the use of two avalanche photodiodes operated independently in reverse bias (“Geiger mode”, or GM-APDs) as a physical source of entropy. By observing the well characterised thermal “dark counts” of this system and assigning the detectors the labels “1” and “0”, high quality random bits can be produced with minimal post-processing. By controlling the temperature and bias voltage of the GM-APD modules, a physical unbiasing technique may be realised.

We also present a method for the engineering of the dark count rate of individual detectors, based on the deliberate irradiation of the active areas with proton beams. We describe a compact physical implementation of this scheme, based on discrete GM-APD modules integrated with a system-on-chip module. This system should prove an attractive alternative to more complicated schemes based on single photon detection, and may be readily scaled down to permit integration into embedded processor architectures, paving the way for widespread adoption.

### **PO.57 Highly confining direct written waveguides for integrated quantum photonics**

James Grieve\*, Bo Xue Tan, Alexander Ling (Centre for Quantum Technologies)

Compact waveguide chips fabricated by femtosecond direct write in glass have become a powerful and mature tool for the realisation of large scale quantum photonics experiments, with a number of implementations discussed extensively in the literature. To date, most work in this area has utilized a femtosecond oscillator with an external amplifier, with the resulting few-kilohertz pulse train providing the high pulse energies needed to achieve permanent modification of the substrate material. These pulses are brought to a focus with relatively low numerical aperture optics, and the resulting waveguides exhibit a pronounced asymmetric cross-section due to the point spread function of the lens. This may be problematic in quantum optics experiments which make use of the polarization of photons to encode quantum information, as shape-induced birefringence may cause degradation of the guided photon state.

We have developed a femtosecond laser direct write waveguide platform that employs a minimally modified commercial oscillator without amplification and a high numerical aperture objective to fabricate waveguides in the flint glass SF11. With high repetition rates and pulse energies only slightly above the threshold for modification, multiple pulses contribute to the waveguide morphology which is no longer dominated by the point spread function. The resulting waveguides exhibit markedly reduced aspect ratio when compared to those produced by amplified systems, and also feature a small mode cross-section (around 1.6 $\mu$ m FWHM), which we attribute to an unusually high peak modification of the refractive index. This increased mode confinement may enable reduced bending radius, and allow for a further reduction in the scale of large photonic circuits.

In this contribution, we will discuss the fabrication process, as well as present data on the performance of bus waveguides and optical components such as directional couplers. It is our belief that this novel fabrication scheme will provide an attractive alternative to conventional, high pulse energy systems. The reduced cost associated with our oscillator-only approach will also help to lower the barriers to participation in this promising area of research.

### **PO.58 A velocimeter by enhanced light-dragging effect in electromagnetically induced transparency**

Chang Huang\*, Pei Chen Kuan, Shau-Yu Lan (Nanyang Technological University)

I will present a new velocimeter based on the light-dragging effect. The new instrument enjoyed the enhancement by cold atoms with electromagnetically induced transparency (EIT), which improved the effect by orders of magnitude. Our measurement demonstrates the probability of setting up a motional sensor beyond the limitation of Doppler broadening in the future.

### **PO.60 Asymmetric magnetic and magnetotransport in Co-rich and Mn-rich mixed valent oxides**

Amit Chanda, D V Maheswar Repaka, Raju V. Ramanujan, Ramanathan Mahendiran\* (National University of Singapore)

Mn-based perovskite oxides ("manganites") show a dramatic decrease of resistance in response to external magnetic fields, known as Colossal Magnetoresistance (CMR), which could

be exploited for spintronic applications. Manganites such as  $\text{Pr}_{1-x}\text{Sr}_x\text{MnO}_3$  are half metallic ferromagnets, whereas, Co-based oxides (e.g.,  $\text{Pr}_{1-x}\text{Sr}_x\text{CoO}_3$ ) are band ferromagnets similar to elemental ferromagnet such as Fe or Ni. Here, we would like to present the effect of Co (Mn) substitution in the  $\text{Pr}_{0.6}\text{Sr}_{0.4}\text{MnO}_3$  ( $\text{Pr}_{1-x}\text{Sr}_x\text{CoO}_3$ ) sublattice on magnetic, dc magnetotransport properties. For the present study, the doping level has been limited upto  $x=0.3$  for both the ends. We show that ferromagnetism in  $\text{Pr}_{0.6}\text{Sr}_{0.4}\text{MnO}_3$  that arises due to the double exchange (DE) coupling between  $\text{Mn}^{3+}$  and  $\text{Mn}^{4+}$  ions is radically annihilated with Co substitution. While ferromagnetism is also destabilized with Mn substitution in  $\text{Pr}_{0.6}\text{Sr}_{0.4}\text{Mn}_{1-x}\text{Co}_x\text{O}_3$ , the Co rich compounds show distinct magnetic properties (e.g. huge coercivity) from the Mn-rich samples. It is also found that Mn substitution in cobaltite is more effective in destabilizing the metallic state than Co substitution in manganites. While large negative magnetoresistance ( $\approx 70\text{-}90\%$ ) was observed in both these series, they have distinct field dependence. Such wide differences in magnetic and electrical properties warrants detail understanding of these compounds.

### **PO.62 Elongated cloud of cold $^{87}\text{Rb}$ for higher optical density**

Adrian Nugraha Utama\*, Mathias Seidler, Victor Xu Heng Leong, Alessandro Cerè, Christian Kurtsiefer (National University of Singapore)

Narrow bandwidth photon pairs are valuable resources for the study of the interaction between single photons and atoms. They can be generated by four-wave mixing in a cloud of cold atoms exploiting a cascade decay scheme [1]. One limitation of this technique is the trade-off between the pair production rate (brightness) and the bandwidth of the generated photons due to collective interaction in the atoms. To study this effect, we prepare an atomic cloud of cold  $^{87}\text{Rb}$  atoms with elongated geometry to achieve high optical density. A racetrack-shaped anti-Helmholtz coil provides the asymmetric magnetic field gradient of the magneto-optical trap necessary for the elongation [2]. We present details of design, construction and progress of the characterization of the cloud, in particular, measurement of the optical and atomic density. In the future, we are going to study the achievable brightness and bandwidth of the photon pairs generated in the elongated atomic cloud.

[1] B. Srivathsan et al., Physical Review Letters 111, 123602(2013). [2] J. Schoser et al., Physical Review A 66, 023410(2002).

### **PO.64 An Atomtronic Flux Qubit: A ring lattice of Bose-Einstein condensates interrupted by three weak links**

Nghia Tin Nguyen, Filip Auksztol, Maria Martinez Valado, Paul Condylis\*, Rainer Dumke (CQT)

We study a physical system consisting of a Bose-Einstein condensate confined to a ring shaped lattice potential interrupted by three weak links. The system is assumed to be driven by an effective flux piercing the ring lattice. By employing path integral techniques, we explore the effective quantum dynamics of the system in a pure quantum phase dynamics regime. Complementarily, the effects of the density's quantum fluctuations are studied through exact diagonalization analysis of the spectroscopy of the Bose-Hubbard model. We demonstrate that a clear two-level system emerges by tuning the magnetic flux at degeneracy. The lattice confinement, platform for the condensate, is realized experimentally employing a spatial light modulator.

## **PO.65 Quantum error correction in the presence of small baths**

Yink Loong Len\*, Yicong Zheng\*, Hui Khoon Ng\* (CQT & Yale-NUS College)

For the implementation of a realistic quantum computer, an important element is quantum error correction (QEC), in which one actively detects and corrects errors that occurs in the physical system. In the standard QEC analysis, the error or noise model usually falls under two categories.

1. Memoryless noise, in which one describes the noise by using completely positive, trace-preserving (CPTP) maps (or Lindblad master equation for continuous time) that acts on the system only. Since any effect from its coupling with the environment or bath is disregarded, the bath carries no information or memory about the system at all.

2. Memory-full noise or Hamiltonian noise, in which one studies the joint unitary evolution of the full system and bath. With the full bath included, one has a closed-system unitary dynamics, such that any initial information encoded in the system is always preserved within the system+bath.

Depending on which error models, one can get very different results for the fault-tolerance threshold, i.e. a theoretical bound below which efficient quantum computer is not possible. However, in reality, we expect the experimental situation to fall somewhere in between the two extremes, with a small number of degrees of freedom providing some memory capacity for information to how to and from the system, but also couple to a dissipative bath that limits the memory.

In this poster, we show some initial steps towards a more realistic analysis of the effective error on the system with QEC, taking into account the presence of a small bath with few degrees of freedom that are most strongly coupled to the system.

## **PO.70 Nonlocal transistor based on pure crossed Andreev reflection in a EuO-graphene/superconductor device**

Yee Sin Ang\*, L. K. Ang\*, Chao Zhang, Zhongshui Ma (Singapore University of Technology and Design)

Crossed Andreev reflection (CAR) is the excitation of a hole in a normal/superconductor/normal hybrid structure when two electrons are coupled nonlocally in different normal leads to form a Cooper pair [1]. In this work, we propose a mechanism of generating widely tunable CAR in an European-oxide-graphene (EuO-G)/superconductor/EuO-G three-terminal device [2]. We found that the inverted band topology between the valence and the conduction spin-split bands in EuO-G completely removes the parasitic local and non-entangled transport processes. This allows the generation of pure CAR over a wide range of bias and Fermi levels. The nonlocal crossed conductance exhibits rapid on/off switching with an exceedingly small subthreshold swing of 15 mV/dec. Furthermore, the nonlocal crossed conductance exhibits an oscillatory behaviour that directly reflects the propagation of the subgap quasiparticle mode in the superconducting graphene lead. Our results suggest that the device can be utilized as a highly tunable transistor that operates in the non-local and spin-polarized transport regime.

References: [1] J. M. Byers and M. E. Flatte, Phys. Rev. Lett. 73, 206 (1995). [2] Y. S. Ang, L. K. Ang, C. Zhang and Z. Ma, Phys. Rev. B 93, 041422(R) (2016).

### **PO.72 Guided modes in a double-well asymmetric potential of a graphene waveguide**

Yi Xu, Yingbin Zhu, Lay-Kee Ang\* (Singapore University of Technology and Design)

The analogy between the electron wave nature in graphene electronics and the electromagnetic waves in dielectrics has suggested a series of optical-like phenomena have drawn considerable attentions. One of them is the graphene-based electron waveguides, which will be useful for various graphene-based devices, such as electronic fiber. The guided modes for an asymmetric double-well potential is investigated using a modified transfer matrix method. It is found that there are two types of guided modes. The first guided mode appears in one well, which is similar to the asymmetric quantum well graphene waveguide. The second guide mode can appear in two potential wells with double-degeneracy. Characteristics of all the possible guide modes are presented. The results of guided modes in graphene waveguide may be helpful for the practical application of various graphene-based quantum electronic devices.

### **PO.75 Towards an efficient light-atom interface in free space**

Yue Sum Chin\*, Matthias Steiner\*, Nick Lewty, Christian Kurtsiefer (Centre for Quantum Technologies; Department of Physics, National University of Singapore)

An efficient light-atom interface is key for many quantum information protocols. We realize such an interface by focusing light onto a single trapped atom with a custom designed high numerical aperture (0.75) aspheric lens which performs at the diffraction limit. For strong light-atom interaction the excitation light needs to be tightly focused onto the atom. We achieve a beam waist at the focus as small as  $0.8\lambda$ . Based on this value, we expect a spatial overlap of 9.3% between the excitation and the atomic dipole mode. We are now in the midst of verifying this overlap experimentally. The expected spatial overlap is larger than in previous free-space experiments and would allow us to test the theory of light matter interaction in the strong focusing limit.

### **PO.76 Cost of counterdiabatic driving and work output**

Yuanjian Zheng\*, Steve Campbell, Gabriele De Chiara, Dario Poletti\* (Singapore University of Technology & Design)

Unitary processes allow for the transfer of work to and from Hamiltonian systems. However, to achieve non-zero power for the practical extraction of work, these processes must be performed within a finite-time, which inevitably induces excitations in the system. We show that depending on the time-scale of the process and the physical realization of the external driving employed, the use of counterdiabatic quantum driving to extract more work is not always effective. We also show that by virtue of the two-time energy measurement definition of quantum work, the cost of counterdiabatic driving can be significantly reduced by selecting a restricted form of the driving Hamiltonian that depends on the outcome of the first energy measurement. Lastly, we introduce a measure, the exigency, that quantifies the need for an external driving to preserve quantum adiabaticity which, unlike counterdiabatic drivings, does not require knowledge of the explicit form of the counterdiabatic drivings, and can thus always be computed. We apply our analysis to systems ranging from a two-level Landau-Zener problem to many-body spin chains, namely the quantum Ising and Lipkin-Meshkov-Glick models.

### **PO.79 Carbon Overcoats for Magnetic Media using High Energy Density Plasmas in Plasma Focus Device**

Sabpreet Bhatti\*, S.N. Piramanayagam, R.S. Rawat (School of Physical and Mathematical Sciences, Nanyang Technological University, Singapore)

Magnetic media overcoat is required to provide chemical and mechanical protection for the media from corrosion agents and accidental head–disk contact, respectively. The amorphous carbon (in particular, diamond-like-carbon [DLC]) is the material of choice for magnetic media overcoats because of its unique mechanical, physical, and chemical properties. Currently, magnetron sputtering is used by industry for carbon overcoat and new deposition techniques are being explored as requirements on carbon coats, in terms of thickness and head-overcoat distance, are fast changing for next generation magnetic media with ever increasing areal density. New effective alternative devices or synthesis techniques will be needed. Dense Plasma Focus device, a source of high energy density plasma, is used in this work for depositing amorphous carbon as the overcoat on magnetic media's surface. The objective of this work is to optimize the Dense Plasma Focus device for deposition of carbon overcoats on magnetic media. The optimization of carbon overcoat deposition process in plasma focus device is being carried out in terms of pressure of the precursor gas, gas mixture, distances and angular positions of deposition. Initial results show successful synthesis of very thin ( $< 3$  nm/shot) carbon films on magnetic media. Extensive analysis of deposited samples is being carried out while the further optimization of deposition conditions is continued.

### **PO.82 Superconducting Vortex Lattices for Ultracold Atoms**

Francesca Tosto\*, Phyo B. Swe\*, Maria M. Valado\*, Christoph Hufnagel\*, Deshui Yu\*, Rainer Dumke\* (Centre for Quantum Technologies (NUS), Nanyang Technological University)

We propose the realization of a magnetic vortex lattice for ultracold  $^{87}\text{Rb}$  atoms in a thin film of type-II superconductor [1]. Combining electric, magnetic and optical fields, atoms can be trapped close to the chip surface in a dense magnetic lattice formed by persistent supercurrents induced in the chip, with shorter lattice spacing than optical arrays. In such nanometer-scale conditions, atoms are positioned at the local minima of the lattice potential, allowing on site interactions due to short-range collisions and tunnelling to neighboring lattice sites, which provides the basis towards the realization of a Hubbard quantum simulator [2]. This work also paves the way to entangle atomic and solid state systems like SQUIDS [3], or the realization of a superconducting charge-atom qubit system [4].

[1] Siercke et al., PRA 85, 041403 (2012) [2] Romero-Isart et al., PRL 111(2013) [3] Singh et al, Optics Express 17, 2600-2610 (2009) [4] Yu et al., arXiv1602.01609v1 (2016)

### **PO.84 Piezoelectricity in Planar Boron Nitride via a Geometric Phase**

Matthias Droth\*, Guido Burkard, Vitor M. Pereira (University of Konstanz)

Van der Waals heterostructures – consisting of different 2D materials stacked atop each other – bear the promise of tailored physical properties [1]. Hexagonal boron nitride (hBN) is likely to play a key role in this novel paradigm of material physics and is already a critical component in state of the art heterostructures [2,3]. Detailed understanding of hBN's physical properties seems therefore paramount for these novel heterostructures.

In contrast to graphene, the two sublattices in two-dimensional hBN are occupied by different types of atoms, which allows for piezoelectricity. The piezoelectric tensor of extended hBN has been calculated via density functional theory (DFT) [4]. While an analytical description of piezoelectricity does exist for hBN nanotubes [5], this is, to our knowledge, not the case for two-dimensional hBN. We set up a Hamiltonian that involves the strain-induced pseudomagnetic field [6] and derive the piezoelectric tensor using the modern theory of polarization. Our findings are in exact agreement with symmetry arguments and give an analytical explanation for the piezoelectric electron-phonon coupling in planar hBN. We also provide an estimation of the coupling strength and a piezoelectric response similar to reported DFT results.

References [1] K. S. Novoselov et al., *Nature (London)* 490, 192 (2012). [2] B. Hunt et al., *Science* 340, 1427 (2013). [3] X. Cui et al., *Nat. Nanotechnol.* 10, 534 (2015). [4] K.-A. Duerloo, M. T. Ong, and E. J. Reed, *J. Phys. Chem.* 3, 2871 (2012). [5] E. J. Mele and P. Král, *Phys. Rev. Lett.* 88, 056803 (2002). [6] H. Suzuura and T. Ando, *Phys. Rev. B* 65, 235412 (2002).

### **PO.86 Quantum State Estimation of a Self-calibrating Experiment**

Jun Yan Sim\*, Jiangwei Shang, Hui Khoon Ng, Berthold-Georg Englert (Centre for Quantum Technologies)

Self-calibrating quantum state estimation is the procedure of reconstructing the quantum state and certain properties of the measurement devices from the same data. We apply self-calibration procedure to the double-crosshair measurement of the BB84 scenario in quantum cryptography for reconstructing the state and detector efficiencies simultaneously. When we perform maximum likelihood estimation, we observe multiple maxima in the likelihood function even when the state parameters and detector efficiencies are uniquely determined by detection probabilities. This problem disappears when prior knowledge of the ratios of detector efficiencies is taken into account. Finally, we construct optimal error regions for self-calibrating quantum state estimation by employing our recently developed Monte Carlo methods to sample over the joint space of quantum states and detector efficiencies.

### **PO.88 Strong Influence of Metallic Conductivity in Fano Resonant Metamaterials at Low Asymmetry**

Yogesh Kumar Srivastava\*, Manukumara Manjappa, Longqing Cong, Wei Cao, Ibraheem Al-Naib, Weili Zhang, Ranjan Singh\* (Nanyang Technological University)

Sharp resonances are vital for applications in many fields such as sensors and non linear optics. To excite sharp resonances, it is important to minimize losses (radiative and non-radiative). Non-radiative losses are due to the resistive losses from the material, mainly metals that are commonly used to fabricate the metamaterial whereas radiative losses are due to strong coupling of the metamaterial with the free space. Fano resonance in metamaterial system provide a simple route to excite sharp resonances with high quality factors. Metals as a constituent of metamaterials are described by various models such as PEC, Drude and DC conductivity metal in terahertz frequency regime. At terahertz frequencies all three above models show similar results. However, in this work we found that Fano resonances are very sensitive to the conductivity of the metal specially at low structural asymmetry. They possess significantly different

amplitude, line-width and Q factor of the resonances. Thus treating metals as PEC at terahertz frequencies becomes highly inaccurate at low asymmetries of the structures.

### **PO.90 Efficient Large Block Codes Ancilla States Preparation for Fault-tolerant Quantum Computation**

Yi-Cong Zheng\*, Ching-Yi Lai, Todd Brun (Centre for Quantum Technology, Yale-NUS college, National University of Singapore)

Fault-tolerant quantum computation (FTQC) schemes using multi-qubit large block codes require a huge amount of clean ancilla states of different types with weak error correlation inside each block. These ancilla states are usually logical stabilizer states of the data code blocks, which are generally difficult to prepare if code size is large. Meanwhile, the yield rate of preparation process are typically extremely low when the distance of block code is large. Here, we propose a protocol to distill various of ancilla states necessarily for FTQC fault-tolerantly using classical codes. Analytical analysis shows that correlated errors can be largely removed. At the same time, the yield rate can be high for general large block code with arbitrary size, using proper classical codes. Numerical Monte-Carlo simulation based on  $[[23,1,7]]$  quantum Golay code and quantum  $[[127, 57, 11]]$  support this conclusion with reasonably low gate error rates.

### **PO.92 Embedding Oxide-encapsulated Ag NPs in Semiconducting Layers: Absorption Gains or Losses?**

Wei Peng Goh, Wee Shing Koh\* (IHPC)

Incorporating plasmonic nanoparticles (NPs) in an organic solar cell (OSC) to improve device performance is well-established. Surface plasmons generated at resonance is accompanied by highly localized electric field enhancement at the immediate vicinity of the NPs. To maximize the advantage of electric field enhancement arising from surface plasmons, NPs are positioned within the active polymeric layer. As plasmonic materials are usually metallic in nature, positioning the NPs within the polymeric semiconducting layer introduces additional charge recombination sites. However, this can be circumvented by encapsulating the NPs with a continuous buffer layer. The buffer layer helps in isolating the NPs from the polymer layer, hence, preventing charge recombination. In our simulation studies, at NP resonance, absorption in poly(3-hexythiophene):phenyl-C61-butyric acid methyl ester (P3HT:PCBM) can be increased by encapsulating 50 nm Ag NPs with  $\text{Al}_2\text{O}_3$ ,  $\text{HfO}_2$ ,  $\text{MoO}_3$  and  $\text{SiO}_2$ . At Ag NP resonance, electric field distribution plots show the extent the plasmonic field extends into the polymer layer. While polymer absorption is improved at NP resonance, overall absorption in the photoactive layer by normalizing against the solar spectrum presents a more useful gauge. By integrating against AM1.5G, overall absorption in P3HT:PCBM is improved when incorporating Ag NPs encapsulated with a thin oxide shell into the polymer film as compared to a neat P3HT:PCBM control film. A thin 2 nm shell of  $\text{Al}_2\text{O}_3$ ,  $\text{HfO}_2$ ,  $\text{MoO}_3$  and  $\text{SiO}_2$  should be sufficient to improve absorption gains in the polymer film. Additional increment in the shell thickness appear to induce absorption losses with varying degree, although overall absorption is still higher than a control film. Maximum oxide thickness is probably about 20 nm before a negative net optical effect is experienced. Modelling studies are also extended to absorption in a  $\text{CH}_3\text{NH}_3\text{PbI}_3$  perovskite layer. It is revealed that both  $\text{Al}_2\text{O}_3$  and  $\text{HfO}_2$  have an optimal shell thickness of about 20 nm to ensure maximum absorption in  $\text{CH}_3\text{NH}_3\text{PbI}_3$ .

### **PO.93 Numerical simulation of quantum computation under non-Markovian noise**

Jing Hao Chai\*, Hui Khoon Ng (Centre of Quantum Technologies)

In the control of quantum systems, noise is a major hurdle to overcome. For a sequence of operations on an input quantum state, noise causes the output quantum state to deviate from the ideal situation. Encoding the qubit in multi-qubit physical systems, applying error correction and using a fault-tolerant design of quantum operations are some of the methods that can be used to protect quantum information from noise. However, these schemes increase the complexity of the system, which increases the error rate of the system. The error rate of such systems is a function of the number of physical qubits in the system, the number of operations to be carried out, as well as the nature of the operations themselves and the overall sequence of operations. The error rate of such systems under these schemes for a given noise model gives us a gauge of the usefulness of the schemes, but the complexity of the overall design makes it difficult to calculate this number. A certain class of such systems and operations is simulable numerically in an efficient manner, via the stabilizer formalism and Gottesman-Knill theorem. In this work, we first verify numerical results obtained by others [1]. We also provide additional numerical evidence of the effects of assumptions such as, quality of ancilla used in error correction, the use of post-selection of ancilla and output states from error correction, counting of possible error locations, on the resulting error rate of such schemes. In such schemes, it is usually assumed that errors are non-correlated between qubits and different times (Markovian) or that such correlations decay exponentially quickly. Though such an assumption is usually reasonable, the concept of fault tolerance involves the question of whether such schemes are robust to different types of noise. Prior study [2] have shown a wide disparity between the predicted feasibility of such schemes under non-Markovian noise than Markovian one, which seems to suggest that that such schemes may not be robust to non-Markovian noise. Hence we seek to clarify the reason for this disparity. We present some simple results within the limits of the stabilizer formalism, by capturing some simple dynamics of non-Markovian noise within a simple toy model for a system-bath interaction that undergoes error corrections.

1. E. Knill, *Nature*, 434, 39 (2005); P. Aliferis, D. Gottesman, and J. Preskill, *Quantum Inf. & Comp.*, 6, 97 (2006). 2. B. Terhal, G. Burkard, *Phys. Rev. A* 71, 012336, 2005

### **PO.96 Fabrication of artificial opals**

Letian Yu\* (Hwa Chong Institution)

Photonic crystal has been widely used in many fields due to its ability to affect the motion of photons. However, difficulties are faced in the synthesis process as the microscale of photons necessarily limit the size of available particles for the crystal. Further control over the effect also requires the structure to be uniform in order for Bragg's law and knowledge on quantum tunnelling to be applied. Currently the secondary nucleation happened during the seeded experiment is minimized through speed controlling methods and this paper will work on this progress by fabricating artificial opals of known sizes and uniform structure. Pragmatic applications of opals will also be discussed with a test on the opals' property.

### **PO.98 Chalcogenide-tuned nanoplasmonic pixels**

Weiling Dong, Xiao Ming Goh, Ye Yu, Joel Yang\*, Robert Simpson\* (Singapore University of Technology and Design)

Colour arising from metallic nanostructures has been used to demonstrate high resolution static colour images[1,2]. Here we investigate the influence of an active chalcogenide layer,  $\text{Ge}_2\text{Sb}_2\text{Te}_5$ , that is used to tune the plasmonic frequency of metallic nanostructures.  $\text{Ge}_2\text{Sb}_2\text{Te}_5$  is a phase change material that exhibits a large property contrast between amorphous and crystalline structural phases. The phase is usually tuned by laser or Joule heating. Here we show that during the amorphous to crystalline transition, the resonant frequency of a nanopillar array composed of  $\text{Ge}_2\text{Sb}_2\text{Te}_5$  and Al is red shifted. This colour switching is demonstrated and measured by colour image analysis and microspectroscopy. Interestingly, we find that  $\text{Ge}_2\text{Sb}_2\text{Te}_5$  is not only useful for switching the refractive index of the material, but also acts as a plasmonic resonator, and crystalline  $\text{Ge}_2\text{Sb}_2\text{Te}_5$  shows stronger resonance due to its higher metallicity. This work paves the way for chalcogenide-tuneable plasmonic materials for application in the next generation displays and tuneable optical filters.

Reference:

1. S. J. Tan, L. Zhang, D. Zhu, X. M. Goh, Y. M. Wang, K. Kumar, C. W. Qiu, and J. K. Yang, Nano letters 14, 4023 (2014). 2. H. Hu, H. Duan, J. K. Yang, and Z. X. Shen, ACS nano 6, 10147 (2012).

### **PO.100 Transient electrical switching of resonant bonds in chalcogenides**

Jitendra Kumar Behera\*, Wei Jie Wang, Xilin Zhou, Janne Kalikka, Robert Edward Simpson\* (Singapore University of Technology and Design)

Phase change data storage materials (PCMs) can rapidly and reversibly switch between covalently and resonant bonding states. Switching between these two different states produces substantial contrast in both electrical and optical properties. For this reason these materials have practical application in optical and electronic memories, as well as in switchable photonics. Here we show that the resonant bonds in the crystalline state of  $\text{Ge}_2\text{Sb}_2\text{Te}_5$  are disrupted by an external electric field, which can in turn be used to modulate the electrical properties of PCMs without going through any structural transition. A prototype phase change random access memory (PCRAM) cell was fabricated by RF sputtering and used for transient resistance measurement. Different electrical pulses covering the voltage range (0 V – 3 V) and pulse duration (10 ns – 60 ns) were applied whilst simultaneously measuring the memory cell's electrical resistance using an ultrafast electrical tester. We observe a sharp volatile increase in the electrical resistance ( $\approx 3$  times in magnitude) of the memory cell during the initial  $\approx 4$  ns of the applied voltage pulse. Thermal excitation of charge carriers then reduces the resistance of the cell for voltage pulse durations longer than 4 ns. A coupled Electric field-Temperature finite element analysis (FEA) model was developed to gain information about the transient temperature profile in the PCRAM cell. We show that the initial increase in the transient electrical resistance is not due to heating, which is in contradiction to the common paradigm for phase change memory switching processes, but due to electric field induced disruption to the resonant bonding mechanism. Transient switching of resonant bonds in phase change materials paves the way to design

an ultimate universal memory, one which would allow high speed logic operations in the same physical location as the memory.

### **PO.101 3D Printed Photonic Crystal Fibre**

Ka Hui Goh\*, Ng Si Min Rachel\*, Rainer Dumke (Hwa Chong Institution)

3D printing of optics equipment, such as lens holders and optical rails, can lead to cost reductions of over 97%. As an extension of this idea, we use PolyJet technology to 3D print photonic crystal fibres, modelling them on conventional ones. We study the relationship between light transmission through the 3D printed fibre and the following: size of fibre, height of fibre above printer platform during printing, and length of fibre. This characterisation of the 3D printed fibre can potentially increase control over the properties of customised 3D printed fibres. The core diameter of the printed fibres range from 0.5-1.0mm, while the printing height and length of fibre vary from 1.0-10.0cm and 0.5-5.0cm respectively. Our measurements suggest that the power  $P$  transmitted through the fibre increases with size and printing height, while decaying exponentially with an increase in length, possibly due to attenuation losses in the fibre. The data collected was fitted to the equation  $P_{out} = P_{in} \times [10^{-A \times L/10}]$ , where  $A$  is attenuation and  $L$  is the fibre length. The values obtained are  $P_{in} = 30 \pm 2 \mu\text{W}$  and  $A = 1.06 \pm 0.06 \text{ dB/cm}$ .

### **PO.102 Dicke simulation with cavity-assisted Raman transition**

Chern Hui Lee\*, Zhiqiang Zhang, Markus Baden, Kyle Arnold, Murray Barrett (Centre for Quantum Technologies)

With the use of cavity-assisted Raman transitions, we study the superradiant phase transition of an effective Dicke model with tunable coupling strength. We demonstrated that it is crucial to satisfy the "phase-matching" condition for a stable superradiant phase. We study the robustness of the many-atom Dicke state thus created, and explore the use of the system to create a heralded single-photon quantum memory.

### **PO.103 Toroidal resonances in terahertz metasurfaces**

Manoj Gupta\*, Dr Vassili Savinov, Longqing Cong, Ms Ningning Xu, Dr Govind Dayal, Dr Ranjan Singh\* (School of Physical and Mathematical Sciences, Nanyang Technological University)

Toroidal dipole response can be induced electromagnetically in specifically designed metamolecule structures. In a unit cell of metasurface, the design features of these metamolecule help them to confine time varying magnetic field in a circular region, which gives rise to the toroidal dipole. We have designed a planar metasurface with resonant response in the terahertz range, which is easy to fabricate and exhibits the signature of a toroidal excitation. The influence of toroidal dipole excitation on overall transmittance of metadvice can be controlled by engineering the degree of asymmetry in the two dimensional planar metasurface. Radiative and non-radiative losses play an important role in the performance of a photonic device. Toroidal dipoles can provide a way in optimizing the device performance by minimizing the radiative losses.

### **PO.104 A Simple Quantum Eraser using Michelson Interferometer**

Ng Si Min Rachel\*, Way Lin\* (Hwa Chong Institution)

A modified Michelson interferometer is used to investigate the relationship between linear polarisation states of photons and superposition. The modified interferometer comprises an additional linear polariser, making the total number of linear polarisers in the set-up to be three. A beamsplitter and neutral density filters split a laser beam into two paths with reflection to transmission ratio being 53:47. 2 linear polarisers, set at orthogonal states of polarisation, are placed at the reflected and transmitted path respectively making the laser beams spatially distinguishable. The third polariser serves to reduce this distinguishability by ‘erasing’/removing the path information of the 2 paths. We can assume the resultant fringes is the superposition of two laser paths. We hypothesize that when the third polariser is added, the visibility of the fringe pattern on the screen will tend to one and when the third polariser is absent, visibility tends to zero. This was proven to be applicable to a small extent where the visibility of the fringe pattern is 0.2138 and when the third polariser is absent, the visibility of the fringe pattern is 0.09639.

### **PO.106 Exploring the Use of Diffraction Gratings and Optics in Measuring Wavelength of Light.**

Zhen Yuan Yeo\*, Yi Ying Ong\*, Yu Wei Zhang\* (nus)

Diffraction gratings are very relevant in astro-spectroscopy due to its ability to separate different wavelengths of light. In this experimental report, we explore the idea of using two diffraction gratings to make astro-spectroscopy more accessible to the public.

The technique explored involves two diffraction gratings being placed at a known distance from one another in hopes of removing the need for calibration in spectroscopy. We have shown that this is possible in the case of a screen but, due to the presence of convex lens, does not work when using an image capturing device (camera).

This series of experiments provided useful insights, guiding our future direction to achieve a non-calibrative equipment. Promising improvements were discussed in future works.

### **PO.107 Coherent transfer of singlet-triplet qubit states across a linear chain of quantum dots**

Chang Jian Kwong\*, Teck Seng Koh\*, Leong Chuan Kwek\* (NUS)

We propose two schemes to coherently transfer arbitrary quantum states of the two electron singlet-triplet qubit across an empty chain of quantum dots. The schemes are based on electrical control over the detuning energy of the quantum dots. The first scheme is a pulse-gating scheme, requiring dc pulses and engineering of inter- and intra-dot Coulomb energies. The second scheme is based on the adiabatic theorem, requiring time-dependent linear control of the detuning energy through avoided crossings at a rate that the system remains in the ground state. For both schemes, an additional waiting time is required to compensate for the residual dynamical phase accumulated between the singlet and triplet states. Both schemes are shown to work for any arbitrary initial state. We simulate the transfer fidelity for 3 dots using typical experimental parameters for silicon quantum dots, then generalize our results to arbitrary number of dots. Our results show that, with optimization of the singlet-triplet qubit relative phase, both schemes give state transfer fidelities in excess of 98.7%, and at sub-nanosecond and tens of nanosecond timescales for the pulse-gated and adiabatic schemes, respectively.

### **PO.108 Measuring Temporal Coherence of Light from a Mercury vapour lamp**

Jun Heng Lor\*, Zheng Yang Choong\*, Yudong Sun\*, Bianca Lee Yanxi\* (Hwa Chong Institution)

Light from a thermal source of narrow spectral width exhibits intensity fluctuations, or photon bunching, on the order of its coherence time  $\tau_c$ . The coherence time  $\tau_c$  can be approximated to  $\approx 1/\Delta\nu$  where  $\Delta\nu$  is the spectral width. The photon bunching signature,  $g(2)(\tau)$ , is 2 for thermal light sources, and is 1 for coherent light sources such as lasers. For a Doppler-broadened spectral linewidth, the coherence time  $\tau_c$  can be described as  $\approx 1/\Delta\nu$ , where  $\Delta\nu$  is the spectral width. As such, we investigate the photon bunching of the mercury vapor lamp using a pair of Silicon Avalanche Photon Detectors (APDs) with timing resolution of approximately 0.6ns. The mercury spectral peak centres at  $546 \text{ nm} \pm 2 \text{ nm}$ , close to the expected value of 546.1 nm, limited by spectrometer resolution (OceanOptics, USB 4000). We used an oscilloscope (LeCroy, 1 GHz bandwidth, sampling rate 1 GHz) to measure the statistical distribution of the time delay between two photo-detection events from two photon detectors. By fitting the coincidence data to a Gaussian, the photon bunching signal of  $g(2)(\tau = 0)$  is found to be  $1.0 \pm 0.2$ , a deviation from the expected value of 2 for thermal sources. We suspect that with the oscilloscope delay, as well as dead time, the photon-bunching signal could well be outside the coincidence timeframe of the oscilloscope. We hope that further experimentation and data collection will shed further light on this matter.

### **PO.109 Sagnac Interferometry in a Non-inertial Frame**

Mingsong Wu\*, Haotian Wang\* (Hwa Chong Institution)

Early astronomers used the “fixed stars” in the night sky as the basis for measuring the Earth’s rate of rotation, known as a sidereal day. However, this process takes days and requires an unobstructed view of the stars as an external source of reference. We demonstrate an alternative method of using light from a source within our own rotating reference frame in which it is stationary to quantify the rotation instead.

We built a turning Sagnac interferometer using fiber optics, and split a laser beam approximating the TEM<sub>00</sub> spatial mode with wavelength= $652.3 \pm 0.1 \text{ nm}$  into two of similar intensity and sending each through a common 5m circular optical path centered at the rotation axis in antiparallel directions. These two beams are superimposed to give a single beam and videoed by a commercial camera, where its relative intensity (from each frame) is recorded with the rotation speed of the setup.

Empirically, we observed a change in relative intensity of about 2.2x and 1.5x as angular frequency increases from 0 to about 0.55 Hz in the clockwise direction and anti-clockwise direction respectively. Our control setup, where only one beam is sent through one direction in the optical loop, did not exhibit the same effect and showed a constant relative intensity, indicating the involvement of the interference of the two counter-propagating beams in producing the effect. We hypothesized an equation of fit for our data based on a simplified model of the interference between the two beams, and with a reduced  $\chi^2$  goodness-of-fit value of 1.93, our statistical result provided fair agreement with our model and justification that rotation relative to the stationary laboratory influences the relative phase of the two interfering beams that produces the observed relation between rotation rate and relative intensity of the observed output beam.

Our setup proves to be able to detect and quantify its absolute rotation, offering an entry point to possible explorations, such as the link between the centripetal acceleration generated in rotation and its effect on the counter-propagating light beams.

**PO.110 Analysis of the zig-zag transition in a 3D ion chain: spectrum, correlations and emergence of the amplitude mode**

Ulf Bissbort\*, Dario Poletti (SUTD)

We analyze the phonon spectrum and mode structure across the zigzag transition of a an ion chain in the rotationally symmetric case. As the system crosses into the zigzag phase, we find the appearance of a massive Higgs amplitude mode in conjunction with an additional gapless helical twisting mode. The transition features a strong analogy to the superfluid-Mott insulator transition in the Bose-Hubbard model, with the (tunable) rotational symmetry in the axial trapping being the counterpart of the  $U(1)$ -particle number conserving symmetry. In contrast to atomic condensates or liquid Helium, the this  $U(1)$  symmetry can directly be broken in ion experiments by deforming the trap. We initially give a self-contained, pedagogical introduction to an operator-based approach to determining the phonon structure, which extends upon the standard approach by James [] in its range of applicability and directly gives access to a phonon ground state containing correlations beyond the classical equilibrium state. Applying the formalism to the linear chain, we determine closed, analytical expressions for the phonon mode energies. We calculate the ground state spatial correlations and susceptibility, both at zero and non-zero temperature across the transitions. To gain a better intuitive understanding of the emergence of the Higgs-amplitude mode at finite momentum, we map the system onto an effective field theory.

**PO.111 A Short Distance Precision Force Sensor**

Colin Teo\*, Jordi Prat-Camps, Carles Navau, Alvar Sanchez, Oriol Romero-Isart (Singapore University of Technology and Design)

Fluctuation forces like the Casimir force and the van der Waals force have been theoretically described since the 1930s. However, due to the vast experimental hurdles and many noise sources, they have only recently been accurate measurements at short distances in the last decades. In this work, we present a proposal for a short distance force sensor using an all-magnetic setup consisting of a single domain nano-magnet levitated above a superconductor. We show that due to the Meissner effect, levitation can be achieved without any applied field, keeping unavoidable noise sources to the bare minimum. We evaluate the main noise sources for realistic materials and show that one can probe interesting regimes of the Casimir force, as well as more exotic forces, like short distance corrections to gravity and quantum friction.

**PO.113 Trilinear Hamiltonian with trapped ions and its applications**

Roland Hablutzel\*, Shiqian Ding\*, Gleb Maslennikov\*, Dzmitry Matsukevich\* (Centre for Quantum Technologies, NUS)

The model of three harmonic oscillators coupled by the trilinear Hamiltonian can describe wide range of physical processes. We experimentally realize such interaction between three modes of motion in the system of 3 trapped Yb ions. We discuss several application of this coupling, including simulation of the non-degenerate parametric down conversion process in the fully quantum regime, implementation of the quantum absorption refrigerator, simulation of the

interaction between light and atoms described by a Tavis-Cummings model, and studies of a simple model of Hawking radiation.

### **PO.115 Realization of Quantum-Dot Hybrid White Light-emitting-diodes via FRET from ZnO Nanowires Surface Defects**

Xin Zhao, Weizhen Liu, Rui Chen, Yuan Gao, Binbin Zhu, Hilmi Volkan Demir, Shijie Wang, Handong Sun\* (Division of Physics and Applied Physics, School of Physical and Mathematical Sciences, Nanyang Technological University)

Energy injection into the colloidal quantum dots (QDs) has provoked long-lasting research efforts towards realizing low-cost and highly efficient solid state lighting (SSL). Amongst the potential applications in SSL, white light emitting diodes (w-LEDs) have attracted tremendous attention due to the increasing demands in display and in-door lighting. However, the current energy injection routes in w-LEDs, including carrier injection via charge transport layer (electroluminescence mode) and photon injection via back-lit LEDs (Photoluminescence mode), exhibit limited injection efficiency as well as low loading of QDs. Also devices working in photoluminescence (PL) mode usually achieve w-LED through physically combining red, green and blue LEDs, which prevents further device miniaturization. In this study, we proposed an all-inorganic and one-chip integrable 3D excitation scheme which incorporated the QDs into GaN/ZnO nanorods (NRs) matrix. For the first time, we demonstrated energy injection from semiconductor defect levels into quantum dots via fluorescence resonant energy transfer (FRET). The existence of the FRET is confirmed via transient PL measurement and a reasonable 17% efficiency is achieved. Also, a prototype electrically driven GaN/ZnO NRs/CdSe QDs hybrid w-LED is fabricated and it exhibited an ideal achromatic light emission ((0.327, 0.330) in CIE 1931 chromaticity coordinate) with a correlated color temperature of 5700 K, which is very similar to that of the sunlight. The high-surface-to volume ratio of the nanowire matrix would also increase the loading ratio of the QDs. In addition, the energy band diagram and electroluminescence model are discussed. In summary, Integrating QDs with semiconductor family paves the way to next-generation high brightness hybrid LEDs with tunable color and lower power consumption.

### **PO.116 Lead-Free Perovskites for Coherent Light Emission**

Guichuan Xing, Mulmudi Hemant Kumar, Subodh Mhaisalkar, Nripan Mathews\*, Tze Chien Sum\* (Division of Physics and Applied Physics, School of Physical and Mathematical Sciences, Nanyang Technological University)

Solution-processed perovskites have recently demonstrated great potential for ultralow threshold amplified spontaneous emission (ASE), high Q lasing and light emitting diodes with >8% external quantum efficiencies. However, such perovskites are still limited to the same lead-based ones in photovoltaics where toxicity concerns have stifled their commercial aspirations. Furthermore, the slow bimolecular recombination in lead-based perovskites that spurs efficient photovoltaic operation is a fundamental limitation towards improving the light emitting properties. Here, we reveal the family of lead-free Sn-based halide perovskite as a new and superior gain medium that can overcome the abovementioned barriers. These remarkable materials yield stable ASE extending to  $\approx 1\mu\text{m}$  at strikingly low thresholds ( $\approx 6\mu\text{J}/\text{cm}^2$ ) due to fast bimolecular process inaccessible to their leaded counterparts. Solution-processability allows for infiltra-

tion into natural photonic crystal corrugations in butterfly wing scales to achieve NIR lasing. These attractive characteristics stem from the large absorption coefficients, high bimolecular recombination, suppressed defect densities and slow Auger recombination. Importantly, these solution-processed materials with good charge transport characteristics will open up new avenues for perovskite light emitting devices and may hold the key to realizing electrically-driven NIR lasing.

#### **PO.117 Reconfigurable Liquid Whispering Gallery Mode Microlasers**

Shancheng Yang, Van Duong Ta, Yue Wang, Rui Chen, Tingchao He, Hilmi Volkan Demir, Handong Sun\* (Division of Physics and Applied Physics, School of Physical and Mathematical Sciences, Nanyang Technological University, Nanyang Link, Singapore)

Engineering the resonant wavelength of whispering gallery mode (WGM) has become the building block of microcavity research due to the enormous applications in bio/chemical sensing, optical filters/switches and quantum information processing. However, up to now, the works on WGM wavelength tuning, especially in liquid environment, is still challenging. Bottlenecks like short cavity lifetime, small tuning range and non-reconfigurable process hinder the development of this research avenue. In our work, reconfigurably tuning of lasing peaks is demonstrated in all-liquid environment with a quasi-disk polymer microlaser fabricated by inkjet printing technique. We show that the size changing of the microlasers, which is caused by the surface tension variation in the solution, is the key of the wavelength manipulation. Detailed studies reveal that by modifying the surfactant concentration in solution, the diameter of the microlasers can reach a maximum reconfigurable change of 40%, which lead to a 10 nm shift of the lasing envelop. In addition, water-soluble organic compounds sensing with free spectral range (FSR) sensitivity of  $19.85 \text{ THz} / (\text{mol}\cdot\text{mL}^{-1})$  and detectivity limit around  $5.56 \times 10^{-3} \text{ mol}\cdot\text{mL}^{-1}$  is achieved. Our work provides not only a novel way to manipulate WGM resonant peaks in liquid environment, but also a new perspective on chemical and biological sensing.

#### **PO.120 Controllable Circular Dichroism of a Chiral Metasurface by Coupling Localized and Propagating Modes**

Zeng Wang\*, Yue Wang, Giorgio Adamo, Qing Yang Steve Wu, Jinghua Teng, Handong Sun\* (Division of Physics and Applied Physics, School of Physical and Mathematical Sciences, Nanyang Technological University, Centre for Disruptive Photonic Technologies, Nanyang Technological University Singapore)

Normally, the enhanced chiral response exhibited in chiral metamaterials and metasurfaces is attributed to the effect of localized surface plasmon resonance that is mostly determined by the materials and geometry. However, how the propagating mode influences chirality is still short of investigation. Here, we demonstrate a novel chiral metasurface composed of a chiral arrangement of nanoslits, in which propagating mode is proven to be a powerful tool to control the chiral response. In further, a very straight-forward strategy is theoretically raised that through modifying the coupling between the localized mode and propagating mode, we experimentally achieved the remarkable strong chiral response which can be also finely tuned in the visible range. This virtue of tunability enables our design as a chiral platform for various potential applications, such as chiral sensing.

### **PO.122 2D-3D bilayer perovskite solar cell with enhanced moisture stability**

Junye Huang\*, Teck Ming Koh, Subodh Mhaisalkar (Energy Research Institute @ NTU)

In the last 5 years, there have been tremendous research efforts in developing high efficiency MAPbI<sub>3</sub> (MA<sup>+</sup> = CH<sub>3</sub>NH<sub>3</sub><sup>+</sup>) inorganic-organic hybrid perovskite solar cells, pushing the record efficiency to 21%. However, the moisture stability remains as the biggest obstacle for large scale commercialization. In this work, a series of two-dimensional CHMA<sub>2</sub>MA<sub>n-1</sub>PbI<sub>3n+1</sub> (n=1, 2, 3, 4 and 5) (CHMA<sup>+</sup> = C<sub>6</sub>H<sub>11</sub>CH<sub>2</sub>NH<sub>3</sub><sup>+</sup>, cyclohexylmethylammonium) perovskite materials was synthesized and studied. This 2D perovskite material has a novel feature of forming a 2D-3D bilayer structure through a simple single step spin-coating process. Using this 2D-3D bilayer perovskite material as the absorber, our first generation device yields an initial power conversion efficiency of 5.70%, with short-circuit current density of 12.46 mA/cm<sup>2</sup>, higher than conventional 2D perovskite solar cells, while maintaining the enhanced moisture stability of 2D perovskite solar cells. The unique 2D-3D bilayer structure brings new insight to combine the advantages of both 2D and 3D perovskites: the moisture stability of 2D perovskite and the high efficiency of 3D perovskite.

### **PO.123 Transition-edge sensor and signal discrimination optimisation for quantum optics experiments**

Jianwei Lee\*, Lijiong Shen, Mathias A. Seidler, Siddarth K. Joshi, Brenda Chng, Alessandro Cerè, Christian Kurtsiefer (Centre for Quantum Technologies)

A loophole-free violation of Bell's inequality implies non-classical correlations [1], and can be used to certify randomness [2]. To simultaneously close the detection and locality loopholes with photon pair sources, we require efficient and fast detectors [3].

We highlight improvements made to previous readout electronics for transition-edge sensors (TES) provided by NIST\*, where we reduced jitter and afterpulsing. By changing detector biasing conditions, we also improved the reliability of detecting single photons efficiently, at acceptable signal-to-noise ratios. Presently, we have designed and implemented a polarisation-entangled photon source [4]. We expect to observe high pair collection efficiency with two TES's.

We intend to violate the Bell inequality first for fixed measurement bases. Subsequently, we will estimate the amount of randomness that could be extracted when the bases are chosen uniformly [5].

Proposals for using the TES's photon-number-resolving capability for other quantum information protocols, such as a complete Bell-state measurement [6], will also be considered.

[1] J. S. Bell, "On the Einstein Podolsky Rosen paradox", *Physics* 1, 195-200 (1964). [2] Colbeck R 2006 PhD Thesis University of Cambridge (arXiv:0911.3814). [3] P. H. Eberhard, "Background level and counter efficiencies required for a loophole-free Einstein-Podolsky-Rosen experiment", *Phys. Rev. A* 47, R747 (1993). [4] M. Fiorentino et al., "Generation of ultrabright tunable polarization entanglement without spatial, spectral, or temporal constraints", *Phys. Rev. A* 69, 041801 (2004). [5] Jean-Daniel Bancal et al., "More randomness from same data", *New Journal of Phys.* 16 (2014) 033011. [6] W. P. Grice, "Arbitrarily complete Bell-state measurement using only linear optical elements", *Phys. Rev. A* 84, 042331 (2011).

### **PO.124 Fast polarization switch and polarization entangled photon pair source optimization for quantum optics experiments**

Lijiong Shen\*, Jianwei Lee, Mathias A. Seidler, Brenda Chng, Siddarth Koduru Joshi, Alessandro Cerè, Christian Kurtsiefer (Centre for Quantum Technologies)

Experimental loophole-free violation of the Bell's inequality [1] demonstrates that local realism does not definitively describe the world, and can be used to certify randomness. Polarization entangled photon pairs are an appealing resource for such experiments because they are easily transmitted, interact little with the environment, and are easily manipulated in their polarization degree of freedom.

We generate polarization entanglement by Sagnac-like geometry [2] in type-II parametric down-conversion (SPDC) process. Periodically poled KTP crystal is pumped by 405nm CW laser in two opposite directions. The generated photon pairs at 810nm have adjustable degree of entanglement in polarization.

We will close the detection loophole using two high detection efficiency (>95%) transition-edge sensors (TES)[3]. Pair generation, basis implementation and photon detection events must be space-like separated to close the locality loophole. To fulfill this condition while reducing the minimal required space-like separation, we reduce the basis implementation time and detection time. A switch capable of changing measurement bases within tens of nanoseconds was designed and will be controlled by a quantum random number generator.

The entanglement source can be applied in long-distance quantum communications and in cryptography links. Together with our TES detectors, this source could also be used to perform a complete Bell-state measurement [4].

[1] J. S. Bell, "On the Einstein Podolsky Rosen paradox", *Physics* 1,195-200 (1964). [2] M. Fiorentino, G. Messin, C. E. Kuklewicz, "Generation of ultrabright tunable polarization entanglement without spatial, spectral, or temporal constraints" *Physical Review A* 69, 041801 (2004). [3] A. E. Lita, A. J. Miller, S. W Nam, "Counting near-infrared single-photons with (> 95 %) efficiency ", *Optics express* 16, 3032-3040 (2008). [4] W.P.Grice, "Arbitrarily complete Bell-state measurement using only linear optical elements" , *Physical Review A*, 84, 042331(2011).

### **PO.125 3D Printed Rechargeable Lithium-ion Batteries and High Performance Anode Materials**

Ye Wang\*, Glenn Joey Sim, Dezhi Kong, Hui Ying Yang\* (SUTD)

3D printed lithium ion batteries (LIBs) based on interdigital anode and cathode electrodes were reported in this work. The whole 3D printed LIB filled with commercial organic liquid electrolyte can deliver a capacity of 0.05 mAh per cell. Moreover, single cell can power 10 red LEDs for several seconds. In order to improve the 3D printed LIBs electrochemical performance, several high performance anode materials with three-dimensional hierarchical nanoarchitectures were developed and evaluated based on the standard half-cell battery configuration. The results show that these designed anode materials exhibit large specific capacity, high rate capability, long cycle stability and high initial coulombic efficiency. We anticipate these designed anode materials can be used for high performance 3D printed LIBs, and the developed 3D printed flexible LIBs may open up a new avenue for next generation LIBs.

### **PO.127 Oscillations of Bouncing Soap Bubbles**

Yunan Fan\*, Bingjie Zhu (Hwa Chong Institution)

Soap bubbles are excellent models to study reconfigurable microfluidics systems. It is found that the addition of surfactants such as glycerol stabilizes the bubble and extends its existence time. The project is to investigate the harmonic behavior of bouncing soap bubbles and the effect of varying concentrations (0.0%, 11.8%, 16.7%, 21.1%, 25.0%) of glycerol in bubble solution on their oscillations. Water and detergent are mixed at a ratio of 19:1 to prepare 5% bubble solution. The falling of bubbles from the highest point after bouncing off a cotton surface is captured by high-speed camera, and analyzed frame by frame using software Image J. Measurements such as minor, major, area, roundness (minor to major ratio when the bubble is fitted to an ellipse) are recorded. Besides observation from pictures, Fast Fourier Transformation (FFT graphs) is performed to obtain frequencies of oscillations. Later we concluded that the frequency of the oscillation falls maximum at certain concentration of glycerol, contrasting our hypothesis that the frequency increased proportionally with the concentration of glycerol. Nonetheless, another hypothesis is confirmed by our experiment as the roundness of the bubble against frame number indeed follows a sine relation. We also found that observable period of oscillation by eye may not be the dominant period shown by FFT graphs. (The roundness here is defined as the ratio of minor to major when the bubble is fitted to an ellipse in ImageJ.)

### **PO.129 Optical nonlinearity in plasmonic metal-cored fibres**

Behrad Gholipour, Duc Minh Nguyen, Paul Bastock, Long Cui, Venkatram Nalla, Christopher Craig, Khouler Khan, Daniel Hewak, Nikolay Zheludev, Cesare Soci\* (CDPT, Nanyang Technological University)

Advanced optical fibre applications like sensing, amplification and frequency conversion rely on strong optical nonlinearities. Here, we demonstrate nonlinearity enhancement in hybrid plasmonic metal-cored glass fibres where, upon pulsed laser excitation, the coupling between plasmonic and dielectric modes induces strong light collimation and suppression of nonlinear absorption, providing a novel platform for tunable fiberized sources and sensors.

### **PO.130 Cobalt doped Zinc metal-organic framework for high-performance capacitive deionization electrodes**

Meng Ding, Hui Ying Yang\* (Singapore University of Technology and Design)

In this study, Cobalt doped Zinc metal-organic frameworks (MOF) were synthesized from the combination of Zinc MOF, ZIF-67 and Cobalt MOF, ZIF-8 in an optimal ratio to achieve high performance for capacitive deionization (CDI). In CDI, the porous electrode is a key component for desalination, which requires high electrical conductivity, electrochemical stability and large specific surface area. However, the typical MOF with a single metal as the precursor is not able to meet those requirements: Zinc MOF has enormous surface area, yet its electrical conductivity is limited. As Cobalt MOF, it has excellent conductivity, while its specific surface area is quite small. The combined MOF exhibits a large specific surface area of 612 m<sup>2</sup>g<sup>-1</sup> and high electrosorptive capacity of 36.578 mg g<sup>-1</sup> at a cell potential of 1.6V. This bimetallic MOF has the potential to avoid these obstacles and enhance the performance of CDI by increase the specific capacitance and ion-accessible specific surface area.

### **PO.131 Hydrothermally synthesized graphene and Fe<sub>3</sub>O<sub>4</sub> nanocomposites for high performance capacitive deionization**

Zhi Yi Leong\*, Hui Ying Yang\* (Singapore University of Technology and Design)

Capacitive deionization (CDI) is a promising desalination technology that is environmentally friendly and consumes less energy when compared to conventional technologies such as reverse osmosis. Current research in CDI technology has focused on developing novel materials and composites that possess high specific adsorption capacities and stable electrochemical behaviour. In this study, we have synthesized a reduced graphene oxide and Fe<sub>3</sub>O<sub>4</sub> nanoparticle composite (RGO@Fe<sub>3</sub>O<sub>4</sub>) via a hydrothermal approach for CDI applications. This novel material combines the conductive characteristics of RGO with the pseudocapacitive properties of Fe<sub>3</sub>O<sub>4</sub> to provide an enhanced specific capacitance and salt adsorption. The electrosorption capacity and current efficiency of RGO@Fe<sub>3</sub>O<sub>4</sub> were found to be nearly two folds higher than that of RGO. This huge improvement can be attributed to the hydroxylation of the Fe<sub>3</sub>O<sub>4</sub> surface. Furthermore, the maximum electrosorption capacity for RGO@Fe<sub>3</sub>O<sub>4</sub> and RGO as predicted from the Langmuir isotherm was 8.33 and 4.63 mg g<sup>-1</sup> respectively.

### **PO.132 Control of plasmon resonances by symmetric in-plane illumination**

Liyong Jiang\*, Tingting Yin, Zhaogang Dong, Alexander M. Dubrovkin, Cheng Qian, Joel K. W. Yang, Zexiang Shen\* (Centre for Disruptive Photonic Technologies, School of Physical and Mathematical Sciences, Nanyang Technological University, 21 Nanyang Link, Singapore 637371)

In conventional optical studies on individual metallic nanostructures, the focused incident beam contains both out-of-plane and in-plane wave vectors with respect to samples. The out-of-plane wave vectors are usually asymmetric (i.e., from one direction) and excite pure localized surface plasmon resonance (LSPR). Previous Mie scattering and hybrid plasmon theories have been well built up to explain the LSPR excited by asymmetric out-of-plane wave vectors on simple (atom-like) and complicated (molecule-like) metallic nanostructures. Recently, the plasmon theory applied for symmetric out-of-plane incidence condition is developed and some very intriguing phenomena, such as coherent perfect absorption (CPA), coherent perfect transmission (CPT), and perfect polarization control (PPC) have been reported. As a comparison, when in-plane wave vectors are asymmetric (e.g., oblique incidence), besides LSPR, the short-range surface plasmon polariton (SR-SPP) which satisfies the standing-wave condition can also be excited when a nanostructure's size is beyond the quasi-static approximation. In this work, we study the plasmon resonance under the fourth condition, i.e., the in-plane wave vectors are symmetric. Our simulation results show that for a symmetric nanostructure, e.g., gold nanodisks, the LSPR and SR-SPP are preferential selected when the symmetric in-plane illumination condition is applied. For a single nanodisk, the LSPR is dramatically disappeared and the SR-SPP is strongly enhanced. For a gold nanodisk chain with an odd number, the LSPR is always disappeared at the central nanodisk. These spectral and spatial selection rules of plasmon resonances are due to the constructive and destructive phase conditions of gold nanodisks. The scanning near-field optical microscopy and the dark-field scattering spectrum for a single nanodisk and can well demonstrate these theoretical results. This work opens a new venue in plasmonic com-

munity for the nanoscale lightwave control, optical communication, and biosensing based on the switching and coding of plasmon resonances.

### **PO.134 Nontopotactic Conversion Reaction in Highly Reversible Sodium Storage of Ultrathin Co<sub>9</sub>Se<sub>8</sub>/rGO Nanosheets**

Xianfen Wang\*, Ye Wang, Zhi Xiang Huang, Hui Ying Yang\* (Singapore University of Technology and Design)

Na-ion batteries have recently experienced renewed interest as a potential energy storage alternative to Li-ion battery system due to the natural abundance and wider distribution of Na resources. Though many cathode materials have emerged as promising candidate in terms of energy density and electrochemical performance, one main obstacle to the commercialization of NIB is the limited choice of anode that can provide suitable stability and rate performance.

We report Co<sub>9</sub>Se<sub>8</sub> as anode materials for sodium ion battery. Co<sub>9</sub>Se<sub>8</sub> was assembled via a modified solvent-induced oriented attachment method through controlling the ratio of precursors to graphene oxide. The obtained Co<sub>9</sub>Se<sub>8</sub> anode delivers a highly reversible capacity of  $\approx 420$  mAh g<sup>-1</sup> showing evident plateau around 1.7 and 1.2 V respectively. The shift of the potential plateau after initial cycle can be related with the formation of SEI, which also induces large capacity fade. The rate performance of Co<sub>9</sub>Se<sub>8</sub> anode is also promising (298 mAh g<sup>-1</sup> at 5 A g<sup>-1</sup>) compared with other anode materials. Impressively the rate capacity of Co<sub>9</sub>Se<sub>8</sub> is higher than that of any carbonaceous materials such as hard carbon and expanded graphite at any current rate. While its performance is also good compared with other transition metal selenides such as Cu<sub>2</sub>Se. The excellent performance can be attributed to the following aspect: (1) the redox process may involve a nontopotactic reaction as shown in the Figure 1(e) during sodiation/desodiation that the materials break down to facilitate complete reduction of redox-active metal ion to elemental metal, therefore allowing for highly reversible capacity. (2) rGO may not only provides suitable site for oriented attachment growth of the candidate Co<sub>9</sub>Se<sub>8</sub> but also prevent the stacking of nanosheets. (3) In addition, the active materials take the advantage of graphene nanosheets as an elastic and conductive matrix to effectively accommodate the volume strain during charge/discharge. (4) the unique feature of Co<sub>9</sub>Se<sub>8</sub> such as excellent conductivity and large surface area make a promising candidate as anode for sodium-ion battery.

### **PO.135 Beyond the theoretical capacity of SnS<sub>2</sub> in Lithium ion batteries: Catalyst mediated reversible decomposition of Li<sub>2</sub>S**

Zhixiang Huang, Ye Wang, Hui Ying Yang\* (Singapore University of Technology and Design)

Tin disulfide (SnS<sub>2</sub>) has a 2D layered CdI<sub>2</sub>-type structure similar to graphite. However, unlike graphite which stores lithium via an insertion mechanism, the lithium storage mechanism in SnS<sub>2</sub> undergoes a different pathway which can be described using the following equations: (1) SnS<sub>2</sub> + x.Li + x.e -> Li<sub>x</sub>SnS<sub>2</sub> (2) Li<sub>x</sub>SnS<sub>2</sub> + (4-x).Li + (4-x).e -> Sn + 2Li<sub>2</sub>S (3) Sn + 4.4.Li <-> Li<sub>4.4</sub>Sn

Briefly, upon initial discharge, lithium intercalates into SnS<sub>2</sub> forming Li<sub>x</sub>SnS<sub>2</sub> (equation 1). On further discharge, a conversion process takes place which decomposes Li<sub>x</sub>SnS<sub>2</sub> into metallic Sn and Li<sub>2</sub>S (equation 2). The following charge-discharge cycles proceeds with Sn and Li forming a Li<sub>4.4</sub>Sn alloy reversibly resulting in a theoretical capacity of 645 mAh g<sup>-1</sup>. Despite the relatively high theoretical capacity (SnS<sub>2</sub>: 645 mAh g<sup>-1</sup> vs graphite: 372 mAh g<sup>-1</sup>), the for-

mation of Li<sub>2</sub>S in the irreversible reaction (equation 2) results in a huge loss of up to 4 moles of lithium ions per mole of Li<sub>x</sub>SnS<sub>2</sub>. Therefore, if equation (2) is reversible, this untapped capacity can be utilized and thus increasing the theoretical capacity of SnS<sub>2</sub> beyond 645 mAh g<sup>-1</sup>. It has been reported that equation 2 is reversible in transitional metal oxides/sulfides anodes due to the catalytic decomposition of Li<sub>2</sub>O/Li<sub>2</sub>S by the transition metals. Therefore, we believe that metal sulfides introduced into SnS<sub>2</sub> will be able to unlock the lithium in the Li<sub>2</sub>S generated in equation 2. In this work, we will demonstrate the enhanced performance of SnS<sub>2</sub> incorporated on 3D graphene (3DG) foam with doping of MoS<sub>2</sub> as a catalyst. The 3DG is able to support growth of hierarchical nanostructures and hence creating binder-free SnS<sub>2</sub>/MoS<sub>2</sub>/3DG electrodes. Furthermore, the binder-free electrodes are able to facilitate ex-situ XRD, TEM and XPS measurements to provide evidence of the catalytic reactions of MoS<sub>2</sub> in the SnS<sub>2</sub>/MoS<sub>2</sub>/3DG composite.

### **PO.136 Ti<sub>3</sub>C<sub>2</sub> Nanosheets as Effective Electrodes for Capacitive Desalination**

Lu Guo, Xianfen Wang, Huiying Yang\* (SUTD)

Water scarcity is one of the most serious global challenges. To address the global demand on fresh water, many desalination technologies have been developed such as thermal distillation and membrane separation. Though relatively high salt removal with excellent stability can be achieved, challenging bottlenecks still exist such as high energy consumption, high maintenance cost, secondary chemical wastes of ion exchange process and unavoidable degradation of membranes. Capacitive desalination (CDI) has been emerging as a promising approach which is not only easy operated, environmentally benign but also energy-saving for additional potable water production. Though CDI has been intensely investigated using various carbon materials such as activated carbon, carbon nanotubes and graphenes with different morphology and structures, it is highly necessary to explore novel materials for better CDI. As one member of a large family in 2D materials, Ti<sub>3</sub>C<sub>2</sub> nanosheets combine good conductivity and hydrophilic surface that are favorable for water treatment. Importantly, Ti<sub>3</sub>C<sub>2</sub>T<sub>x</sub> nanosheets have been demonstrated as high volumetric capacitor and cation interactions such as Na<sup>+</sup>, K<sup>+</sup>, Mg<sup>2+</sup> and Al<sup>3+</sup>. In addition, Ti<sub>2</sub>CT<sub>x</sub> nanosheets have been investigated as anodes for Na-ion battery applications displaying great promise as pseudocapacitor. In this study, MXene Ti<sub>3</sub>C<sub>2</sub> nanosheets have been prepared via HF treatment of commercial Ti<sub>3</sub>AlC<sub>2</sub> powder, followed by exfoliation in NaOH solution and Ar-plasma treatment subsequently. CDI electrodes were prepared and pasted onto carbon paper, batch-mode experiments were conducted in a continuously recycling system. As for the CDI unit, it comprises one pair of MXene Ti<sub>3</sub>C<sub>2</sub> electrodes. During CDI process, the NaCl solution was continuously flowed through the MXene Ti<sub>3</sub>C<sub>2</sub> based CDI unit cell at constant rate of 30 mL/min. The volume and temperature of the solution were maintained at 40 mL and 298 K, respectively. XRD revealed an evident shift of (002) peak to the lower angle implying the increased interlayer distance after exfoliation. SEM demonstrated the characteristic morphology of nanosheets in multilayers. XPS confirmed that the surface wettability can be closely related with high density of OH groups. CDI unit made of Ti<sub>3</sub>C<sub>2</sub> nanosheets displayed good ion adsorption/desorption upon charging/discharging process depending on the potential applied the electrode pair. The unit revealed a maximum removal capacity of 13 mg/g with relatively high efficiency of 31% at the voltage of 1.2 V and initial salt concentration of 250 mg/L. The adsorption performance demonstrated that MXene Ti<sub>3</sub>C<sub>2</sub> nanosheets hold high promise for seawater desalination and purification.

### **PO.137 Enhanced performance in Inorganic Halide Perovskites Green Light Emitting Diodes using Bathophenanthroline as Electron Transport Layer**

Irukuvarjula Venkata Kameshwar Rao\* (NTU)

Earth abundant solution processed organo metal halide perovskites has a major breakthrough of achieving power conversion efficiencies above 20%. This is mainly ascribed to higher diffusion length (0.1 – 0.3 $\mu$ m), charge carrier mobility's (8- 33 cm<sup>2</sup> V<sup>-1</sup>.s<sup>-1</sup>) and low temperature processing. Higher photoluminescence quantum yield, easily tuned emission colors and good color purity of these materials pave the way of these perovskites for light emission devices (PELEDs). Here we report CsPbBr<sub>3</sub> perovskite as a green light emitter for devices. The inclusion of the Bathophenanthroline (BPhen) as an ETL between the active layer and cathode, the device performance is substantially improved compared to the control. The devices with BPhen showed an improvement of the luminance by 500% with reduced threshold voltage to 2.5V from 3.0V and current efficiency improvement of five folds.

### **PO.139 The design and implementation of an adapted configuration for unconventional integrated system of quadrotor and hexacopter**

Yuying Qian\*, Kan Liu, Lijun Zhang, Junzhe Lin, Zixuan Lu (Hwa Chong Institution)

The project aims to modify the conventional configuration of Unmanned Aerial Vehicles (UAV) with rotary wings and develop an integrated system of quadrotor and hexacopter based on a redesigned mechanical structure and adapted dynamics modelling. Special implementation of detachable rotor arms, non-perpendicular X-configuration and altered arrangement of motors enable the UAV to execute tasks with either one of the two selectable configurations including quadrotor and hexacopter, thus obtaining advantage in higher resilience to hardware failures and versatility in applications. The flight control of the integrated system is realized by the mathematic modelling of force and momentum generation and an improved program architecture which accepts multiple sets of data for different configurations. Accurate parameter identification methods, like level scale setup to calculate thrust and torque coefficients of motors and the trifilar pendulum method to measure the moment of inertia of UAV, are employed to ensure better flying performance in terms of both stability and agility. The full model is verified through actual flight tests, of which the results reflect a success in the system development.

### **PO.140 Bubbles between graphene layers by electrolysis of water**

Hongjie An, Beng Hau Tan, Claus-Dieter Ohl\* (Nanyang Technological University)

Electrolysis of water have been proved an effective method to generate bulk bubbles, which is of great promising in flotation, waste water treatment and aquaculture industry. Electrolysis of water is also becoming one of amazing techniques in cleaning by forming surface nanobubbles. In this work, we are trying to use atomic force microscope (AFM) to study dynamics and formation mechanics of surface nanobubble through electrolysis of water. Highly oriented pyrolytic graphite (HOPG) was used as the working electrode, while a wire of platinum or copper used as counter electrode immersed in diluted salt solutions on HOPG. When a small DC voltage was applied, surface nanobubbles formed on HOPG surfaces. Some bubbles between graphene layers formed when increase the applied voltage or elongate the reaction time. Herein, we developed some methods to distinguish surface nanobubbles and bubbles between graphene

layers. These bubbles between graphene do not disappear after removal water, and they can also distinguish themselves in water with their special physical properties, such as stiffness. Bubble formation mechanics and impact factors were discussed. This discovery has great potential in using graphene as energy storage materials in near future.

#### **PO.141 Methylammonium lead iodide perovskite field-effect transistors**

Francesco Maddalena\*, Xin Yu Chin, Kar Cheng Lew, Daniele Cortecchia, Ummu Sumaiyah Binte Eliase, Annalisa Bruno, Cesare Soci (Energy Research Institute @ NTU)

In recent years, solution-processable hybrid organic–inorganic perovskites have become one of the focus of research in material science due to their potential in photovoltaic applications. However applications in light-emitting devices is also garnering attention, especially in the field of light-emitting diodes. Recently we showed that FETs are an excellent testbed to investigate charge transport in hybrid organic–inorganic perovskites, and demonstrated the feasibility of perovskite light-emitting field-effect transistors (PeFETs) at low temperature. Here we present a study of the mobility and FET characteristics of methylammonium lead iodide perovskite ( $\text{CH}_3\text{NH}_3\text{PbI}_3$ ) at different stoichiometric concentrations of the perovskite precursors, methylammonium iodide and lead iodide. We investigate the impact of the stoichiometry on the field-effect mobility of the charge carriers at different temperatures and the impact on light-emission.

#### **PO.142 Harvesting wasted heat using graphene material**

Shijun Liang\*, Lay Kee Ang (Singapore University of Technology and Design)

60 percentage of energy input into our society is lost as wasted heat, therefore it is of practical significance to harvest or recycle these wasted energy to generate electricity. In this paper, we are going to exploit the thermionic emission mechanism to converting thermal energy into electricity, based on two-dimensional material graphene. Our results predicate that the traditional Richardson's law (for which Owen W. Richardson won the Nobel Prize in Physics in 1928.) does not holds for graphene, but a new scaling exists. The predicated scaling is verified with experiment. Based on this new mechanism, we identify two ideal systems Graphene/ $\text{WSe}_2$ /Graphene and Graphene/ $\text{MoSe}_2$ /Graphene, which have high efficiency (above 10 %) in transforming wasted heat into electricity. These findings are very helpful in the field of heat management and energy harvesting.

#### **PO.143 Using Sequential Remote Sensing Data to Monitor and Predict Urban Growth of Yangtze River Delta, China**

Yikai Wu\*, Soo Chin Liew (Hwa Chong Institution)

Yangtze River Delta, China has experienced rapid urban development over the last three decades. Satellite remote sensing provides us cost-effective data to study urban development. This study examined urban expansion of selected cities (Suzhou, Wuxi, and Changzhou) in Yangtze River Delta, China using time-series satellite remote sensing data from 1986 to 2014. We emphasize using free satellite remote sensing images and open source image analysis/statistical software packages. A total of 16 cloud-free Landsat satellite images for the study area were downloaded and three classes (impervious cover, vegetated area, and water) land-cover map products were developed using advanced remote sensing image classification techniques. Image classification training data points were selected from 1986 and 2014 images, focusing on

common/no-changed areas within the 28-year time period. The locations of such training area were then used to extract training data points from each individual satellite image and fed into a random forest classifier to support land cover classification. Image classification accuracy assessment was conducted for year 2014. Overall classification accuracy was 88.9% and accuracy for impervious surface class was 76.7%. From 1986 to 2014, total impervious surface area increased from 375 km<sup>2</sup> to 1073 km<sup>2</sup>, corresponding to a very high annual urban growth rate of 7%. By examining all 16 land cover maps from 1986 to 2014, we observed increased level of landscape fragmentation. Furthermore, there was a linearly increasing trend of total impervious surface. A simple linear trend model predicted 1423.8 km<sup>2</sup> ( $\approx$  66% of land area) of impervious surface area in 2030.

#### **PO.145 Advanced Characterization techniques of Cu-Nb metallic nanolayers due to interface**

Hashina Parveen Anwar Ali\*, Ihor Radchenko, Arief Budiman (Singapore University of Technology and Design)

Through the tailoring of layer thicknesses, Cu-Nb metallic nanolayers have shown great promise, exhibiting extraordinary mechanical properties due to very high flow strength, stable plastic flow to large strains and enhanced radiation damage tolerance. Two different synthesis techniques of physical vapour deposition (PVD) and accumulated roll bonding (ARB) have shown contrasting mechanical behaviour for Cu-Nb metallic nanolayers due to their different interface crystallographic characters. To understand the mechanics behind the differences, novel advanced characterization techniques are revealed with initial results with nanolayers. Through atomic engineering of interfaces through synthesis and advanced characterization techniques, these multilayers can be used as a platform to develop more systematic design methodologies.

#### **PO.146 Highly stable, luminescent core-shell type methylammonium-octylammonium lead bromide layered perovskite nanoparticles**

Saikat Bhaumik, Sjoerd A. Veldhuis, Yan Fong Ng\*, Muduli Subas Kumar, Mingjie Li, Tze Chien Sum, Damodaran Bahulayan, Subodh Mhaisalkar, Nripan Mathews (Energy Research Institute @ NTU (ERI@N))

A new protocol for the synthesis of highly stable (over 2 months in ambient) solution-processed core-shell structure of mixed methylammonium-octylammonium lead bromide perovskite nanoparticles (size of 5-12 nm), with spherical shape, color tunability in the blue to green spectral region (438-521 nm) and high photoluminescence quantum yield (PLQY) of up to 92% is described. The color tunability, high PLQY and stability is due to the quantum confinement effect imparted by the crystal engineering associated with core-shell nanoparticle formation during growth.

#### **PO.147 Charge Modulation Mapping of Ambipolar Polymer Field-Effect Transistors**

Xin Yu Chin\*, Giuseppina Pace, Cesare Soci, Mario Caironi (Division of Physics and Applied Physics, School of Physical and Mathematical Sciences, Nanyang Technological University, Singapore.)

We study the device physics of an ambipolar organic field-effect transistor (FET) with charge modulation spectroscopy (CMS) and microscopy (CMM), an optical probing method which is capable to unveil both the transport properties and the spatial distribution of the charge carriers generated under different device operating regime. To perform CMS and CMM studies, we fabricated ambipolar FETs with DPP-DTT (poly(N-alkyldiketopyrrolo-pyrrole dithienylthieno[3,2-b]thiophene)), a high mobility donor-acceptor copolymer, as the active material. By exploiting the high spatial resolution of a confocal optical microscope, we clearly identify a linear and ambipolar operating regime of the device by mapping distribution of holes and electrons charge across the active channel under different drain-source voltages. Interestingly, our measurements are also sensitive to contact resistance upon charge injection, revealing a lower carrier distribution along the channel when the contact resistance is high. Furthermore, the high spatial resolution allows discriminating electroabsorption (EA) and charge-induced absorption contributions from the electrode edges and active channel, respectively. Understanding of the nature of hole and electron transport in donor-acceptor copolymer enabled by this technique will allow optimizing the molecular design of higher performance ambipolar polymer materials.

### **PO.148 Effect of Annealing Temperature on Film Morphology of CH<sub>3</sub>NH<sub>3</sub>PbBr<sub>3</sub> based Light Emitting Diodes**

Nur Fadilah Jamaludin\*, Natalia Yantara (NTU)

Organic-inorganic halides have garnered much interest from the photovoltaic community in recent years with efficiencies exceeding 20% in less than a decade. Its success as a light absorber can be attributed to its plethora of unique properties namely balanced long range charge transport, benign grain boundaries and high charge mobilities. This class of materials has also been identified as promising emitters for light emitting applications due to their photoluminescent properties. Though innate, the film characteristics are also largely influenced by film morphology, which in turn is affected by deposition conditions and surface treatments. Here, we investigate the effect of annealing temperature on the film formation of CH<sub>3</sub>NH<sub>3</sub>PbBr<sub>3</sub>. Although sufficiently high annealing temperature is required to remove excess solvent and induce grain growth, excessive heating for prolonged periods resulted in formation of PbBr<sub>3</sub>. The effect of annealing temperature on film characteristics and the correlation to device performance will be assessed.

### **PO.154 Implementation of optical oracle in laser written waveguide network**

Maria Vazquez, Vibhav Bharadwaj, Belen Sotillo, Duc Minh Nguyen, Shane Eaton, Cesare Soci\* (Nanyang Technological University)

Direct femtosecond-laser writing into transparent glasses is a robust technology for the fabrication of three-dimensional optical waveguide networks, including waveguide couplers, beam shapers and resonators. We are implementing a compact optical oracle, laser written into a borosilicate platform, to solve the Hamiltonian path problem, the famous non-polynomial (NP) complexity problem of finding whether a set of towns can be travelled via a path in which each town is visited exactly once. The Hamiltonian path problem is solved optically by sending femtosecond lasers pulses into a waveguide network that maps the topology of the network of towns, and monitoring the time delay of the output pulses. If the Hamiltonian path exists, this delay will be equal to the sum of the travel times needed to visit all nodes of the network, which is

made unique by design. Direct laser writing will allow integration of relatively large “cognitive photonic networks”, which may be used to solve complex mathematical problems faster than brute-force electronic computing.

1 An optical fibre network oracle for NP-complete problems, K. Wu, J. García de Abajo, C. Soci, P.P. Shum, N.I. Zheludev, *Light: Science & Applications* 3, e147 (2014).

### **PO.155 Hybrid organic-inorganic perovskite nanostructures**

Kar Cheng Lew, Daniele Cortecchia, Xin Yu Chin, Paola Lova, Annalisa Bruno, Cesare Soci\* (Physics and Applied Physics, School of Physical and Mathematical Sciences, Nanyang Technological University, Singapore)

Within the past few years, perovskites have exhibited extremely good performance in solar cells, with exceptional efficiencies, which are comparable to Silicon silicon cells, opening a new era in photovoltaics. More recently, hybrid perovskites have also attracted great interest for application in light emission and photodetectors. However, up to now, research has focused extensively more on application of the bulk materials, and only few cases examples related to nanostructures have been reported. In this work, we present show the synthesis of methylammonium lead iodide (MAPbI<sub>3</sub>) nanostructures with different morphology, and discuss investigating their possible integration into nanoscale devices to exploit their superior optoelectronic properties and size scalability. Different MAPbI<sub>3</sub> nanostructures of MAPbI<sub>3</sub> were synthesized through ad hoc by proper engineering/modification of the synthetic method/conditions. Using double and single-step spin coating deposition techniques, we were able to obtain high quality perovskite nanocubes, nanowire meshes, as well as isolated individual single nanowires. Synthetic conditions, morphological and compositional characterization will be presented, along with preliminary the characterization of the optoelectronic properties of low-dimensional perovskite characterization of these nanostructures. Our measurements results indicate that such nanostructures are promising for application in highly sensitive efficiency photodetectors with intrinsic excellent photosensitivity and photoconductivity gain, and we envision that further design developments will lead to the fabrication of single wire transistors and laser devices, the development of which would extend pushing the use implementation of hybrid perovskites to the nanoscale.

### **PO.156 Plasmonic Enhancement of Spontaneous Emission in Metal-Perovskite Slabs**

M Danang Birowosuto\*, Daniele Cortecchia, Lew Kar Cheng, Paola Lova, Annalisa Bruno, Cesare Soci (CNRS International - NTU - Thales Research Alliance)

We investigated the radiative properties of a white light emitting hybrid organic-inorganic perovskite film (EDBEPbBr<sub>4</sub>) embedded into metal-perovskite (MP) and metal-perovskite-metal (MPM) slabs. We show that coupling of surface plasmon polaritons excited in the metal slabs with emissive dipoles in the perovskite film results in the large enhancement of spontaneous emission intensity, and in the significant shift of the photoluminescence emission wavelength in MP and MPM configurations. Time-resolved photoluminescence measurements indicate a corresponding enhancement of radiative emission rate of about 2- and 5-fold for MP and MPM, respectively, compared to the  $\approx 0.2 \text{ ns}^{-1}$  emission rate of the bare EDBEPbBr<sub>4</sub> film. This is in excellent agreement with analytical computations of Purcell enhancement due to the tight

confinement of plasmonic gap modes at specific distances from a metallic plate, and between two metallic plates at resonant wavelength. Demonstration of plasmonic enhancement of the radiative properties of hybrid organic-inorganic perovskites may provide new ways to improve the energy efficiency of light-emitting devices such as LEDs and displays; similar concepts may also be implemented to increase light absorption in thin-film perovskite solar cells.

### **PO.157 Partially Depolarized Photoluminescence in Dolmen-like Plasmonic Nanoantennas**

Tingting Yin\*, Liyong Jiang, Zhaogang Dong, Joel K. W. Yang, Zexiang Shen\* (NTU)

Similar to semiconductors, photoluminescence (PL) from bulk noble metals is naturally and completely depolarized due to fast energy and momentum relaxation processes of photoexcited electrons. However, in plasmonic atom (e.g., metallic nanodisk or nanorod), the strongly polarization-dependent radiative channels of plasmonic resonance will modulate the polarization properties of the PL. In this presentation, we show comprehensive experimental studies on the partially depolarized PL of a plasmonic molecule, i.e. a dolmen-like plasmonic nanoantenna, where an interconversion between Lorentz- and Fano-like lineshape PL is reported by simply controlling the excitation-collection polarization configurations. More importantly, the depolarization ratio of such PL is relied on the spectral overlap of the excitation energy and the transverse/longitudinal plasmon resonance band of the components of the plasmonic nanoantennas. An energy transfer and microdynamic model is proposed to well explain the complicated depolarized PL in dolmen-like plasmonic nanoantennas.

### **PO.158 Optimal binary device-independent witnessing of depolarizing, erasure, and amplitude-damping channels**

Sarah Brandsen\*, Michele Dall'Arno, Francesco Buscemi (Centre for Quantum Technologies)

In arxiv:1511.05260, we introduced the framework of universal optimal device-independent witnessing of quantum channels as a method to characterize any unknown quantum channel given as a black-box, drawing only upon its experimentally observed input-output statistics.

Here we apply our framework to derive a closed-form characterization of such input-output statistics in the case where both the input and output are binary, for various relevant channels such as the erasure, depolarizing, and amplitude damping. Our results provide an explicit answer to questions such as: what is the smallest value of the noise parameter  $\lambda$  such that the experimentally observed conditional binary probability  $p_{y|x}$  of output  $y$  given input  $x$  could have been generated by an erasure (or depolarizing, or amplitude damping) channel with parameter  $\lambda$ ?

### **PO.159 Layer-dependent electro and optical properties in 2D materials and Perovskites**

Zexiang Shen\*, Jiaxu Yan\*, Juan Xia, Zheng Liu (NTU)

The optical and electronic structures of two dimensional transition metal dichalcogenide (2D TMD) materials and perovskite often show very strong layer-dependent properties. Detailed understanding of the inter-layer interaction will help greatly in tailoring the properties of 2D TMD materials for applications. Raman/Photoluminescence (PL) spectroscopy and imaging have been extensively used in the study of nano-materials and nano-devices. They provide

critical information for the characterization of the materials such as electronic structure, optical property, phonon structure, defects, doping and stacking sequence. In this talk, we use Raman and PL techniques to study few-layer 2D TMD samples and perovskites under low temperature and high pressure. The Raman and PL spectra show clear correlation with layer-thickness and stacking sequence. Our ab initio calculations reveal that difference in the electronic structures mainly arises from competition between spin-orbit coupling and interlayer coupling in different structural configurations.

#### **PO.160 Absolute Te<sub>2</sub> reference for barium ion at 455.4 nm**

Tarun Dutta\*, Manas Mukherjee (CQT,NUS)

Precision atomic spectroscopy is presently the work horse in quantum information technology, metrology, trace analysis and even for fundamental tests in Physics. Stable lasers are inherent part of precision spectroscopy which in turn requires absolute wavelength markers suitably placed according to the probed atomic spectra. Here we present, new lines of tellurium (Te<sub>2</sub>) which allows locking of external cavity diode laser for precision spectroscopy of singly charged barium ion. For the first time we have observed seven resonance lines in the neighbourhood of barium ion dipole transition S<sub>1/2</sub> – P<sub>3/2</sub>, the closest being only 80 MHz away. The S/N ratio of this closest line is close to 100 which leads to a robust lock of frequency.

#### **PO.161 Nanostructuring mixed-dimensional perovskites: a route towards tunable, efficient photovoltaics**

Vignesh Shanmugam\*, Teck Ming Koh, Johannes Schlipf, Lukas Oesinghaus, Peter Müller-Buschbaum, Ramakrishnan Narayanan, Varghese Swamy, Nripan Mathews, Pablo P. Boix, Subodh G. Mhaisalkar (Monash University)

2D perovskites are one of the proposed strategies to obtain higher moisture resistance solar cells, since the presence of the larger organic cations may serve as a barrier. Nevertheless, these moisture resisting layers commonly become charge transporting barriers, and up to date none of the 2D perovskites have delivered high power conversion efficiency. Here, we present a nanostructuring approach in mixed-dimensionality perovskites, (IC<sub>2</sub>H<sub>4</sub>NH<sub>3</sub>)<sub>2</sub>(CH<sub>3</sub>NH<sub>3</sub>)<sub>n-1</sub>Pb<sub>n</sub>I<sub>3n+1</sub>, showing an overall power conversion efficiency over 9%.

#### **PO.162 Exact diagonalization and steady state of quadratic bosonic quantum open system**

Chu Guo\*, Dario Poletti\* (Singapore University of Technology and Design)

We study the set of quantum open systems whose dynamics are described by the Lindblad quantum master equation. In particular, the Hamiltonian and the dissipator of the systems we considered are all of quadratic forms of the bosonic creation and annihilation operators. We find that for such system of size N, we can perform a transformation which corresponds to the Bogoliubov transformation of the unitary system, to diagonalize the Liouvillian super operator and get the 4N normal modes. We also find the analytic form of the similarity transformation which relates the steady state of the Liouvillian to the vacuum state of the corresponding unitary system. In the end, we propose an algorithm to solve the eigenvalues of the Liouvillian super operator and the binary observables, in which we only need to diagonalize an N by N non-Hermitian matrix, together with a few matrix multiplication.

### **PO.163 Quantum Supremacy of Many-Particle Thermal Machines**

Juan Diego Jaramillo\*, Mathieu Beau, Adolfo Del Campo (National University of Singapore)

While the emergent field of quantum thermodynamics has the potential to impact energy science, the performance of thermal machines is often classical. We ask whether quantum effects can boost the performance of a thermal machine to reach quantum supremacy, i.e., surpassing both the efficiency and power achieved in classical thermodynamics. To this end, we introduce a non-adiabatic quantum heat engine operating an Otto cycle with a many-particle working medium, consisting of an interacting Bose gas confined in a time-dependent harmonic trap. It is shown that thanks to the interplay of nonadiabatic and many-particle quantum effects, this thermal machine can outperform an ensemble of single-particle heat engines with same resources, demonstrating quantum supremacy in many-particle thermal machines.

J. Jaramillo, M. Beau and A. del Campo, arXiv:1510.04633v3 (2016).

### **PO.164 Investigation into the Properties of Plasma Deposited Polyterpenol Thin Films Subjected to Ionising Radiation**

Daniel Grant\*, Rajdeep Sawat (NTU)

Plasma polymerisation is a novel method for fabricating polymer thin films. These films are characterised as being ultrathin (10-1000 nm), pinhole free, and exhibit superb adhesion to a wide variety of substrate materials. Whilst these films express reasonable diversity with respect to their surface chemistry and morphology, there remains considerable room for tailoring these characteristics.

This course of research investigates the utility of various types of ionising radiation (including gamma rays, monoenergetic ions, and plasma sources) to induce chemical and structural changes in plasma polymerised polyterpenol thin films. The information generated by this research will facilitate the development of irradiation processes to selectively tailor the chemical, electrical, optical, and mechanical properties of polyterpenol thin films, with potential applications to the development of biomedical and organic electronic devices.

### **PO.165 Coherent light manipulation of cold Sr**

Chang Chi Kwong\*, Frédéric Leroux, Manan Jain, Vincent Mançois, Riadh Rebhi, David Wilkowski\* (SPMS, Nanyang Technological University; Centre for Quantum Technologies, National University of Singapore; Majulab)

We are developing scientific activities around a cold gas of strontium atoms. We achieved a high performance setup in particular in term of atoms loading rate, of control of the laser frequency stability and of stray magnetic field cancellation. Several experiments have been carry out to probe cooperative effects on light scattering. They have led to the observation of a coherent superflash and of a new type of pulse train. In parallel, we are developing state manipulation on the strontium fermionic isotope to generate non-abelian gauge fields.

### **PO.166 Modelling Cell Extrusion Mechanics with 3D Vertex Model**

Lester Lin\*, Sabyasachi Dasgupta (National University of Singapore)

Cells in a packing can undergo apical or basal extrusion at the onset of apoptosis, or when triggered by crowding-induced mechanical stresses. From confocal imaging of cells undergoing

extrusion, the observations of actomyosin accumulation on the extruding cell lateral surfaces suggest surface contractility is important to mediate cell apical extrusions. We have adapted the Surface Evolver tool (by Kenneth Brakke) to create a 3-dimensional vertex cell-packing model to study the physical considerations for cell extrusion. We demonstrate the importance of establishing a gradient of active tensions on the lateral surface, induced by build-up of hydrostatic pressure within the extruding cell, can lead to successful cell extrusion.

### **PO.167 Effect of Electric Field on Laser-induced Actuation of CNTs**

Ning Lu\*, Yun Ling Selina Ho\* (DHS/Dept of Physics NUS)

Carbon nanotubes (CNTs) with its unique ability to exhibit laser induced actuating effect with high sensitivity and durability, has led to it being proclaimed as a potential candidate for future opto-mechanical micro-electronic devices. To gain further insights into this effect, a focused laser beam was used to craft out an actuating CNTs piece from an entire array of CNTs. In this work, effect of the following parameters on the actuating ability of the CNTs actuator is studied: (1) width and length of actuator, (2) power of the laser that induces the actuating phenomenon, as well as (3) trench width separating the actuator from its surrounding CNTs array. Based on the above findings, the ideal condition leading to most significant actuating effect was used in our further study regarding the effect of the actuator on applied electric field. For CNTs actuators to be implemented in opto-mechanical micro-electronic devices, it is crucial for us to determine its effect on applied electric field running through the system. Parameters such as orientation of actuators, bias, laser power and laser positions were explored. It was discovered that actuation is significant in increasing the conductivity of CNTs. Laser power and laser position affect the current by affecting actuation, bias affects the flow of charge carriers and orientation of actuators affect the actuation's effect on the electron pathways. We believe that the findings presented in this report will play a significant role in directing the future application of CNTs actuators in opto-mechanical micro-electronic devices.

## 5 Technical Sessions

### T1: Solid State Physics 1

Time: Monday 7 Mar, 11:15am; Venue: TT16

Time allocated for invited talks is 20 min speaking time, plus 5 min Q&A, and time allocated for contributed talks is 12 min speaking time plus 3 minutes Q&A.

#### T1.4 (INVITED) Weyl Semimetals and Chirality-dependent Electron Dynamics

Shengyuan Yang\* (Singapore University of Technology and Design)

11:15am – 11:40am

The topological classification of solids has been extended from insulators to semimetals. These topological semimetals have bandstructure featuring nontrivial topological invariants and there exist exotic topological boundary states. There has been a lot of research effort in the search for new topological semimetal materials and in understanding their unusual physical properties. We have predicted several new topological semimetal phases in both 2D and 3D, including 2D semimetals with fully-unpinned Dirac point and 3D spin-orbit-free Weyl-loop semimetals. We also formulated a semiclassical theory for Weyl electron dynamics. We predict universal transverse shifts of the wave-packet center in transmission and reflection. The anomalous shifts are opposite for electrons with different chirality, leading to a chirality-dependent Hall effect, and they can be further made imbalanced by breaking inversion symmetry.

#### T1.8 Momentum signatures of the Anderson transition

Sanjib Ghosh\* (Centre For Quantum Technologies)

11:40am – 11:55am

Quantum particle (wave) travelling through a disordered medium has an extra probability density along the backward direction of its initial momentum. This phenomenon is called the coherent backscattering (CBS). CBS can be explained by the maximally crossed diagram, where two Green's functions are connected by two maximally crossed infinite series of scattering lines. This diagram can be visualise by two counter propagating waves experiencing same series of scattering events, on average. Conventionally, CBS is known as the weak localization effect and a precursor of Anderson localization.

By developing a finite-time scaling theory for the angular width of the CBS peak, we demonstrate that this observable can be experimentally used to characterize the 3D Anderson transition. We apply this method to coherent backscattering of cold atoms in laser speckle potentials and verify the one-parameter scaling theory of Anderson localization.

#### T1.54 Floquet Weyl Phases in a Three Dimensional Network Model

Hailong Wang\*, Longwen Zhou, Yidong Chong\* (Division of Physics and Applied Physics, NTU)

11:55am – 12:10pm

We study the topological properties of 3D Floquet bandstructures, defined using unitary evolution matrices rather than Hamiltonians. Previously, 2D bandstructures of this sort have been

shown to exhibit anomalous topological behaviors, such as topologically-nontrivial zero-Chern-number phases. We show that the bandstructure of a 3D network model can exhibit Weyl phases, which feature “Fermi arc” surface states like those found in Weyl semimetals. Tuning the network’s coupling parameters can induce transitions between the Weyl phase and various topologically distinct insulator phases. We identify a connection between the topology of the insulator phases and the topology of Weyl point trajectories in k-space. The model is feasible to realize in custom electromagnetic networks, using reflection measurements to probe the Weyl point trajectories.

### **T1.77 Calculation of Thermal Expansion Coefficients of Low-symmetry Crystals Based on the Gruneisen Formalism**

Chee Kwan Gan\*, Yun Liu (Institute of High Performance Computing)

12:10pm – 12:25pm

We present a method that is based on the Gruneisen formalism [1], to enable calculation of thermal expansion coefficients (TEC) of any low-symmetry orthorhombic system. Our method is applied to antimony sulfide (Sb<sub>2</sub>S<sub>3</sub>) which belongs to a class of semiconductors for optoelectronics, photovoltaics, and thermoelectrics. Our method [1] allows practical calculation of the TECs of Sb<sub>2</sub>S<sub>3</sub> without having to carry out an extensive search in the three parameter space for a, b, and c lattice parameters as required in a routine yet expensive quasiharmonic calculation. We find that Sb<sub>2</sub>S<sub>3</sub> exhibits a large thermal expansion anisotropy where the TEC in the b direction is seven and two times larger than that in the a and c directions, respectively. Our method opens the door for efficient screening of materials [2] with desired TECs.

[1] C.K. Gan, J.R. Soh, and Y. Liu, *Phys. Rev. B* 92 (2015) 235202.

[2] C. Toher, J.J. Plata et al., *Phys. Rev. B* 90 (2014) 174107.

## T2: Solid State Physics 2

Time: Monday 7 Mar, 11:15am; Venue: TT17

Time allocated for invited talks is 20 min speaking time, plus 5 min Q&A, and time allocated for contributed talks is 12 min speaking time plus 3 minutes Q&A.

### T2.23 Excitations and dynamics in the extended bose-hubbard model

Benoît Grémaud\*, George Batrouni (Centre for Quantum Technologies - UMI 3654 CNRS)

11:15am – 11:30am

Using the time evolving block decimation method, we study the excitation spectrum above the ground state of the one dimensional extended Bose Hubbard model in different phases. First, at unit filling, we discuss the properties of the structure factor across the Mott insulating phase, the Haldane insulating phase and the charge density wave phase. In particular, in the Haldane phase, we emphasize the competition between the single particle and two particle excitations, resulting in different values for the neutral and the charge gap. In the supersolid phase appearing by doping the charge density wave phase, we find that the structure factor depicts additional gapless modes at a finite momentum that depends on the density. This feature and the low energy spectrum can be explained by a mapping of the system onto the Heisenberg model for a spin 1/2 chain in a finite magnetic field. Finally, we discuss the excitation spectrum of the phase obtained by underdoping the charge density wave at half-filling, emphasizing the difference with the supersolid phase.

### T2.41 The classical-quantum divergence of complexity in the Ising spin Chain

Whei Yeap Suen\*, Jayne Thompson\*, Andrew Garner\*, Mile Gu\*, Vlatko Vedral\* (Centre for Quantum Technologies, National University of Singapore)

11:30am – 11:45am

Can quantum information fundamentally change the way we perceive what is complex? Here, we study statistical complexity, a popular quantifier of complexity that captures the minimal memory required to classically model a process. We construct a quantum variant of this measure, and evaluate it analytically for a classical Ising spin chain. The resulting complexity measure - quantum statistical complexity - exhibits drastically different qualitative behaviour. Whereas the classical statistical complexity of the spin chain grows monotonically with temperature, its quantum complexity rises to a maximum at some finite temperature then tends back towards zero for higher temperatures. This demonstrates that our notion of what is complex depends fundamentally on which information theory we employ.

### T2.73 Topological non-trivial States in Shastry-Sutherland Kondo Lattice Model

Munir Shahzad\*, Pinaki Sengupta\* (NTU/SPMS)

11:45am – 12:00pm

The charge-spin coupled systems arranged on geometrically frustrated lattices give rise to rich novel phases. Recently these systems have got much attention from the condensed matter community since the observation of Topological Hall effect in pyrochlore-structure compound such as  $\text{Nd}_2\text{Mo}_2\text{O}_7$  and  $\text{Pr}_2\text{Ir}_2\text{O}_7$ . We present the results of our study of the Kondo Lattice Model

on Shastry-Sutherland lattice. This model is a framework to study magnetic and electronic properties of the family of rare-earth tetraborides  $RB_4$ , where itinerant electrons interact with the localized moments on the rare earth ions. This interaction of the itinerant electrons strongly affects their properties inducing some non-conventional magnetic states and transport phenomena. For a particular set of the parameters involved in the Hamiltonian we have found the existence of non-coplanar ground state at itinerant electron density  $n_e = 1/4$  and  $3/4$ , on applying a longitudinal magnetic field there is a first order phase transition from this non-coplanar ground state to a Ferromagnetic state magnetic field. When magnetic field exceeds a critical strength we have found magnetization plateaus at itinerant electron density  $n_e = 1/2$ . To our knowledge this is the first time magnetization plateaus are being observed in Kondo lattice model on Shastry-Sutherland lattice. Also turning on the Dzyaloshinskii-Moriya interaction stabilizes the non-coplanar ground state over a wide range of parametric space.

### **T2.94 Strange correlator probe in transverse field Ising model**

Rakesh Kumar\*, Pinaki Sengupta (Nanyang Technological University)

12:00pm – 12:15pm

We have studied transverse field Ising model (TFIM) by measuring a recently proposed quantity termed as strange correlator in stochastic series expansion quantum Monte-Carlo framework. This correlator is a two-point correlation function of some local operator and measured at the interface of two different wave functions. Of which, one is a wave function under examination and the other some trivial wave function. The strange correlator is primarily used to distinguish trivial and nontrivial short-range entanglement states, and it works well in spin-1 Heisenberg antiferromagnets and generalized Kane-Mele-Hubbard model. In our work, we show that the results of strange correlator probe in TFIM agree well with the results of other probes. The log-log plot of strange correlator with respect to distance is nearly flat at zero magnetic field, shows power-law behaviour in the close vicinity of critical magnetic field, and decays exponentially at very high magnetic field. The critical points of quantum phase transition match well with the existing reliable results.

### **T3: Soft Condensed Matter**

Time: Monday 7 Mar, 11:15am; Venue: TT18; Chair: Julian Martinez MERCADO

Time allocated for invited talks is 20 min speaking time, plus 5 min Q&A, and time allocated for contributed talks is 12 min speaking time plus 3 minutes Q&A.

#### **T3.144 In-situ imaging of nanobubbles with Transmission Electron Microscope (TEM) - Observations and Analysis**

Meera Kanakamma Mohan\*, Beng Hau Tan, Zahava Barkay, Utkur Mirsaidov, Claus-Dieter Ohl (NTU)

11:15am – 11:30am

In situ transmission electron microscopy is a powerful technique for imaging of liquids with high spatial and temporal resolution. In this work, we imaged confined water trapped between graphene layers which are called as “graphene liquid cells” with TEM. Interestingly, we observed that the nanobubbles formed inside the liquid cells as a result of the radiolytic break down of the etchant used for preparing graphene liquid cells are stable for hours in the absence of the beam and persists only for  $\approx 10$ s in the presence of the beam. The predictions of sub-second dissolution by Classical theories are violated by this observations. Using graphene liquid cells, we also observed various bubble dynamics like shrinkage, coalescence, liquid film retraction etc.

#### **T3.121 Insights from the dynamic imaging of nanobubbles**

Beng Hau Tan\*, Hongjie An\*, Zahava Barkay, Utkur Mirsaidov, Meera Mohan, Claus-Dieter Ohl\* (Nanyang Technological University)

11:30am – 11:45am

Nanobubbles are nanoscale gaseous domains that are found in bulk liquids or attached onto surfaces immersed in liquids. However, progress in understanding the fundamental properties of nanobubbles is limited, due to the use of ‘blind’ or ‘slow’ methods of characterisation such as atomic force microscopy (AFM), which cannot capture dynamic processes. In this talk I discuss some insights we have gleaned from studying nanobubbles in various modes of dynamic imaging.

First, we use a transmission electron microscope to study the merger and shrinkage of bulk nanobubbles of radius  $\approx 10$  nm that are nano-confined in water between graphene sheets. These bubbles are remarkably stable, surviving for  $\approx 10$  s under an electron beam and for several hours without. With the aid of simple scaling relations and diffusion theory, we show that this enhanced stability is provided by the very high viscosity of the confined water.

The contact line pinning of a nanobubble is an important quantity that various research groups have attempted to estimate, without success. The second half of my talk covers the pulling and depinning of nanobubbles using an AFM tip. The dynamics of this process can be observed with optical microscopy, allowing us to quantify the pinning force on a nanobubble for the first time.

### **T3.80 Bioinspired nanomotors made of engineered DNA molecules**

Long Ying Loh\* (National University of Singapore)

11:45am – 12:00pm

Many important biological processes such as intracellular organelle transport, cell division, and muscle contraction are powered by biological motors like kinesins, dyneins, and myosins. These motors bind to and walk along specific tracks, converting chemical energy (ATP hydrolysis) to mechanical work. Inspired by these biological nanomotors, artificial track-walking nanomotors are developed and could be critical for constructing nanomachines that perform sophisticated tasks. Despite the efforts, inventing these nanomotors remains challenging. We borrow the concept of modular design found in modern cars, spatially and functionally separated engine for energy consumption and force generation and wheels for track binding, to reduce the technical requirements for self-directed nanomotors. Found on this modular design principle, we devised a bipedal DNA nanomotor that is waste-free and beyond the previously reported burn-the-bridge types. This modular design principle bears remarkable resemblance to biological motor dynein and has the potential to convert many bi-state nanoswitches into self-directed nanomotors.

### **T3.119 Droplets on inclined superhydrophobic surfaces: from a sandwiched to a jumping motion**

Julian Martinez Mercado\*, Claus-Dieter Ohl (PAP-SPMS NTU)

12:00pm – 12:15pm

In recent years, the motion of liquid droplets on superhydrophobic substrates has frequently been a research topic within the fluid dynamics community. Yet the effect of confinement or transport of within the droplet has received little attention. In this work we focus on the effect that confinement has on the motion of a droplet. For this purpose, two cell geometries are considered. In the first one, a droplet is confined between two superhydrophobic plates (Hele-Shaw cell), for the second geometry only the initial half of the cell consists of two plates (semi Hele-Shaw cell), hence the droplet is released from the confinement. The cells are inclined such that gravity drives the droplet motion. The dynamics is captured from two views to reveal centre of mass motion and the three dimensional motion. We also image the flow inside the droplet by means of a laser light sheet illumination and fluorescence particles. Additionally, 2D volume of fluid simulations are also performed. We found that the flow inside a sandwiched droplet corresponds to a plug flow, i.e. trajectories of fluid particles are nearly straight lines parallel to the substrate. Droplets being released jump off the substrate converting considerable amount of the surface energy into potential energy. In this case, we observe that the flow inside the droplet changes from the plug flow case to a rotational (vortex like) one. The numerical simulations show similar features as the experimental observations.

### **T3.138 Photoacoustic shock wave emission and cavitation from structured optical fiber tips**

Milad Mohammadzadeh\*, Silvestre Roberto Gonzalez-Avila, Yin Chi Wan, Xincan Wang, Hongyu Zheng, Claus-Dieter Ohl (Nanyang Technological University)

12:15pm – 12:30pm

Optical fibers are commonly used in medical applications for laser ablation of tissue. Strong thermoelastic waves could be emitted upon absorption of a high-intensity laser pulse on the tip of a fiber optic. If the fiber tip is flatly cleaved, these waves consist of a planar compressive shock wave, followed by tensile diffraction waves that form a cavitation cloud along the fiber axis. We demonstrate that modifying the geometry of the fiber tip changes the photoacoustic field and the resulting cavitation cloud. Particularly, by using structured fiber tips multiple shock waves can be emitted from a single laser pulse and strong tensile stress can be generated away from the fiber axis. The shock waves emitted from five different tip structures are studied experimentally using stroboscopic photography and pressure measurements with a hydrophone. The experimental observations agree quantitatively with numerical solutions of the linear wave equation. The complex photoacoustic fields achieved by structured fiber tips may be useful for simulating histotripsy effects via surgical catheters for enhanced ablation of soft tissue in micro scale.

## **T4: Optics and Photonics 1**

Time: Monday 7 Mar, 1:30pm; Venue: TT16; Chair: Joe FITZSIMONIS

Time allocated for invited talks is 20 min speaking time, plus 5 min Q&A, and time allocated for contributed talks is 12 min speaking time plus 3 minutes Q&A.

### **T4.2 Engineering high brightness and high efficiency in downconversion sources**

Brigitta Septriani\*, James Grieve, Kadir Durak, Alexander Ling (Centre for Quantum Technologies)

1:30pm – 01:45pm

We present the first systematic investigation into the performance of photon pair sources based on spontaneous parametric downconversion in thick crystals. We investigate a Type I collinear experimental geometry built around a  $\beta$ -Barium Borate (BBO) crystal which produces non-degenerate photon pairs in the visible and near-infrared.

We observe a broadening in the spectrum of the downconverted light when compared to numerical simulation, which we associate with an effective interaction length defined only by the overlap of the pump and collection modes within the crystal volume. This contrasts with commonly used “thin-crystal” geometries, in which the interaction length is defined by the length of the crystal. We note that this reduction in the effective interaction length is the result of spatial walk-off of the pump beam, and conduct a systematic mapping of the brightness and efficiency that can be achieved using a variety of pump and collection mode sizes. Our data convincingly demonstrates high brightness and efficiency over a range of focusing conditions, highlighting the robust nature of this source design.

This work will be of interest to optical designers and those involved in the construction and operation of photon pair sources, particularly where high brightness and efficiency are required simultaneously. Field deployment of these devices often imposes strict limits on size, weight and power (SWAP), and we believe the adoption of a thick-crystal BBO strategy may open up new opportunities for entangled photon pair sources in real-world scenarios.

### **T4.5 A scheme for estimating accidental coincidence rates between saturated single photon detectors: the effective duty cycle**

James A. Grieve\*, Zhongkan Tang, Rakhitha Chandrasekara, Cliff Cheng, Alexander Ling\* (Centre for Quantum Technologies)

01:45pm – 02:00pm

In the field of quantum photonics, the correlated detection of single photons is a routine task, with applications in experiments as diverse as metrology and quantum key distribution. In any such experiment, two or more single photon detectors are operated in parallel, with their signals combined via hardware or post-processing to produce a coincidence signal.

Since two uncorrelated streams of photons will occasionally produce coincidences by chance, care must be taken to minimise the contribution of such “accidental” coincidences, typically by operating the entire experiment at a very low throughput. In many cases however, it is sufficient to simply subtract these spurious events in post-processing, for which a good estimation of their

rate is essential. Unfortunately, such estimations typically require assumptions which are only valid at low rates, where the detector count rates respond in an approximately linear fashion to the incoming event stream. At higher rates, so-called “saturation” behaviour of the single photon detector results in markedly non-linear behaviour, reducing the useful range of event rates which can be detected.

In this presentation we discuss a general method for estimating rates of accidental coincidence at rates commonly associated with these saturation effects and non-linear behaviour. By combining the effects of the recovery time of both detector circuits and the waiting-time statistics of the light source into an “effective duty cycle” we are able to accommodate arbitrarily complex recovery behaviour at high event rates.

In our discussion, we provide a detailed high-level model for the recovery process of passively quenched avalanche photodiodes, and demonstrate effective accidental coincidence subtraction at rates commonly considered outside of the range of these detectors. By post-processing experimental data using our model, we observe an improvement in the visibility of polarization correlation fringes from 88.7% to 96.9% over a large dataset with highly varying flux.

We believe this technique will be useful in improving the signal-to-noise ratio in applications which depend on coincidence measurements, especially in situations where rapid changes in flux may make a rate-limiting strategy impossible. Although we will present a detailed treatment for passively quenched APDs, we emphasise the very general nature of this estimation strategy, and will provide explicit protocols for its application to arbitrary detector technologies and incoming event statistics.

#### **T4.10 Spin transport of exciton-polaritons in low-dimensional systems with disorder**

Anastasiia Pervishko\*, Vincent Sacksteder Iv, Ivan Shelykh (Nanyang Technological University)

02:00pm – 02:15pm

In past decades an idea to use spin properties of various particles as alternative ingredient in novel technological devices gave a start for a new field of physics, called spintronics. Since carrier spin evolves with time and depends on structure parameters, nowadays, one of the fundamental challenges in spintronics is to find a way to control the initial spin direction and predict its dynamics.

In this work, we show theoretically the prospects for creation of spin states with selected direction and the effects leading to initial alignment loss in polariton systems with disorder. In particular, we demonstrate that in a two-dimensional system the spin-orbit and Zeeman splittings acting separately or in combination result in the transfer from in-plane spin state to out-of-plane spin state, and contrariwise. We also show the appearance of spin multipole spin patterns in the plane of the system, which under the influence of external magnetic field start to rotate and twist with strong dependence to the spin-orbit interaction strength. In addition, we discuss the difference between prevalent spin relaxation mechanisms, such as Elliott-Yafet and D'yakonov-Perel' regimes, which can be used for theoretical prediction of spin evolution and estimation of the spin-orbit strength in diffusive regime.

#### **T4.25 Switching Waves in Multi-Level Incoherently Driven Polariton Condensates**

Helgi Sigurdsson\*, Ivan Shelykh, Timothy Liew (Nanyang Technological University - SPMS)  
02:15pm – 02:30pm

It can be shown theoretically that an open-dissipative microcavity exciton-polariton condensate confined within a generic 2D trapping potential in the plane of the microcavity quantum well gives rise to bistability between odd and even eigenmodes of the trapping potential. The origin of the bistability comes from driving the system by an incoherent pumping scheme which causes non-trivial rates of polariton generation in different eigenmodes of the potential.

Switching from one bistable state to the other can be controlled via incoherent pulsing which becomes an important step towards construction of low-powered optoelectronic devices. The effect can be explained as a modulational instability between odd and even states of the trapping potential governed by the nonlinear polariton-polariton interactions.

#### **T4.152 “Remote Control” of coherent absorption with quantum metamaterials**

Charles Altuzarra\*, Stefano Vezzoli, Joao Valente, Cesare Soci, Daniele Faccio, Christophe Couteau, Nikolay Zheludev\* (CDPT/Optoelectronics Research Centre and Centre for Photonic Metamaterials, University of Southampton)  
02:30pm – 02:45pm

Here we show the first experimental demonstration of controlling coherent absorption of a plasmonic metamaterial remotely by acting on the polarization of entangled photon pairs. By introducing one of the entangled photons in an interferometer, we demonstrate that by measuring the polarization state of its twin photon, we can nonlocally control absorption and plasmon generation in the subwavelength thin metamaterial absorber.

## **T5: Energy Conversion and Storage**

Time: Monday 7 Mar, 1:30pm; Venue: TT17; Chair: YANG Hui Ying

Time allocated for invited talks is 20 min speaking time, plus 5 min Q&A, and time allocated for contributed talks is 12 min speaking time plus 3 minutes Q&A.

### **T5.128 3D whisker-like $\text{Co}_3\text{O}_4@ \text{Co}_3\text{S}_4$ nanoarrays as cathode materials for flexible pseudocapacitor**

Bo Liu, Hui Ying Yang\* (SUTD)

1:30pm – 01:45pm

To design and develop hierarchical hybrid  $\text{Co}_3\text{O}_4@ \text{Co}_3\text{S}_4$  nanostructure with large specific surface area, high electron conductivity and excellent energy storage capability for electrochemical application, we have successfully synthesized the 3D whisker-like  $\text{Co}_3\text{O}_4@ \text{Co}_3\text{S}_4$  nanoarrays on Ni foam as cathode materials. The ultrathin and large-scale  $\text{Co}_3\text{S}_4$  whiskers were fully grown onto the mesoporous  $\text{Co}_3\text{O}_4$  NNAs with  $\text{Co}_3\text{O}_4$  as capacitive core and  $\text{Co}_3\text{S}_4$  as highly conductive shell. The core/shell structure can increase the contact in an electrolyte, enable the fast redox reaction, and protect the inner  $\text{Co}_3\text{O}_4$  core as a result of promoting long cycling stability. From advantages of the synergistic contribution from the structure composition, the resulting  $\text{Co}_3\text{O}_4@ \text{Co}_3\text{S}_4$  electrode exhibits a high capacitance of  $1284.3 \text{ F}\cdot\text{g}^{-1}$  at  $2 \text{ mV}\cdot\text{s}^{-1}$  with a capacitance retention of 93.1%. Moreover, a solid asymmetric supercapacitor composed of  $\text{Co}_3\text{O}_4@ \text{Co}_3\text{S}_4//\text{AC}$  exhibits excellent electrochemical performance, which can drive the DC motor for 5 min or power five LEDs for 10 min after full charging. This facile electrode preparing process may also open up a new opportunity for fabricating next generation energy storage devices.

### **T5.91 (INVITED) Energy Storage studies on thin and bulk materials**

M V Reddy\* (National University of Singapore)

01:45pm – 02:10pm

Commercial lithium ion batteries (LIBs) use layer-type compounds, lithium cobalt oxide ( $\text{LiCoO}_2$ ) or  $\text{LiFePO}_4$  as the cathode (positive electrode) and graphite (C) as the anode (negative electrode) material, and a non-aqueous Li- ion conducting electrolyte. The liquid electrolyte in the form of a solution or immobilized in a gel-polymer. LIBs with an operating voltage of 3.6 V are extensively used in the present-day portable electronic devices like, cell phones and other low power operated devices. For high-power applications like, electric/hybrid electric vehicles and back-up power supplies and, the LIBs need to satisfy several criteria, namely, cost-reduction, improvement in the energy density, safety-in-operation at high current charge/discharge rates and improvement in the low-temperature-operation. To satisfy the above criteria, researches are being carried out worldwide to find alternative novel nanostructured electrode materials. In my talk, I will discuss our group studies on thin and bulk select metal oxides and nitrides electrode materials for Li-ion batteries. Also our recent studies on graphene and its metal oxide composites. Specifically, i will focus on nano- CoN, Ni doped CoN, CrN, MO (M=Co,Ni, Cu, Mn) and metal oxides graphene composites. Materials were prepared variety of chemical methods It includes Rf-sputtering, molten salt method, carbothermal/Grapheno reduction method and ammonolysis

methods. Materials were characterized by Rietveld refinement X-ray diffraction, X-ray absorption spectroscopy, Raman, XPS, SEM, TEM, density and BET surface area methods. Electro analytical studies like cyclic voltammetry, galvanostatic cycling and electrochemical impedance spectroscopy techniques

### **T5.89 Synthesis and structural studies of Sodium electrodes for rechargeable batteries**

Rayavarapu Prasada Rao\*, Stefan Adams\* (National University of Singapore)

02:10pm – 02:25pm

Sodium ion batteries attracted large research community because of earth-abundance and low cost of sodium. Despite the cost motivation of the research a considerable fraction of this activity still focuses on cathode materials analogous to those in Li-ion batteries containing costly transition metals such as Co, which appears problematic for various reasons: differences in reaction mechanisms of the Na analogues to the Li transition metal oxides, different structural requirements for  $\text{Na}^+$  mobility, the fact that a cost advantage of Na over Li will only translate into low cost batteries. Hence, research on transition metal electrode materials for Na-ion batteries will have to concentrate on abundant transition metals (essentially Fe, Ti, Mn, and possibly Cr, V). On the other hand, O3-type  $\text{NaFeO}_2$ , and P2-type  $\text{Na}_x[\text{Fe}_{0.5}\text{Mn}_{0.5}]\text{O}_2$  utilizing the  $\text{Fe}^{4+}/\text{Fe}^{3+}$  redox couple are known to suffer from limited reversible capacity and low operating potential. Here we report the preparation of  $\text{Na}_2\text{Fe}(\text{SO}_4)_3$  and structural variation with temperature. The target compound was synthesized by mechanical milling of stoichiometric amounts of  $\text{Na}_2\text{SO}_4$  and  $\text{FeSO}_4$  followed by annealing at  $400^\circ\text{C}$  under argon environment. The  $\text{Na}_2\text{Fe}(\text{SO}_4)_3$  formed with lattice constants  $a=12.654(1)\text{\AA}$   $b=12.761(9)\text{\AA}$   $c=6.503(5)\text{\AA}$ ,  $\beta=115.52(1)^\circ$  with space group C12/c. When it comes to anode transition metal oxides, the number of low potential lithium insertion compounds is rather limited owing to the competition of insertion vs conversion reactions, the former being only favored for early 3d metal (Ti, V) oxides. Along that line,  $\text{Na}_x\text{VO}_2$  was recently found to reversibly react with Na at ca. 1.5 V but sensibly lower operation voltages would be needed for enhanced energy density. Titanium-based systems are considered as best alternatives.  $\text{Na}_2\text{Ti}_3\text{O}_7$  was prepared from anatase  $\text{TiO}_2$  and anhydrous  $\text{Na}_2\text{CO}_3$  mixtures with 10% excess of the latter with respect to stoichiometric amounts. These mixtures were milled and treated at  $800^\circ\text{C}$  for 20 h with intermediate regrinding. X-ray diffraction pattern indicated the formation of pure crystalline phase as shown in the figure with space group P121/m. A modified BV approach [1] is used to locate ‘accessible’ sites for a mobile  $\text{Na}^+$  ion in a local structure model. Using empirical relationships between the bond length, R and a bond valence  $s_{\text{Na}^+-\text{X}} = \exp[(R_0 - R)/b]$  with bond-softness adjusted values of the parameter b, sites are considered to be accessible, if the bond valence sum (BVS),  $V(\text{Li})$ , over the  $s_{\text{Na}-\text{X}}$  from all adjacent counterions, X approaches the ideal valence,  $V_{\text{id}}(\text{Li})$  (which equals its oxidation state). Ion transport pathways are then identified with regions of low values of BVS mismatch for a hypothetical  $\text{Na}^+$  ion.

### **T5.18 Integrated Photo-supercapacitor based on PEDOT Modified Printable Perovskite Solar Cell**

Jing Xu, Zhiliang Ku, Hong Jin Fan\* (PAP-SPMS Nanyangtechnological University)

02:25pm – 02:40pm

Solar-charging power source is highly useful for portable electronic devices. Previous reports are all based on wire-connected tandem cells. Here, we present an individual photo-supercapacitor cell (PSC) by integrating a printable perovskite solar cell and a supercapacitor to realize simultaneous energy conversion and storage. Bridged by a PEDOT-carbon electrode, the photo-generated charges are stored in situ into supercapacitor electrodes without external wire connection. This device delivers a maximum overall efficiency up to 4.70 % with a high energy storage efficiency of 73.77 %. Furthermore, it is also found that the work function of the carbon-PEDOT top electrode can be tuned by charging the supercapacitor, thus affecting the PSC open circuit voltage.

### **T5.118 The Surface and Bulk Photophysics in Organic-inorganic Halide Perovskite Single Crystals**

Bo Wu, Huy Tiep Nguyen, Hong Jin Fan, Tze Chien Sum\* (Nanyang Technological University)

02:40pm – 02:55pm

Solution-processed organic-inorganic halide perovskite single crystals have recently gained great popularity as materials for optoelectronic applications in photovoltaics, photo detections, etc. In this work, we present an all-optical approach to distinguish the surface kinetics from the bulk kinetics in the representative MAPbBr<sub>3</sub> and MAPbI<sub>3</sub> SCs using the ubiquitous transient spectroscopy techniques of transient photoluminescence and transient absorption spectroscopy. The surface region was photoexcited using single photon-absorption (1PA) while the true bulk region was stimulated using two-photon absorption (2PA). For the representative MAPbBr<sub>3</sub> SC system, contrasting differences in the recombination dynamics are found with the bulk lifetime of  $\approx 34$  ns shortening significantly to  $\approx 1$  ns at the surface. The surface trap density is estimated to be around two order larger than that of the bulk. Correspondingly, the bulk carrier diffusion lengths are  $\approx 2.6$ - $4.3 \mu\text{m}$  as compared to only  $\approx 130$ - $160$  nm near the surface.

## **T6: Quantum Information**

Time: Monday 7 Mar, 1:30pm; Venue: TT18; Chair: Valerio SCARANI

Time allocated for invited talks is 20 min speaking time, plus 5 min Q&A, and time allocated for contributed talks is 12 min speaking time plus 3 minutes Q&A.

### **T6.34 (INVITED) Universal optimal device-independent witnessing of quantum channels**

Michele Dall'Arno\*, Sarah Brandsen\*, Francesco Buscemi (Centre for Quantum Technologies, National University of Singapore)

1:30pm – 01:55pm

Quantum channels, including state preparations, measurements, and their most general transformations, comprise the fundamental building blocks of any experiment involving quantum systems. Quantum process tomography, the standard method to characterize any unknown quantum channel provided as a "black-box", is affected by a circular argument: in order to obtain meaningful information, one needs a full characterization of the tomographic preparation and measurement.

In arXiv:1511.05260 we break this loop by designing an operational framework able to universally and optimally characterize any unknown quantum channel provided as a "black-box" in a device-independent fashion, namely drawing upon the sole assumption that quantum theory is valid. That is, given any (thus universality) experimentally observed input-output statistics, we rule out all (thus optimality) channels that are incompatible with it. As a proof of principle, we apply our framework to the device-independent witnessing of any finite-dimensional unitary, trace-class, erasure, depolarizing, or amplitude-damping channel.

### **T6.52 Powerful charging of quantum batteries**

Sai Vinjanampathy\*, Felix Binder, John Goold, Kavan Modi (Centre for Quantum Technologies, NUS)

01:55pm – 02:10pm

We study the problem of charging a quantum battery in finite time. We demonstrate an analytical optimal protocol for the case of a single qubit. Extending this analysis to an array of  $N$  qubits, we demonstrate that an  $N$ -fold advantage in power per qubit can be achieved when global operations are permitted. The exemplary analytic argument for this quantum advantage in the charging power is backed up by numerical analysis using optimal control techniques. It is demonstrated that the quantum advantage for power holds when, with cyclic operation in mind, initial and final states are required to be separable.

## **T6.42 Non-local games and optimal steering at the boundary of the quantum set**

Yi-Zheng Zhen, Koon Tong Goh\*, Yu-Lin Zheng, Wen-Fei Cao, Xingyao Wu, Kai Chen, Valerio Scarani (Centre for Quantum Technologies, National University of Singapore)

02:10pm – 02:25pm

The violation of Bell inequalities is one of the clearest examples in which quantum resources outperform classical ones: the outcomes of local measurements on a shared entangled quantum state cannot in general be reproduced by reading shared classical information. In other words, the quantum set of probability distributions is strictly larger than the (classical) local set. It is also known that shared entanglement cannot be used at a later time to exchange a message, but quantum theory does not achieve all the possible no-signaling probability distribution.

The resources “shared quantum states” thus hang somehow between two easily formulated types of resources. This observation has triggered the effort to find a physical or information-theoretical principle that would identify the quantum set. However, formulation at the level of probability distributions failed to reach the quantum set [1]. On the other hand, Oppenheim and Wehner (OW) proved that the point of maximal Bell violation by quantum resources is characterized by both full steerability and an amount of certainty as high as allowed by some uncertainty relations for several examples [2].

A link between bipartite nonlocality and local uncertainty relations is definitely an observation worth closer scrutiny. In particular, it is natural to ask whether the link holds beyond the examples studied by OW, and ultimately for the whole of the boundary of the quantum set. A few months ago, Ramanathan and coworkers answered negatively, by producing explicit counterexamples to the OW link [3]. In this paper, we show that these counterexamples can be circumvented by exploiting an arbitrariness in the definition of non-local games. We then proceed to show that the OW link holds for a much larger portion of the quantum boundary than previously proved, and conjecture that it may hold for all of it.

[1] Nat. Comm. 6, 6288 (2015) [2] Science 330, 1072 (2010) [3] arXiv:1506.05100 (2015)

## **T6.67 Permutation-invariant codes encoding more than one qubit**

Yingkai Ouyang\*, Joseph Fitzsimons (Singapore University of Technology and Design)

02:25pm – 02:40pm

A permutation-invariant code on  $m$  qubits is a subspace of the symmetric subspace of the  $m$  qubits. We derive permutation-invariant codes that can encode an increasing amount of quantum information while suppressing leading order spontaneous decay errors. To prove the result, we use elementary number theory with prior theory on permutation invariant codes and quantum error correction.

## **T6.81 Implementation of bipartite or remote unitary gates with repeater nodes**

Li Yu\*, Kae Nemoto (National Institute of Informatics (Japan))

02:40pm – 02:55pm

We propose some protocols to implement various classes of bipartite unitary operations on two remote parties with the help of repeater nodes in between. We also present a protocol to im-

plement a single-qubit unitary with parameters determined by a remote party with the help of up to three repeater nodes. It is assumed that the neighboring nodes are connected by noisy photonic channels, and the local gates can be performed quite accurately, while the decoherence of memories is significant. A unitary is often a part of a larger computation or communication task in a quantum network, and to reduce the amount of decoherence in other systems of the network, we focus on the goal of saving the total time for implementing a unitary including the time for entanglement preparation. We review some previously studied protocols that implements bipartite unitaries using local operations and classical communication (LOCC) and prior shared entanglement, and apply them to the situation with repeater nodes. We find that the protocols using piecewise entanglement between neighboring nodes often require less total time compared to preparing entanglement between the two end nodes first and then performing the previously known protocols. Some of the protocols work for an arbitrary bipartite unitary, hence the time needed by these protocols provide upper bounds for the total time needed to implement an arbitrary bipartite unitary as a function of the number of repeater nodes. We also prove the corresponding lower bounds when there is a small number of repeater nodes. The application to position-based cryptography is discussed.

## T7: Topological Systems

Time: Monday 7 Mar, 3:30pm; Venue: TT16; Chair: Jens MARTIN

Time allocated for invited talks is 20 min speaking time, plus 5 min Q&A, and time allocated for contributed talks is 12 min speaking time plus 3 minutes Q&A.

### T7.22 (INVITED) STM/STS Studies of Organic-2D Heterointerfaces

Andrew Wee\* (NUS)

3:30pm – 03:55pm

Graphene, an atomically thin layer of carbon, is a semi-metal that can be used in applications such as transparent conducting electrodes in flexible electronics. The electronic and chemical properties of graphene can be engineered through a variety of methods such as by molecular adsorption [1,2], or fabricating graphene nanoribbons [3,4]. Unlike graphene, transition metal dichalcogenides (TMDs) such as MoS<sub>2</sub> and WSe<sub>2</sub>, are semiconductors with tunable direct bandgaps dependent on the number of atomic layers, and have potential electronic and optoelectronic applications. We use high resolution scanning tunneling microscopy/spectroscopy (STM/STS) to study the atomic structure and intrinsic electronic properties of MoS<sub>2</sub> layers (mono-, bi-, tri-) directly deposited on HOPG substrates by chemical vapour deposition (CVD) [5]. We report an unexpected bandgap tunability with distance from the grain boundary in single-layer MoS<sub>2</sub>, which also depends on the grain misorientation angle. We have similarly investigated the atomic scale electronic properties of CVD-grown WSe<sub>2</sub> monolayers as well as their interactions with molecules. In particular we show that a monolayer TMD can effectively screen an Organic-Inorganic Heterointerface [6]. We also demonstrate giant photoluminescence enhancement in WSe<sub>2</sub>-gold plasmonic hybrid structures [7].

[1] W. Chen, S. Chen, D.C. Qi, X.Y. Gao, A.T.S. Wee, *J. Am. Chem. Soc.* 129 (2007) 10418. [2] H.Y. Mao, Y. Hong, Y.H. Lu, J.D. Lin, S. Zhong, A.T.S. Wee, W. Chen, *Prog. Surf. Sci.* 88 (2013) 132. [3] H. Huang, D.C. Wei, J.T. Sun, S.L. Wong, Y.P. Feng, A.H. Castro Neto, A.T.S. Wee, *Scientific Reports* 2 (2012) 983. [4] D.C. Wei, L.F. Xie, K.K. Lee, Z.B. Hu, S.H. Tan, W. Chen, C.H. Sow, K.Q. Chen, Y.Q. Liu, A.T.S. Wee, *Nature Commun.* 4 (2013) 1374. [5] Y.L. Huang, Y.F. Chen, W.J. Zhang, S.Y. Quek, C.H. Chen, L.J. Li, W.T. Hsu, W.H. Chang, Y.J. Zheng, W. Chen, A.T.S. Wee, *Nature Commun.* 6 (2015) 6298. [6] Y.J. Zheng, Y.L. Huang, Y.F. Chen, W.J. Zhao, G. Eda, C.D. Spataru, W.J. Zhang, Y.-H. Chang, L.-J. Li, D.Z. Chi, S.Y. Quek, A.T.S. Wee, *ACS Nano* (2016) DOI: 10.1021/acsnano.5b07314. [7] Zhuo Wang et al., *Nature Comm.*, under revision.

### T7.7 Heterointerface Screening Effects between Organic Monolayers and Monolayer Transition Metal Dichalcogenides

Yu Jie Zheng\*, Yu Li Huang, Yifeng Chen, Weijie Zhao, Yung-Huang Chang, Wenjing Zhang, Spataru Catalin Dan, Eda Goki, Lain-Jong Li, Dongzhi Chi, Su Ying Quek\*, Andrew Thye Shen Wee\* (NUS)

03:55pm – 04:10pm

The nature and extent of electronic screening at heterointerfaces and their consequences on energy level alignment are of profound importance in numerous applications, such as solar cells,

electronics etc. The increasing availability of two-dimensional (2D) transition metal dichalcogenides (TMDs) brings additional opportunities for them to be used as interlayers in “van der Waals (vdW) heterostructures” and organic/inorganic flexible devices. These innovations raise the question of the extent to which the 2D TMDs participate actively in dielectric screening at the interface. Here we study perylene-3,4,9,10-tetracarboxylic dianhydride (PTCDA) monolayers adsorbed on single-layer tungsten diselenide ( $\text{WSe}_2$ ), bare graphite and Au(111) surfaces, revealing a strong dependence of the PTCDA HOMO-LUMO gap on the electronic screening effects from the substrate. The monolayer  $\text{WSe}_2$  interlayer provides substantial – but not complete – screening at the organic/inorganic interface. Our results lay a foundation for the exploitation of the complex interfacial properties of hybrid systems based on TMD materials.

### **T7.63 2D materials: exploring the orthorhombic crystal classes**

Alexandra Carvalho\*, Aleksandr Rodin, Lidia Gomes, Leandro Seixas, Antonio Castro Neto\* (CA2DM, NUS)

04:10pm – 04:25pm

Black phosphorus has recently been brought to the limelight following the unveiling of the properties of its monolayer form, phosphorene. While most known 2D materials have hexagonal structures, resembling graphene, phosphorene has a curious wavelike structure that gives its properties an anisotropic flavor. In less than two years, the studies about phosphorene have been multiplying with exciting results including stress-induced metal to semiconductor transition, high carrier mobility, high optical absorption, superconductivity and thermoelectricity; and the list continues to grow. However, phosphorene is only one of a series of orthorhombic 2D materials with exciting properties. In this talk, we will consider what sets phosphorene aside from other 2D materials. Then, we will consider how the bandstructure of phosphorene-like group IV monochalcogenides makes them suitable for valleytronics applications. Finally, we will consider how multiferroic systems can be engineered from 2D oxides.

### **T7.126 Controlled Synthesis of Organic/Inorganic van der Waals Solid for Tunable Light-matter Interactions**

Lin Niu, Xinfeng Liu, Chunxiao Cong, Chunyang Wu, Di Wu, Tay-Rong Chang, Hong Wang, Qingsheng Zeng, Jiadong Zhou, Xingli Wang, Wei Fu, Qundong Fu, Sina Najmaei, Zhuhua Zhang, Boris I. Yakobson, Beng kang Tay, Peng Yu, Wu Zhou, Horng-Tay Jeng, Hsin Lin, Sum Tze Chien, Chuanhong Jin, Haiyong He\*, Ting Yu, Zheng Liu (Nanyang technological university)

04:25pm – 04:40pm

Van der Waals (vdW) solids, as a new type of artificial materials that consist of alternating layers bonded by weak interactions, have shed light on fascinating optoelectronic device concepts. As a result, a large variety of vdW devices have been engineered via layer-by-layer stacking of two-dimensional materials, although shadowed by the difficulties of fabrication. Alternatively, direct growth of vdW solids has proven as a scalable and swift way, highlighted by the successful synthesis of graphene/h-BN and transition metal dichalcogenides (TMDs) vertical heterostructures from controlled vapor deposition. Here, we realize high-quality organic and inorganic

vdW solids, using methylammonium lead halide (CH<sub>3</sub>NH<sub>3</sub>PbI<sub>3</sub>) as the organic part (organic perovskite) and 2D inorganic monolayers as counterparts. By stacking on various 2D monolayers, the vdW solids behave dramatically different in light emission. Our studies demonstrate that h-BN monolayer is a great complement to organic perovskite for preserving its original optical properties. As a result, organic/h-BN vdW solid arrays are patterned for red light emitting. This work paves the way for designing unprecedented vdW solids with great potential for a wide spectrum of applications in optoelectronics.

### **T7.66 Remarkable anisotropic phonon response in uniaxially strained few-layer black phosphorus**

Yanlong Wang\*, Chunxiao Cong, Ruixiang Fei, Weihuang Yang, Yu Chen, Bingchen Cao, Li Yang, Ting Yu (NTU)

04:40pm – 04:55pm

Strain serves an effective tool to tune the properties of 2D materials. By virtue of the excellent ability to sustain high strain and remarkably anisotropic mechanical properties as a result of the unique puckered structure, black phosphorus (BP) is deemed as a good candidate to further study strain effects on 2D materials following graphene and transition metal dichalcogenides. In this work, we report a systematic in situ strained Raman spectroscopy investigation of the phonon frequency dependence on crystallographic orientations in uniaxially strained few-layer BP. It is found that the out-of-plane  $A_g^1$  mode is sensitive to uniaxial tensile strain along armchair direction while the in-plane  $B_g^2$  and  $A_g^2$  modes are susceptible to zigzag direction strain. Under uniaxial strain applied along the direction roughly intermediate between the two edge orientations, all of the three phonon modes linearly redshift. Our density functional theory calculation results clearly illustrate the anisotropic influence of uniaxial strain on structural properties of few-layer BP owing to its unique puckered crystal structure and could be used to elucidate the striking dependence of strained phonon frequencies on crystal orientations. This work demonstrates the possibility of selective tuning of in-plane and out-of-plane phonon modes in BP by uniaxial strain and suggests that strain engineering holds a promising future for extensive modulation of optical and mechanical properties in 2D materials.

## **T8: Optics and Photonics 2**

Time: Monday 7 Mar, 3:30pm; Venue: TT17; Chair: NG Hui Khoon

Time allocated for invited talks is 20 min speaking time, plus 5 min Q&A, and time allocated for contributed talks is 12 min speaking time plus 3 minutes Q&A.

### **T8.28 (INVITED) Experimental Quantum Fingerprinting**

Juan Miguel Arrazola\*, Feihu Xu, Norbert Lutkenhaus, Hoi-Kwong Lo (Centre for Quantum Technologies)

3:30pm – 03:55pm

Quantum communication holds the promise of creating disruptive technologies that will play an essential role in future communication networks. For example, the study of quantum communication complexity has shown that quantum communication allows exponential reductions in the information that must be transmitted to solve distributed computational tasks. Here we report a proof-of-concept experimental demonstration of a quantum fingerprinting system that is capable of transmitting less information than the best known classical protocol. Our implementation is based on a modified version of a commercial quantum key distribution system using off-the-shelf optical components over telecom wavelengths, and is practical for messages as large as 100 Mbits, even in the presence of experimental imperfections. Our results provide a first step in the development of experimental quantum communication complexity.

### **T8.45 Using CubeSat nanosatellites for fundamental physics experiments.**

Robert Bedington\*, Daniel Oi, Alexander Ling\* (Centre for Quantum Technologies, NUS)

03:55pm – 04:10pm

Space is the ideal place for performing many fundamental physics experiments. It offers long lines of sight, microgravity, high relative velocities and varying gravitational potentials. Accordingly many physics missions have been imagined and proposed, including investigations into gravity waves, general relativity, Bose-Einstein condensates and cold atoms. Tangible development work towards such missions is often limited however due to high costs, long development times, launcher availabilities and national space policies.

The CubeSat standards for nanosatellites (satellites as small as 10cm<sup>3</sup>) however are revolutionising access to space. Increasingly, plug & play CubeSat subsystems and off-the-shelf CubeSat satellites are becoming available, and standardised launcher interfaces have created a flexible global market for launching them into space. CubeSats have enabled cheap, quick and regular access to space albeit with payload volumes and available power greatly reduced compared with traditional missions. While these tiny satellites cannot accommodate the experiments proposed for traditional satellites, the bar to entry is greatly lowered so small groups with innovative miniaturised experiments now have the chance to fly them in space. Such developments can also feed back into the traditional satellite development programmes to accelerate their development also.

With long range tests of entanglement and quantum key distribution in mind, CQT has been developing SPEQS (Spontaneous Photon Entangling Quantum System) miniaturised entangled photon sources. CubeSats enable a fast, iterative design methodology, so early SPEQS devices

have already been integrated and demonstrated on third-party CubeSats. Upcoming CubeSats assembled at CQT will host the second generation versions of the payload. This talk will cover our experiences so far in designing and building CubeSat satellites.

### **T8.59 Optimization of TM modes for Amorphous Slab Laser**

Shampy Mansha\*, Yidong Chong\*, Qi Jie Wang, Zeng Yongquan (Nanyang Technological University)

04:10pm – 04:25pm

Random lasers are lasers which confine light through multiple scattering in a random media. Due to their low spatial coherence, they may have applications in imaging and sensing. Recently, the first random laser emitting in the mid-infrared region was reported, based on a semiconductor QCL (quantum cascade laser) wafer with etched air holes. However, an important property of a QCL is that it supports TM (Transverse Magnetic) modes only, and there has not been much work on designing random structures supporting high-Q TM modes. We show numerically that high-performance TM-emitting random lasers can be realized using an amorphous lattice of dielectric rods joined by veins. For vein widths comparable to the rod radius, strong light confinement can be obtained due to the presence of short-range order, resulting in Q-factors at least two orders of magnitude larger than those reported in previous work.

### **T8.69 Rectification of light in the quantum regime**

Jibo Dai\*, Alexandre Roulet, Huy Nguyen Le, Valerio Scarani (CQT, NUS)

04:25pm – 04:40pm

On the road towards a quantum network built with integrated optoelectronic components, several devices have been proposed and studied. Two-level emitters (atoms) coupled strongly to one-dimensional (1D) waveguide have recently emerged as a prominent candidate in building this network. However, one of the key elements that is still missing is a rectifying device playing the role of an optical diode. Ultimately, one would like to achieve passive and state-independent rectification with such a device. A proposal based on a pair of atoms strongly coupled to a 1D waveguide showed a promising behavior based on a semi-classical study. In this work, we present a full quantum mechanical analysis of this set-up, both for coherent input pulse and single photon input pulse, using Heisenberg equations of motion. It is shown that, in such a device, rectification is a purely multi-photon effect. We find that the set-up under study cannot achieve rectification for single-photon states, contrary to the hope stated in the initial proposal. Fortunately, when the incident light is a coherent pulse, the efficiency of the diode can reach up to approximately 70% in a range of power, for suitable detuning of the atoms and interatomic distance, whereas no rectification is predicted for low and high power. By studying the dynamics of excitation of the two atoms, we obtain a clear physical picture for the origin of the rectification. For input field in a coherent state, rectification is high in which one of the two atoms is excited, but not both. This detailed understanding may inspire improved designs of passive and state-independent optical diodes.

### **T8.83 PT symmetry Breaking and Nonlinear Optical Isolation in Coupled Microcavities**

Xin Zhou\*, Yidong Chong\* (Nanyang Technological University)

04:40pm – 04:55pm

The implementation of compact optical isolators is a major research goal in integrated optics. Recently, record low-power on-chip optical isolators were experimentally demonstrated in a pair of coupled microcavities, using "PT symmetric" gain and loss within the microcavities along with nonlinear gain saturation. However, the reason for adopting a PT symmetric configuration was previously not well understood. Using coupled-mode theory, we show that the phenomenon of PT symmetry breaking in the linear regime is closely linked to the isolation ratio in the nonlinear regime. This analysis also indicates that the nonlinear isolation ratio can be tuned through several orders of magnitude by small shifts in the inter-cavity coupling strength.

### **T8.1 Survivor! Analysis of a photon pair source recovered intact from a catastrophic launch failure.**

Tang Zhongkan Xavier\*, Rakhitha Chandrasekara, Yue Chuan Tan, Cliff Cheng, Kadir Durak, Alexander Ling (National University of Singapore)

04:55pm – 05:10pm

Motivated by the vision of a global quantum communication network, we present a compact and rugged photon pair source that can be embedded into small cost-effective satellites called CubeSats. We report on the performance of one such photon pair source, recovered intact from the site of a catastrophic launch failure (Cygnus CRS Orb-3). The ability of the source to survive very dramatic conditions yields lessons for designers of practical quantum technology. It demonstrates that with adequate engineering quantum devices need not be delicate instruments confined to laboratory environments. Our work combines cutting-edge quantum engineering with the on-going revolution in small satellite systems and demonstrates that the financial and technical barriers to scientific experiments in space are rapidly falling. In this talk, we will discuss the steps taken in assembling the source, discuss how possible points of failure can be addressed in future designs, and describe future missions that are in the pipeline.

## **T9: Atomic, Molecular and Optical Physics 1**

Time: Monday 7 Mar, 3:30pm; Venue: TT18; Chair: Shau-Yu LAN

Time allocated for invited talks is 20 min speaking time, plus 5 min Q&A, and time allocated for contributed talks is 12 min speaking time plus 3 minutes Q&A.

### **T9.55 (INVITED) Time-resolved Scattering of a Single Photon by a Single Atom**

Victor Leong, Mathias Alexander Seidler\*, Matthias Steiner, Alessandro Cere, Christian Kurt-siefer (Centre for Quantum Technologies, NUS)

3:30pm – 03:55pm

The efficiency of light-matter interfaces between single photons and single atoms depends on the bandwidth and temporal shape of the single photon, and is crucial for realistic implementations of many quantum information protocols. In particular, an exponentially rising single photon is predicted to excite a single atom with a higher efficiency compared to any other temporal shape [1].

A four-wave mixing photon pair source, in conjunction with an asymmetric cavity, generates heralded single photons of tunable bandwidth with exponentially decaying or rising shapes [2,3]. We combine the photon pair source with a trapped single atom and investigate the free space scattering for different bandwidths and temporal shapes.

We study the scattering dynamics by measuring the atomic emission and the reduction in the number of transmitted photons. We observe that the atomic absorption dynamics are imprinted in the single-photon excitation mode.

[1] Y. Wang et al., PRA 83, 063842 (2011) [2] B. Srivathsan et al., PRL 111, 123602 (2013) [3] B. Srivathsan et al., PRL 113, 163601 (2014)

### **T9.40 A velocimeter based on enhanced light-dragging effect in electromagnetically induced transparency**

Pei Chen Kuan\*, Chang Huang, Shau-Yu Lan (Nanyang Technological University)

03:55pm – 04:10pm

I will present a new velocimeter based on the light-dragging effect. The new instrument enjoyed the enhancement by cold atoms with electromagnetically induced transparency (EIT), which improved the effect by orders of magnitude. Our measurement demonstrates the probability of setting up a motional sensor beyond the limitation of Doppler broadening in the future.

### **T9.48 Linear and nonlinear magneto-optical rotation on the narrow strontium intercombination line**

Kanhaiya Pandey, Chang Chi Kwong\*, Mysore Srinivas Pramod, David Wilkowski\* (SPMS, Nanyang Technological University; Centre for Quantum Technologies, National University of Singapore; Majulab CNRS-University of Nice-NUS-NTU International Joint Research Unit UMI 3654)

04:10pm – 04:25pm

In presence of an external static magnetic field, an atomic gas becomes optically active. The light transmitted through the gas displays a magneto-optical rotation (MOR) of its polarization. In the

saturated regime, the coherence among the excited substates gives a nonlinear contribution. In contrast with the linear magneto-optical rotation, the width of the nonlinear counterpart is insensitive to Doppler frequency shift. The narrow strontium intercombination line is probed in our experiment. Both the linear and nonlinear MOR effects are studied by varying the temperature of the atomic gas. For this narrow transition, the sensitivity to a small and static magnetic field is typically three orders of magnitude larger than for a standard broad transition in the alkali atoms. These experiments were performed using an active stabilization of the stray magnetic field.

### **T9.97 Molecular spectroscopy of ${}^6\text{Li}-{}^{40}\text{K}$ : Towards STIRAP transfer to absolute ground state.**

Sambit Pal\*, Mark Lam, Kai Dieckmann (Centre for Quantum Technologies)

04:25pm – 04:40pm

${}^6\text{Li}-{}^{40}\text{K}$  molecules in its absolute ground state have a large dipole moment of 3.6 debye, which makes them a suitable candidate for investigating long range dipole-dipole interactions. Starting from Feshbach molecules, we plan to transfer them to the ground state using stimulated Raman adiabatic passage (STIRAP). We give an overview of our single-photon spectroscopic measurements of the (1)1 $\Pi$  and (2)1 $\Sigma$  potentials of  ${}^6\text{Li}-{}^{40}\text{K}$  molecules. Latest results of 2-photon spectroscopic search for the deeply-bound vibrational states of the X1 $\Sigma$  ground-state potential, will also be presented.

### **T9.105 Progress towards an optical clock with Lu+**

Eduardo Paez, Kyle Arnold, Elnur Hajiyev, Murray Barrett\* (Centre for Quantum Technologies, NUS)

04:40pm – 04:55pm

We have recently identified singly ionizing Lu+ as a promising clock candidate. A unique set of atomic properties, and a novel averaging technique, provides a reference frequency with extremely low systematic shifts. In addition, we have shown that a judicious choice of operating conditions enables cancellation of important frequency shifts from the trapping fields themselves and from neighboring ions which provides the unique opportunity of implementing clock operation with a large Coulomb crystal. We will present our current progress towards this goal.

## **T10: 2D Materials - Future Directions**

Time: Tuesday 8 Mar, 10:00am; Venue: TT16

Time allocated for invited talks is 20 min speaking time, plus 5 min Q&A, and time allocated for contributed talks is 12 min speaking time plus 3 minutes Q&A.

### **T10.78 Transport properties of a two-dimensional electron gas dressed by light**

Skender Morina\*, Oleg Kibis, Ivan Shelykh (Nanyang Technological University)

10:00am – 10:15am

We show theoretically that the strong interaction of a two-dimensional electron gas (2DEG) with a dressing electromagnetic field drastically changes its transport properties. Particularly, the dressing field leads to a giant increase of conductivity (which can reach thousands of percents), resulting in nontrivial oscillating dependence of conductivity on the field intensity. As a consequence, the developed theory opens an unexplored way to control transport properties of 2DEG by a strong high-frequency electromagnetic field. From an experimental viewpoint, this theory is applicable directly to quantum wells exposed to a laser-generated electromagnetic wave.

### **T10.6 Topological Transistors Based on Dirac Semimetals and 2D Topological Insulators**

Ying Liu\*, Shengyuan Yang (Singapore University of Technology and Design)

10:15am – 10:30am

Topological materials, including topological insulators and topological semimetals, hold great promising for designing novel low-dissipation electronic devices. These materials have topological surface or edge states protected by the nontrivial topology of their band structures in the bulk. Here we present two separate designs of topological field effect transistors (TFET). The first one is based on a Dirac semimetal thin film. We show that it is possible to induce and control the topological phases in a Dirac semimetal thin film by using a vertical electric field, realizing a phase transition between a trivial band insulator and a quantum spin Hall insulator (QSHI). This offers a simple scheme to realize a TFET. Our second design is more close to the Datta-Das spin transistor, consisting of two ferromagnetic leads connected by a channel. However, instead of using the Rashba spin-orbit coupling in a semiconducting structure, we utilize the edge channels of a QSHI channel material. We show that the conductance of the device can be controlled in a simple and all-electric manner by a side-gate voltage, which effectively rotates the spin-polarization of the carrier. Our study provides promising routes to realize topological electronic devices, and these devices may also be used to probe the intriguing fundamental properties of topological materials.

Journal Ref: [1] Hui Pan, Meimei Wu, Ying Liu, and Shengyuan A. Yang. Electric control of topological phase transitions in Dirac semimetal thin films. *Scientific Reports*, 5, 14639 (2015). [2] Xianbo Xiao, Ying Liu, Zhangfang Liu, Guoping Ai, Shengyuan A. Yang, and Guanghui Zhou. All-electric spin transistor based on a side-gate-modulated two-dimensional topological insulator. *Applied Physics Letters*, accepted.

### **T10.49 Graphene Electrodynamics in the presence of the Extrinsic Spin Hall Effect**

Chun Li Huang\*, Yidong Chong, Giovanni Viganale, Miguel Cazalilla\* (National Tsing Hua University, Taiwan)

10:30am – 10:45am

We extend the electrodynamics of two dimensional electron gases to account for the extrinsic spin Hall effect (SHE). The theory is applied to doped graphene decorated with a random distribution of adsorbates that induce spin-orbit coupling (SOC) by proximity. The formalism extends previous semiclassical treatments of the SHE to the non-local dynamical regime. Within a particle-number conserving approximation, we compute the conductivity, dielectric function, and spin Hall angle in the small frequency and wave vector limit. The spin Hall angle is found to decrease with frequency and wave number, but it remains comparable to its zero-frequency value around the frequency corresponding to the Drude peak. The plasmon dispersion and linewidth are also obtained. The extrinsic SHE affects the plasmon dispersion in the long wavelength limit, but not at large values of the wave number. This result suggests an explanation for the rather similar plasmonic response measured in exfoliated graphene, which does not exhibit the SHE, and graphene grown by chemical vapor deposition, for which a large SHE has been recently reported. Our theory also lays the foundation for future experimental searches of SOC effects in the electrodynamic response of two-dimensional electron gases with SOC disorder.

### **T11: Solid State Physics 3**

Time: Tuesday 8 Mar, 10:00am; Venue: TT17; Chair: Ricky ANG

Time allocated for invited talks is 20 min speaking time, plus 5 min Q&A, and time allocated for contributed talks is 12 min speaking time plus 3 minutes Q&A.

#### **T11.19 A space-fractional model of space charge limited current**

Muhammad Zubair\*, L. K. Ang (Singapore University of Technology and Design)

10:00am – 10:15am

In general we can assume that space and space-time dimensions are of integer order. Non-integer (fractional) dimensional spaces and method of dimensional regularization are initially emerged in statistical mechanics and quantum field theory. Recently, the concept of fractional-dimensional space has been used as an effective physical description of restraint conditions in the physical systems. We will present some recent developments of space charge limited (SCL) current in the framework of fractional-dimensional space which may account for the effect of imperfectness or roughness of the electrode surface. For SCL current in free space, the governing law is known as the Child-Langmuir (CL) law. Its analogy in a trap-free solid (or dielectric) is known as Mott-Gurney (MG) law. This work extends the one-dimensional CL Law and MG Law for the case of  $\alpha$ -dimensional fractional space with  $0 < \alpha \leq 1$ ; where parameter  $\alpha$  defines the degree of roughness of the electrode surface. Such a fractional dimensional space generalization of SCL current theory can be used to characterize the charge injection by the imperfectness or roughness of the surface in applications related to high current cathode and organic electronics.

#### **T11.33 Solid State Materials for Magnetic Cooling : New Materials and Emerging Physics**

Mahendiran Ramanathan\* (National University of Singapore)

10:15am – 10:30am

Liquid Helium is indispensable not only for studying physics of matter but also for operation of superconducting magnets in MRI scanning, liquefaction of industrial gases and linear accelerators. To attain temperatures of the order of few tens of micro kelvin to  $\approx 1$  K, magnetic entropy of paramagnetic salts has been exploited in commercial adiabatic magnetic refrigerators (ADR). However, ferromagnetic and antiferromagnetic magnetic materials can be tailored to produce cooling effect (refrigeration) from room temperature down 1 K. Recently, there has been revival of interest in magnetic refrigeration near room temperature and also at cryogenic temperatures. In this talk, I will give a short overview of new magnetic materials and current technologies being developed worldwide, followed by some important contributions (in magnetic oxides) to this field from my laboratory in NUS.

### **T11.153 Experimental and theoretical evidence of the visible range plasmons in topological insulators**

Alexander M. Dubrovkin\*, Jun Yin, Giorgio Adamo, Yasaman Kiasat, Bo Qiang, Lan Wang, Qi Jie Wang, Cesare Soci, Nikolay I. Zheludev (Nanyang Technological University, Centre for Disruptive Photonic Technologies)

10:30am – 10:45am

Chalcogenide topological insulators were recently identified as plasmonic materials with highly conductive surface states, thus providing a novel platform for development of metamaterials. We report real-space observation of the visible range plasmons in  $\text{Bi}_{1.5}\text{Sb}_{0.5}\text{Te}_{1.8}\text{Se}_{1.2}$  (BSTS) topological insulator at optical wavelengths, where bulk permittivity is positive and therefore plasmonic response can only be attributed to the conductive surface states of the material. Direct near-field imaging of localized plasmons in nano and micro structures shows a clear evidence of dipolar and higher order surface plasmon modes with well-defined field amplitude and phase profiles. Experimental data are supported by full wave numerical simulations. We experimentally map propagating plasmons in both ultrathin and optically thick films of the material and match the experimental dispersion of BSTS plasmons with the numerically calculated one. We also report ab-initio band structure calculations explaining the origin of plasmonic response in chalcogenide compounds and perform a systematic study of the optical and plasmonic properties of a family of chalcogenide topological insulator compounds. Knowledge of surface charge distribution in thin TI slabs allows isolating plasmonic contribution coming from surface electrons, which indicates that a conventional three dimensional Drude model for a  $\approx 2$  nm metallic layer appropriately describes the optical response of the topologically protected surface states in the visible range. These results will help designing new hybrid electro-optical and plasmonic devices that exploit plasmonic peculiarities of the band structure and topologically protected surface in the chalcogenide compounds.

## **T12: Solid State Physics 4**

Time: Tuesday 8 Mar, 10:00am; Venue: TT18

Time allocated for invited talks is 20 min speaking time, plus 5 min Q&A, and time allocated for contributed talks is 12 min speaking time plus 3 minutes Q&A.

### **T12.85 Magnetoelectronic properties of graphene dressed by a high-frequency field**

Oleg Kibis, Skender Morina, Kevin Dini\*, Ivan Shelykh (University of Iceland)

10:00am – 10:15am

We solved the Schrödinger problem for electrons in graphene subjected to both a stationary magnetic field and a strong high-frequency electromagnetic wave (dressing field). The found solutions of the problem are used to describe the magnetoelectronic properties of dressed graphene. It follows from the analysis that both optical characteristics and electronic transport are very sensitive to the dressing field. Particularly, the field strongly changes the spectra of optical absorption and the Shubnikov-de Haas oscillations. As a result, the developed theory opens a way for controlling magnetoelectronic properties of graphene with light.

### **T12.74 Electron transport through double time-periodic barriers on silicene**

Yi Xu, Shengyuan Yang, Lay Kee Ang\* (Singapore University of Technology and Design)

10:15am – 10:30am

We applied a transfer matrix method to studying the photon-assisted charge transport through double time-periodic barriers on silicene. For zero energy gap silicene, the electrons in silicene show similar behaviors as that of Dirac Fermions in graphene. And the time reversal symmetry is broken by adding time-periodic potentials with a phase lag. The transmission asymmetry can be as high as almost 1 for the central band with a critical phase lag though there is no difference in the total transmission properties at normally incidence. The time reversal symmetry is also broken even without a phase lag for a gapped silicene. These features may be helpful in designing various novel silicene-based devices, such as electronic filters.

### **T12.68 Thermoelectric transport in the two-dimensional Bose-Hubbard model**

Jian-Ping Lv\*, Jian-Sheng Wang\* (Department of Physics, National University of Singapore)

10:30am – 10:45am

Using a large-scale quantum Monte Carlo simulation and the maximum entropy analytic continuation, we investigate various transport properties of the two-dimensional Bose-Hubbard model. In this talk we shall present a highly accurate estimate of universal charge conductivity at quantum critical point. We shall also discuss the Seebeck effect in a broad range of interaction strength and particle density, and reveal extremely high thermoelectric efficiencies under certain conditions.

## **T13: Atomic, Molecular and Optical Physics 2**

Time: Tuesday 8 Mar, 11:15am; Venue: TT16; Chair: Manas MUKHERJEE

Time allocated for invited talks is 20 min speaking time, plus 5 min Q&A, and time allocated for contributed talks is 12 min speaking time plus 3 minutes Q&A.

### **T13.61 Towards an atom interferometer inside an optical fiber.**

Mingjie Xin\*, Wui Seng Leong, Arpan Roy, Shau-Yu Lan (Nanyang Technological University)  
11:15am – 11:30am

Precision measurement with light-pulse grating atom interferometry in free space have been used in the study of fundamental physics and applications in inertial sensing. Recent development of photonic band-gap fibers allows light for traveling in hollow region while preserving its fundamental Gaussian mode. The fibers could provide a very promising platform to transfer cold atoms. Optically guided matter waves inside a hollow-core photonic band-gap fiber can mitigate diffraction limit problem and has the potential to bring research in the field of atomic sensing and precision measurement to the next level of compactness and accuracy. Here, we will show our experimental progress towards an atom interferometer in optical fibers. We designed an atom trapping scheme inside a hollow-core photonic band-gap fiber to create an optical guided matter waves system. The guiding potential is created by a far-off resonance dipole trap propagating inside the fiber with a hollow core of  $65 \mu\text{m}$ . In the guiding system, millions of atoms can be transferred through a 40 mm long piece of hollow core fiber. Here, I will present our experimental progress towards an atom interferometer inside an optical fiber.

### **T13.112 (INVITED) A quantum parametric oscillator with trapped ions**

Gleb Maslennikov\*, Shiqian Ding, Roland Hablutzel, Huanqian Loh, Dzmitry Matsukevich\* (Centre for Quantum Technologies, NUS)  
11:30am – 11:55am

We report experimental investigation of nonlinear coupling between two normal modes of motion in a system of two Yb171 ions. This coupling is induced by the anharmonicity of the Coulomb interaction between the ions and is equivalent to a degenerate optical parametric oscillator. We observe that under the resonance conditions two phonon Fock state in the radial out-of phase mode is coupled to a single phonon state in the axial mode, while the one phonon state in the radial mode does not evolve. We use this coupling to directly measure the parity of different quantum motional states and their corresponding Wigner functions.

### **T13.47 Doppler-free approach to optical pumping dynamics in the $6S_{1/2} - 5D_{5/2}$ electric quadrupole transition (E2) of Caesium vapour**

Eng Aik Chan\*, Syed Abdullah Aljunid\*, Nikolay Zheludev, David Wilkowski\*, Martial Ducloy\* (LPL/CDPT)  
11:55am – 12:10pm

The  $6S_{1/2} - 5D_{5/2}$  electric quadrupole transition is investigated in Caesium vapour at room temperature via nonlinear Doppler-free 6P-6S-5D three-level spectroscopy. Frequency-resolved studies of individual E2 hyperfine lines allow one to analyse optical pumping dynamics, po-

larization selection rules and line intensities. It opens the way to studies of transfer of light orbital angular momentum to atoms, and the influence of metamaterials on E2 line spectra.

### **T13.99 Production of fermionic 6Li quantum gas in a single optical transport trap**

Christian Gross\*, Jaren Gan, Kai Dieckmann (CQT)

12:10pm – 12:25pm

Lithium offers a broad Feshbach resonance that allows the tuning of the two-body interaction strength, enabling the experimental investigation of quantum many-body physics. We present our scheme for the efficient all-optical production of a fermionic Lithium quantum gas utilizing a simplified transport method. A crossed optical dipole trap (cODT) is loaded from a magneto-optical trap (MOT) on the narrow  $2S_{1/2} - 3P_{3/2}$  ultra-violet (UV) transition. For optimal optical access, the cODT is then displaced by 30 cm with a translation stage, which brings the atoms into a glass cell. A quantum degenerate Fermi gas or a molecular Bose-Einstein condensate (mBEC) is obtained by evaporative cooling of the atoms at selected magnetic fields. In our setup we have included a Channel Electron Multiplier for the detection of ions. This offers an alternative, highly sensitive probe of the atoms, which should allow the investigation of weak spectroscopic transitions, especially when used in conjunction with tunable two-body interactions.

### **T14: Optics and Photonics 3**

Time: Tuesday 8 Mar, 11:15am; Venue: TT17

Time allocated for invited talks is 20 min speaking time, plus 5 min Q&A, and time allocated for contributed talks is 12 min speaking time plus 3 minutes Q&A.

#### **T14.150 Dielectric Super-Oscillatory Lens for Achromatic Sub-Diffraction Focusing**

Guanghai Yuan\*, Edward Rogers, Nikolay Zheludev (Centre for Disruptive Photonic Technologies, Nanyang Technological University)

11:15am – 11:30am

We design and demonstrate an achromatic far-field sub-diffraction focusing device using dielectrics at the wavelengths of 1300 nm and 1550 nm.

#### **T14.151 Switching negative refraction in a hyperbolic metamaterial**

Harish N. S. Krishnamoorthy\*, Behrad Gholipour, Nikolay Zheludev, Cesare Soci\* (Center for Disruptive Photonic Technologies, Nanyang Technological University)

11:30am – 11:45am

We report our work on developing a reconfigurable hyperbolic metamaterial (HMM). We accomplished this by using the chalcogenide alloy  $\text{Ge}_2\text{Sb}_2\text{Te}_5$  (GST) as one of the constituents of a multilayer HMM. By exploiting the reversible amorphous to crystalline phase change property of GST, we demonstrate a Type-I HMM in which the spectral region of negative refraction can be switched from the near infra-red (IR) to visible upon thermal annealing.

The HMM was composed of 7 periods of alternating layers of silver and GST of thicknesses, 15nm and 24nm, respectively, deposited by RF sputtering on pre-cleaned glass substrates. An ultrathin layer ( $\approx 1$  nm thick) of germanium was used as a wetting layer in order to ensure good quality silver films. Optical characterization of the HMM was performed by carrying out ellipsometric measurements on the HMM sample. By using a uniaxial anisotropic model, the effective in-plane and out-of-plane dielectric constants of the HMM were determined from ellipsometry. When the GST layers in the HMM are in the amorphous phase, the HMM shows Type-I hyperbolic dispersion (the out-of-plane dielectric constant being negative and the in-plane dielectric constant being positive) in the near-IR region and elliptical dispersion (both the dielectric constants are positive) in the visible region. Subsequently, the sample is annealed above the GST crystallisation temperature to convert the GST phase from amorphous to crystalline. In this phase, the HMM exhibits Type-I hyperbolic dispersion in the visible region and elliptical dispersion in the near-IR region. Finite element method simulations showed that the HMM exhibits negative refraction in the near-IR region and positive refraction in the visible region when the GST layers are in the amorphous phase. This situation is reversed after conversion of the GST layers to their crystalline phase, where the negative refraction is exhibited in the visible region.

In conclusion, we demonstrated a hyperbolic metamaterial containing a chalcogenide phase change constituent in which both positive and negative refraction coexist in the visible and near-IR spectral regions, respectively; the sign of refraction in both spectral regions can be inverted by simply switching the phase of the chalcogenide glass.

### **T14.3 Optical properties of an atomic ensemble coupled to a band edge of a photonic crystal waveguide**

Ewan Munro\*, Leong Chuan Kwek, Darrick Chang (CQT)

11:45am – 12:00pm

In recent years there has been significant interest in the intersection of quantum optics and nanophotonics, where quantum emitters ('atoms') are coupled to structures such as cavities and waveguides whose characteristic dimensions are comparable to the resonant wavelength of the atom. Primarily conceived as a route to more efficient atom-photon coupling and improved scalability compared to traditional quantum optics setups, such systems also allow for the exploration of qualitatively new classes of light-matter interactions. One example of this is to couple atoms to photonic band-gap materials, where it is possible to engineer long-range coherent interactions between the atoms. Motivated by recent advances in experimental capabilities along such lines, we study the fundamental optical properties of such a system in both the linear and several-photon regimes. In particular, we show how a modification is required of the basic characterisation tools of standard atomic ensemble physics, and consider how the system may be used to produce non-classical states of light.

### **T14.114 Tailoring the slow-light behavior in terahertz metamaterials.**

Manukumara Manjappa\*, Sher-Yi Chiam, Longqing Cong, Andrew A. Bettiol, Weili Zhang, Ranjan Singh\* (Center for Disruptive Photonic Technologies, Division of Physics and Applied Physics, School of Physical and Mathematical Sciences, Nanyang Technological University, 21 Nanyang Link, Singapore 637371)

12:00pm – 12:15pm

Light is one among the primary constituents of the universe. Manipulating and capitalizing on its exotic properties have led to exceptional inventions over the centuries. Metamaterials exhibiting the unnatural properties have contributed immensely in manipulating the behaviour of light waves in a desired manner by modifying their structures and geometries. Metamaterials are the sub-wavelength resonators that exhibit near field effects, whose strengths are dominating close to the meta-atoms and they abate faster with increase in the coupling distance. In this presentation we discuss on tailoring the near field coupling that induces the classical analogue of electromagnetically induced transparency in the metamaterial system under various system asymmetries and there by tuning the slow light behavior in the system. These systems can show potential application in the broadband telecom networks and as efficient amplitude and phase modulators at terahertz frequencies.

### **T14.36 Infrared Nonlinear Spectroscopy Without Spectral Selection**

Anna Paterova\*, Shaun Lung\*, Dmitry Kalashnikov\*, Leonid Krivitsky\* (data storage institute)

12:15pm – 12:30pm

The infrared (IR) optical spectrum range contains vibrational resonances of many molecules. Probing materials in the IR allows obtaining a set of unique molecular fingerprints. This is why the IR optical spectroscopy is a powerful tool for many applications including material

analysis, environmental sensing, health diagnostics and others. Being well-developed for VIS-NIR range optical spectrometers and refractometers face challenges, when they are applied in the IR range. The reason is inferior performance (in terms of noise level and efficiency) and high cost of IR optics, IR light sources and IR detectors. Recently, an elegant approach to the IR spectroscopy was suggested, which is fully based on using well-developed and low-cost optical instruments for the visible range [1]. The idea is to introduce frequency correlation between infrared and visible light, through the process of Parametric Down Conversion (PDC). A specific interferometric scheme allows measurement of a transmission spectrum of the sample in the IR-range from the interference pattern observed for a visible photon. This technique does not require the use of IR-range optical equipment. However, the technique requires careful spectral and spatial selection using a spectrograph and the slit to avoid overlapping of spatial and frequency modes and to allow observation of the interference pattern. Use of the spectrograph for spectral selection makes the system more bulky, expensive and requires long readout time to mitigate poor signal to noise ratio. Here we engineered a device for measurement of both real (refraction) and imaginary (absorption) part of the refractive index in the IR-range by measuring an interference pattern in the visible range without need for any spectral and spatial selection. The SPDC sources are set subsequently into the common pump beam to produce interference pattern at the output of the scheme. The parameters of the setup are chosen in such a way that the interference fringes for signal photons are parallel to the horizontal frequency axis and do not overlap. As a result the interference pattern can be measured without the need for any spectrally filtering element. In this case the interference pattern takes the form of the ring-like structure and can be directly detected with a CCD camera. (see attached paper for pictures). Interference pattern depend on medium properties at the gap between crystals. The refractive index and the absorption coefficient can be found from the distorted interference pattern by comparing experimental results for a vacuum gap and a gap filled with some medium. The technique is applicable to different media of different types (solid, gases and liquids) and provides broadband tunability in wavelength by tilting the crystals.

[1] D. A. Kalashnikov, A. V. Paterova, S. P. Kulik and L. A. Krivitsky, “Infrared spectroscopy with visible light”, *Nature Photonics*, 10, 98–101 (2016).

## **T15: Density Functional Theory of 2D Materials**

Time: Tuesday 8 Mar, 11:15am; Venue: TT18; Chair: Feng Yuan Ping

Time allocated for invited talks is 20 min speaking time, plus 5 min Q&A, and time allocated for contributed talks is 12 min speaking time plus 3 minutes Q&A.

### **T15.30 Effective Coulomb interaction and the Metal-Insulator transition in graphene**

João Rodrigues\*, Shaffique Adam (Centre for Advanced 2D Materials, National University of Singapore)

11:15am – 11:30am

We have recently shown [H.-K. Tang et al., PRL 115, 186602 (2015)] that the application of isotropic strain to graphene is a more promising route to make it an antiferromagnetic Mott insulator than substrate manipulation. That numerical work considered graphene's pi-electrons interacting through an effective Coulomb potential that is finite at short-distances due to screening effects by graphene's sp<sup>2</sup>-electrons. We have demonstrated that the magnitude of the effective Coulomb interaction at short distances plays a fundamental role in determining the semimetal to Mott insulator phase transition in graphene. Here we will overview these results and explore the phase diagram of graphene by studying a field theoretical model of Dirac fermions interacting through an effective Coulomb-like potential with both short and long-range interactions. This model attempts to bridge the gap between I. F. Herbut's work [PRL 97, 146401 (2006)], that concentrates on the effect of onsite interactions, and the work of D. T. Son [PRB 75, 235423 (2007)], which puts the emphasis on the long-range interactions. This work was supported by the Singapore National Research Foundation (NRF-NRFF2012-01 and CA2DM medium-sized centre program) and by the Singapore Ministry of Education and Yale-NUS College (R-607-265-01312).

### **T15.71 Two-dimensional group-IV monochalcogenides: Structural, electronic and optical properties.**

Lídia Gomes\*, Alexandra Carvalho, Aleksandr Rodin, Antonio Helio Castro Neto (Centre for Advanced 2D Materials and Graphene Research Centre-NUS)

11:30am – 11:45am

The layered group-IV monochalcogenides-SnS, SnSe, GeS and GeSe- has gained attention as a promising group with potentially useful applications in diverse fields. We use first principles calculations to explore structural, electronic and optical properties of this group, with focus in their two-dimensional forms. We show that all those binary compounds are semiconducting, with bandgap energies covering most of the visible range. They have multiple valleys in the valence and conduction bands, with substantial spin-orbit splitting. An enhanced static dielectric permittivity is found for the monolayers. Structural analysis shows that the 2D form of these materials presents very high piezoelectric constants, exceeding values recently observed for other 2D-systems. Further, a useful method of write and read valley states is proposed for SnS, taking advantage of its orthorhombic form.

### **T15.87 Theoretical Study of Coulomb Drag in Double Monolayer Graphene Heterostructures**

Derek Ho\*, Indra Yudhistira, Ben Yu-Kuang Hu, Shaffique Adam\* (Department of Physics and Centre for Advanced 2D Materials, National University of Singapore, and Yale-NUS College)  
11:45am – 12:00pm

The double monolayer graphene heterostructure is a promising system for realizing a highly energy-efficient transistor, a vital requirement for the continued improvement of semiconductor processor technology. There is thus an effort across several groups worldwide to understand the underlying physics. A particularly important effect that must be understood in this regard is the Coulomb Drag, in which driving a current in one of the layers induces an electric field across the other. At this point in time, a quantitative understanding of this effect is still lacking. We will review the current state-of-the-art theory in the Coulomb Drag literature and share our current ongoing work. Our investigation suggests that the effects of charge inhomogeneity in the two layers play a centrally important role in the Coulomb Drag effect but have not yet been treated in a quantitatively rigorous manner. This work was supported by the Singapore National Research Foundation (NRF-NRFF2012-01 and CA2DM medium-sized centre program) and by the Singapore Ministry of Education and Yale-NUS College (R-607-265-01312).

### **T15.95 Non-linear photocurrent in hexagonal lattices**

Fábio Hipólito\*, Thomas Garm Pedersen, Vítor M. Pereira (National University of Singapore - NGS)  
12:00pm – 12:15pm

The second order response of the electrical current to an electromagnetic field is analyzed within the framework of a perturbative expansion of density matrix using direct coupling to the radiation, i.e. the length gauge. This paper focus on the generation of non-linear DC currents on mono and bilayer hexagonal lattices of hexagonal Boron Nitride (hBN) and graphene. Inversion symmetry is naturally absent in mono and bilayer hBN, whereas in graphene the symmetry is broken by interaction with substrates or the presence of external static fields. The induced DC current is computed at finite temperature, and its tunability is analyzed as a function of electron density, which can be experimentally varied by means of a global gate voltage applied to the sample. Results indicate that the response of both hBN mono and bilayers is robust and occurs at in ultra-violet range due to the very large gap. However, the presence of finite doping opens a low energy channel at the low energy, i.e. the separation between the valence (conduction) bands. The response in graphene, particularly in the biased bilayer is much more rich and highly tunable with respect to both temperature and electron density.

## **6 Committees**

### **Program Committee**

Dario Poletti, SUTD

Cesare SOCI, SPMS, NTU

KOH Wee Shing, IHPC, A\*STAR

Rainer DUMKE, CQT and SPMS, NTU

Jens MARTIN, CA2DM and Physics Dept, NUS

Christian KURTSIEFER, CQT and Physics Dept, NUS

### **Organizing Committee**

Dario Poletti, SUTD

TAN Si Hui, SUTD (Exhibitors)

Atul MANTRI, SUTD

LIM Kim Yong, NUS (SPho Event)

LIM Jit Ning, HCI (IPS Finances)

Cesare SOCI, SPMS, NTU

KOH Wee Shing, IHPC, A\*STAR

Christian KURTSIEFER, CQT and Physics Dept, NUS

special thanks for logistics help to the technical support staff and many students at SUTD!

## Author List

A. Bettioli, Andrew, 82  
Adam, Shaffique, 6  
Adam, Shaffique, 84, 85  
Adamo, Giorgio, 34, 77  
Adams, Stefan, 61  
Al-Naib, Ibraheem, 25  
Aljunid, Syed Abdullah, 79  
Alodjants, Alexander, 19  
Altuzarra, Charles, 59  
An, Hongjie, 41, 54  
Ang, L. K., 22, 76  
Ang, Lay Kee, 42, 78  
Ang, Lay-Kee, 23  
Ang, Yee Sin, 22  
Anwar Ali, Hashina Parveen, 43  
Arnardottir, Kristin Bjorg, 19  
Arnold, Kyle, 29, 73  
Arpan, Roy, 18  
Arrazola, Juan Miguel, 69  
Aukstol, Filip, 21

B. Swe, Phyo, 24  
Baden, Markus, 29  
Bahulayan, Damodaran, 43  
Bai, Xueliang, 17  
Bancal, Jean-Daniel, 17  
Barkay, Zahava, 54  
Barrett, Murray, 29, 73  
Bastock, Paul, 37  
Batrouni, George, 52  
Beau, Mathieu, 48  
Bedington, Robert, 17, 69  
Behera, Jitendra Kumar, 28  
Bharadwaj, Vibhav, 44  
Bhatti, Sabpreet, 24  
Bhaumik, Saikat, 43  
Binder, Felix, 63  
Birovosuto, M Danang, 45  
Bissbort, Ulf, 32  
Boix, Pablo P., 47  
Bornheimer, Ulrike, 11

Brandsen, Sarah, 46, 63  
Brun, Todd, 26  
Bruno, Annalisa, 42, 45  
Budiman, Arief, 43  
Burkard, Guido, 24  
Buscemi, Francesco, 46, 63

Caironi, Mario, 43  
Campbell, Steve, 23  
Cao, Bingchen, 16, 68  
Cao, Wei, 25  
Cao, Wen-Fei, 64  
Carvalho, Alexandra, 67, 84  
Castro Neto, Antonio, 67  
Castro Neto, Antonio Helio, 84  
Catalin Dan, Spataru, 66  
Cazalilla, Miguel, 75  
Cerè, Alessandro, 21, 35, 36  
Cere, Alessandro, 72  
Chai, Jing Hao, 27  
Chan, Aik Hui, 16  
Chan, Eng Aik, 79  
Chan, Wei Sheng, 18  
Chanda, Amit, 20  
Chandrasekara, Rakhitha, 10, 19, 57, 71  
Chang, Darrick, 82  
Chang, Tay-Rong, 67  
Chang, Yung-Huang, 66  
Chen, Kai, 64  
Chen, Rui, 33, 34  
Chen, Yifeng, 66  
Chen, Yu, 16, 68  
Cheng, Cliff, 10, 17, 57, 71  
Cheng, Lew Kar, 45  
Chi, Dongzhi, 66  
Chiam, Sher-Yi, 82  
Chien, Sum Tze, 67  
Chin, Xin Yu, 42, 43, 45  
Chin, Yue Sum, 23  
Chng, Brenda, 10, 35, 36  
Chong, Yidong, 10, 50, 70, 71, 75

Choong, Zheng Yang, 31  
 Christian, Kurtsiefer, 10  
 Chua, Hou, 15  
 Condylis, Paul, 21  
 Cong, Chunxiao, 16, 67, 68  
 Cong, Longqing, 14, 25, 29, 82  
 Cortecchia, Daniele, 42, 45  
 Couteau, Christophe, 59  
 Craig, Christopher, 37  
 Cui, Long, 37  
  
 Dai, Jibo, 15, 70  
 Dall'Arno, Michele, 46, 63  
 Dasgupta, Sabyasachi, 48  
 Dayal, Dr Govind, 29  
 De Chiara, Gabriele, 23  
 Del Campo, Adolfo, 48  
 Demir, Hilmi Volkan, 33, 34  
 Dieckmann, Kai, 73, 80  
 Dimova, Emiliya, 11  
 Ding, Meng, 37  
 Ding, Shiqian, 32, 79  
 Dini, Kevin, 78  
 Dong, Weiling, 28  
 Dong, Zhaogang, 38, 46  
 Droth, Matthias, 24  
 Dubrovkin, Alexander M., 38, 77  
 Ducloy, Martial, 79  
 Dumke, Rainer, 18, 21, 24, 29  
 Durak, Kadir, 10, 57, 71  
 Dutta, Tarun, 47  
  
 Eaton, Shane, 44  
 Eliase, Ummu Sumaiyah Binte, 42  
 Engardt, Sara, 19  
 Englert, Berthold-Georg, 25  
 Ew, Chee Howe, 18  
  
 Faccio, Daniele, 59  
 Fan, Hong Jin, 11, 62  
 Fan, Yunan, 37  
 Fei, Ruixiang, 68  
 Feng, Shun, 16  
 Feng, Yuan Ping, 13  
 Fitzsimons, Jack, 12  
  
 Fitzsimons, Joseph, 12, 64  
 Fu, Qundong, 67  
 Fu, Wei, 67  
  
 Gan, Chee Kwan, 51  
 Gan, Jaren, 80  
 Gao, Yuan, 33  
 Garner, Andrew, 52  
 Gholipour, Behrad, 37, 81  
 Ghosh, Sanjib, 12, 50  
 Goh, Ka Hui, 29  
 Goh, Koon Tong, 64  
 Goh, Wei Peng, 26  
 Goh, Xiao Ming, 28  
 Goki, Eda, 66  
 Gomes, Lídia, 84  
 Gomes, Lidia, 67  
 Gonzalez-Avila, Silvestre Roberto, 56  
 Goold, John, 63  
 Grémaud, Benoît, 52  
 Grant, Daniel, 48  
 Grieve, James, 19, 20, 57  
 Grieve, James A., 57  
 Gross, Christian, 80  
 Grémaud, Benoît, 11  
 Gu, Mile, 52  
 Guimond, Pierre-Olivier, 15  
 Guo, Chu, 47  
 Guo, Lu, 40  
 Gupta, Manoj, 29  
  
 Hablutzel, Roland, 32, 79  
 Hajiyev, Elnur, 73  
 He, Haiyong, 67  
 He, Tingchao, 34  
 Hewak, Daniel, 37  
 Hipólito, Fábio, 85  
 Ho, Derek, 85  
 Ho, Yun Ling Selina, 49  
 Hu, Ben Yu-Kuang, 85  
 Huang, Chang, 20, 72  
 Huang, Chun Li, 75  
 Huang, Junye, 35  
 Huang, Wei, 11

Huang, Yu Li, 66  
 Huang, Zhi Xiang, 39  
 Huang, Zhixiang, 39  
 Hufnagel, Christoph, 18, 24  
  
 Iorsh, Ivan, 19  
  
 Jain, Manan, 48  
 Jamaludin, Nur Fadilah, 44  
 Jaramillo, Juan Diego, 48  
 Jeng, Horng-Tay, 67  
 Jiang, Liyong, 38, 46  
 Jin, Chuanhong, 67  
 Joshi, Siddarth K., 35  
  
 Kalashnikov, Dmitry, 82  
 Kalikka, Janne, 28  
 Khan, Khouler, 37  
 Kiasat, Yasaman, 77  
 Kibis, Oleg, 74, 78  
 Koduru Joshi, Siddarth, 36  
 Koh, Teck Ming, 35  
 Koh, Teck Seng, 30  
 Koh, Wee Shing, 26  
 Kong, Dezhi, 36  
 Krivitsky, Leonid, 82  
 Ku, Zhiliang, 62  
 Kuan, Pei Chen, 20, 72  
 Kumar, Muduli Subas, 43  
 Kumar, Mulmudi Hemant, 33  
 Kumar, Rakesh, 53  
 Kurtsiefer, Christian, 16, 21, 23, 35, 36, 72  
 Kwek, Leong Chuan, 30, 82  
 Kwong, Chang Chi, 48, 72  
 Kwong, Chang Jian, 30  
 Kyoseva, Elica, 11  
  
 Lai, Ching-Yi, 26  
 Lam, Mark, 73  
 Lan, Shau-Yu, 20, 72, 79  
 Landra, Alessandro, 18  
 Le, Huy Nguyen, 15, 70  
 Lee Yanxi, Bianca, 31  
 Lee, Chern Hui, 29  
 Lee, Jianwei, 35, 36  
  
 Lei, Yisheng, 18  
 Len, Yink Loong, 22  
 Leong Wui Seng, Wui Seng, 18  
 Leong, Victor, 72  
 Leong, Victor Xu Heng, 21  
 Leong, Wui Seng, 79  
 Leong, Zhi Yi, 38  
 Leroux, Frédéric, 48  
 Lew, Kar Cheng, 42, 45  
 Lewty, Nick, 23  
 Leykam, Daniel, 10  
 Li, Lain-Jong, 66  
 Li, Mingjie, 43  
 Liang, Shijun, 42  
 Liew, Soo Chin, 42  
 Liew, Timothy, 59  
 Lim, Chin Chean, 18  
 Lim, Tian Yi, 13  
 Lin, Hsin, 67  
 Lin, Junzhe, 41  
 Lin, Lester, 48  
 Lin, Way, 29  
 Ling, Alexander, 7, 10, 17, 19, 20, 57, 69,  
     71  
 Liu, Bo, 60  
 Liu, Kan, 41  
 Liu, Weizhen, 33  
 Liu, Xinfeng, 67  
 Liu, Ying, 74  
 Liu, Yun, 51  
 Liu, Zheng, 46, 67  
 Lo, Hoi-Kwong, 69  
 Loh, Huanqian, 79  
 Loh, Iong Ying, 55  
 Lor, Jun Heng, 31  
 Lova, Paola, 45  
 Lu, Jun Peng, 14  
 Lu, Ning, 49  
 Lu, Zixuan, 41  
 Lung, Shaun, 82  
 Lutkenhaus, Norbert, 69  
 Lv, Jian-Ping, 78  
  
 M. Valado, Maria, 24

Müller-Buschbaum, Peter, [47](#)  
Ma, Zhongshui, [22](#)  
Maddalena, Francesco, [42](#)  
Mahendiran, Ramanathan, [20](#)  
Mañcois, Vincent, [48](#)  
Manjappa, Manukumara, [25](#), [82](#)  
Mansha, Shampy, [70](#)  
Martinez Mercado, Julian, [55](#)  
Martinez Valado, Maria, [21](#)  
Maslennikov, Gleb, [32](#), [79](#)  
Mathews, Nripan, [33](#), [43](#), [47](#)  
Matsukevich, Dzmitry, [32](#), [79](#)  
McKague, Matthew, [17](#)  
Mhaisalkar, Subodh, [33](#), [35](#), [43](#)  
Mhaisalkar, Subodh G., [47](#)  
Ming Koh, Teck, [47](#)  
Miniatura, Christian, [11](#)  
Mirsaidov, Utkur, [54](#)  
Mishra, Jatadhari, [19](#)  
Modi, Kavan, [63](#)  
Mohammadzadeh, Milad, [56](#)  
Mohan, Meera, [54](#)  
Mohan, Meera Kanakamma, [54](#)  
Morina, Skender, [74](#), [78](#)  
Mukherjee, Manas, [47](#)  
Munro, Ewan, [82](#)  
  
Najmaei, Sina, [67](#)  
Nalla, Venkatram, [37](#)  
Narayanan, Ramakrishnan, [47](#)  
Navau, Carles, [32](#)  
Nemoto, Kae, [64](#)  
Ng, Hui Khoo, [22](#), [25](#), [27](#)  
Ng, Yan Fong, [43](#)  
Nguyen, Duc Minh, [37](#), [44](#)  
Nguyen, Huy Tiep, [62](#)  
Nguyen, Nghia Tin, [21](#)  
Niu, Lin, [67](#)  
  
Oesinghaus, Lukas, [47](#)  
Ohl, Claus-Dieter, [41](#), [54–56](#)  
Oi, Daniel, [69](#)  
Ong, Yi Ying, [30](#)  
Ouyang, Yingkai, [64](#)  
  
Pace, Giuseppina, [43](#)  
Paez, Eduardo, [73](#)  
Pal, Sambit, [73](#)  
Pandey, Kanhaiya, [72](#)  
Paterova, Anna, [82](#)  
Pedersen, Thomas Garm, [85](#)  
Peimyoo, Namphung, [16](#)  
Pereira, Vítor M., [85](#)  
Pereira, Vitor M., [24](#)  
Pervishko, Anastasiia, [58](#)  
Piramanayagam, S.N., [24](#)  
Poletti, Dario, [23](#), [32](#), [47](#)  
Popkirov, George, [11](#)  
Pramod, Mysore Srinivas, [72](#)  
Prasada Rao, Rayavarapu, [61](#)  
Prat-Camps, Jordi, [32](#)  
  
Qian, Cheng, [38](#)  
Qian, Yuying, [41](#)  
Qiang, Bo, [77](#)  
Quek, Su Ying, [66](#)  
  
Rachel, Ng Si Min, [29](#)  
Radchenko, Ihor, [43](#)  
Ramanathan, Mahendiran, [76](#)  
Rangelov, Andon, [11](#)  
Rawat, R.S., [24](#)  
Rebhi, Riadh, [48](#)  
Rechtsman, Mikael, [10](#)  
Reddy, M V, [60](#)  
Reddy, M. V., [13](#)  
Reddy, M. V. Venkatasamy, [12](#)  
Repaka, D V Maheswar, [20](#)  
Rodin, Aleksandr, [67](#), [84](#)  
Rodrigues, João, [84](#)  
Rogers, Edward, [81](#)  
Romero-Isart, Oriol, [32](#)  
Roulet, Alexandre, [15](#), [70](#)  
Roy, Arpan, [79](#)  
  
S. Krishnamoorthy, Harish N., [81](#)  
Sacksteder Iv, Vincent, [58](#)  
Sanchez, Alvar, [32](#)  
Savinov, Dr Vassili, [29](#)  
Sawat, Rajdeep, [48](#)

Scarani, Valerio, [15](#), [17](#), [64](#), [70](#)  
 Schlipf, Johannes, [47](#)  
 Seidler, Mathias, [21](#)  
 Seidler, Mathias A., [35](#), [36](#)  
 Seidler, Mathias Alexander, [72](#)  
 Seixas, Leandro, [67](#)  
 Sengupta, Pinaki, [52](#), [53](#)  
 Septriani, Brigitta, [57](#)  
 Shahzad, Munir, [52](#)  
 Shang, Jiangwei, [25](#)  
 Shang, Jingzhi, [16](#)  
 Shanmugam, Vignesh, [47](#)  
 Shelykh, Ivan, [19](#), [58](#), [59](#), [74](#), [78](#)  
 Shen, Lijiong, [35](#), [36](#)  
 Shen, Zexiang, [38](#), [46](#)  
 Shi, Yicheng, [10](#)  
 Sigurdsson, Helgi, [59](#)  
 Sim, Glenn Joey, [36](#)  
 Sim, Jun Yan, [25](#)  
 Simpson, Robert, [28](#)  
 Simpson, Robert Edward, [28](#)  
 Singh, Dr Ranjan, [29](#)  
 Singh, Ranjan, [14](#), [25](#), [82](#)  
 Soci, Cesare, [37](#), [42–45](#), [59](#), [77](#), [81](#)  
 Soh, Yong Sheng, [13](#)  
 Sotillo, Belen, [44](#)  
 Sow Miaoer, Belle, [14](#)  
 Sow, Chornng Haur, [14](#)  
 Srivastava, Yogesh, [14](#)  
 Srivastava, Yogesh Kumar, [25](#)  
 Steiner, Matthias, [23](#), [72](#)  
 Suen, Whei Yeap, [52](#)  
 Sum, Tze Chien, [33](#), [43](#), [62](#)  
 Sun, Handong, [33](#), [34](#)  
 Sun, Yudong, [31](#)  
 Swamy, Varghese, [47](#)  
  
 Ta, Van Duong, [34](#)  
 Taisne, Benoit, [5](#)  
 Tan, Beng Hau, [41](#), [54](#)  
 Tan, Bo Xue, [20](#)  
 Tan, Peng Kian, [16](#)  
 Tan, Pinxi, [15](#)  
 Tan, Yue Chuan, [17](#), [71](#)  
  
 Tang, Zhongkan, [57](#)  
 Tay, Beng kang, [67](#)  
 Teng, Jinghua, [34](#)  
 Teo, Colin, [32](#)  
 Thompson, Jayne, [52](#)  
 Tosto, Francesca, [24](#)  
 Truong Cao, Edward, [17](#)  
  
 Utama, Adrian Nugraha, [21](#)  
  
 V. Ramanujan, Raju, [20](#)  
 Valente, Joao, [59](#)  
 Vazquez, Maria, [44](#)  
 Vedral, Vlatko, [52](#)  
 Veldhuis, Sjoerd A., [43](#)  
 Venkata Kameshwar Rao, Irukuvarjula, [41](#)  
 Venkatakrisnan, Ashwin, [15](#)  
 Vezzoli, Stefano, [59](#)  
 Viganale, Giovanni, [75](#)  
 Vinjanampathy, Sai, [63](#)  
  
 Wan, Yin Chi, [56](#)  
 Wang, Hailong, [50](#)  
 Wang, Haotian, [31](#)  
 Wang, Hong, [67](#)  
 Wang, Jian-Sheng, [78](#)  
 Wang, Lan, [77](#)  
 Wang, Qi Jie, [70](#), [77](#)  
 Wang, Shijie, [33](#)  
 Wang, Wei Jie, [28](#)  
 Wang, Xianfen, [39](#), [40](#)  
 Wang, Xincan, [56](#)  
 Wang, Xingli, [67](#)  
 Wang, Yanlong, [68](#)  
 Wang, Ye, [36](#), [39](#)  
 Wang, Yue, [34](#)  
 Wang, Zeng, [34](#)  
 Wee, Andrew, [66](#)  
 Wee, Andrew Thye Shen, [66](#)  
 Wen, Bruce, [12](#)  
 Wilkowski, David, [48](#), [72](#), [79](#)  
 Wu, Bo, [62](#)  
 Wu, Chunyang, [67](#)  
 Wu, Di, [67](#)  
 Wu, Mingsong, [31](#)

Wu, Qing Yang Steve, 34  
 Wu, Xingyao, 17, 64  
 Wu, Yikai, 42  
  
 Xia, Juan, 46  
 Xin, Mingjie, 18, 79  
 Xing, Guichuan, 33  
 Xu, Feihu, 69  
 Xu, Jing, 62  
 Xu, Ms Ningning, 29  
 Xu, Yi, 23, 78  
  
 Yakobson, Boris I., 67  
 Yan, Jiaxu, 46  
 Yang, Hui Ying, 36–39, 60  
 Yang, Huiying, 40  
 Yang, Joel, 8, 28  
 Yang, Joel K. W., 38, 46  
 Yang, Li, 68  
 Yang, Shancheng, 34  
 Yang, Shengyuan, 50, 74, 78  
 Yang, Weihuang, 68  
 Yantara, Natalia, 44  
 Yeo, Zhen Yuan, 30  
 Yin, Jun, 77  
 Yin, Tingting, 38, 46  
 Yongquan, Zeng, 70  
 Yu, Deshui, 18, 24  
 Yu, Letian, 27  
 Yu, Li, 64  
 Yu, Peng, 67  
 Yu, Ting, 16, 67, 68  
 Yu, Ye, 28  
 Yuan, Guanghui, 81  
 Yudhistira, Indra, 85  
  
 Zeng, Qingsheng, 67  
 Zhang, Chao, 22  
 Zhang, Lijun, 41  
 Zhang, Weili, 25, 82  
 Zhang, Wenjing, 66  
 Zhang, Yongqi, 11  
 Zhang, Yu Wei, 30  
 Zhang, Zhiqiang, 29  
 Zhang, Zhuhua, 67  
  
 Zhao, Weijie, 66  
 Zhao, Xin, 33  
 Zhao, Zhikuan, 12  
 Zheludev, Nikolay, 37, 59, 79, 81  
 Zheludev, Nikolay I., 77  
 Zhen, Yi-Zheng, 64  
 Zheng, Hongyu, 56  
 Zheng, Yi-Cong, 26  
 Zheng, Yicong, 22  
 Zheng, Yu Jie, 66  
 Zheng, Yu-Lin, 64  
 Zheng, Yuanjian, 23  
 Zhongkan Xavier, Tang, 71  
 Zhou, Jiadong, 67  
 Zhou, Longwen, 50  
 Zhou, Wu, 67  
 Zhou, Xilin, 28  
 Zhou, Xin, 71  
 Zhu, Binbin, 33  
 Zhu, Bingjie, 37  
 Zhu, Yingbin, 23  
 Zou, Chenji, 16  
 Zubair, Muhammad, 76